Introduction into HEP Experiments

Jim Freeman

FNAL

Some Sources Used

- http://www-physics.lbl.gov/~spieler/physics_198_notes/PDF/ Helmuth Spieler UC-Berkely Detectors
- B. Alpat, INFN Perugia, AMS
- http://www.physics.ohio-state.edu/~kass/teaching.html Richard Kass, Detectors
- Cerenkov Counter, Litt and Meunier, http://www.annualreviews.org/doi/pdf/10.1146/annurev.ns.23.120173.000245
- R. Forty, ICFA School,
  lhcb-doc.web.**cern**.ch/lhcb-doc/presentations/lectures/**Forty**1.ppt

Outline-Experiments

- Collider/fixed target beams
- Scintillation Counters
- HPDs and Silicon Detectors
- Wire Chambers
- Cerenkov Counters
- Discovery of Antiproton
- Calorimeters
- Water Cerenkov calorimeters: Super-Kamiokande, IceCube
- Fixed target detector: NuTeV
- LHC experiments CMS, LHCb

Overview

- Many of the HEP experiments use a limited number of particle detectors repeatedly
  - Scintillators
  - Cerenkov counters
  - Time-of-flight
  - Calorimeters
  - Wire tracking chambers
  - Silicon tracking detectors
- Goal of particle detectors is to determine properties of particles, P, V, M, charge, …
- Important to be familiar with these. (Can help with physics analyses, …)

Detector Subsystems

Particle type	Tracking	ECAL	HCAL	Muon
γ				
e				
μ				
Jet				
Et miss				

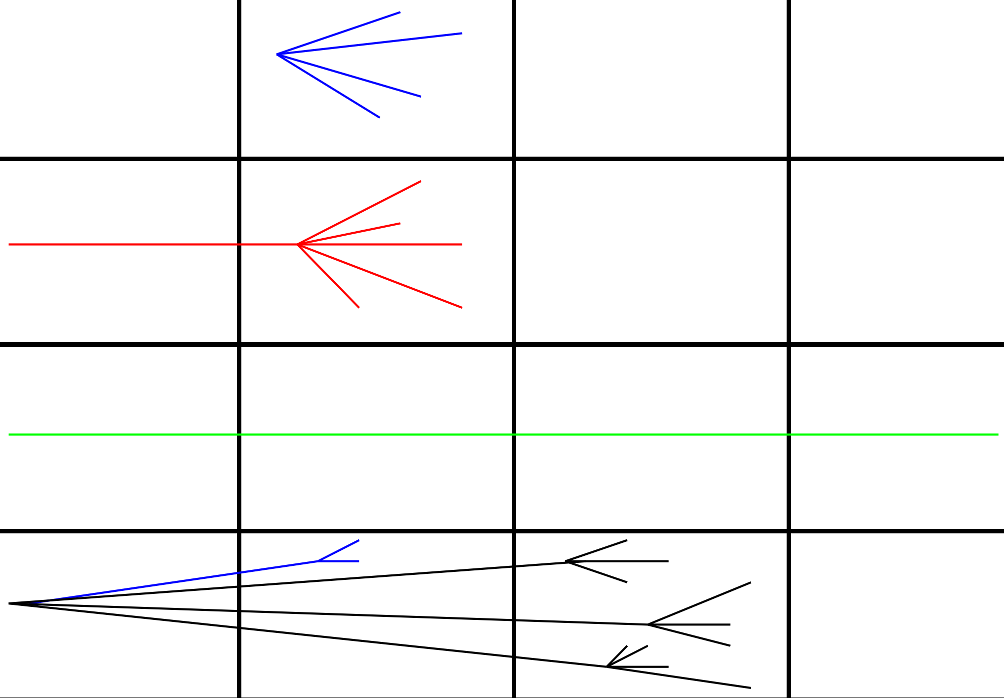

CERN LHC

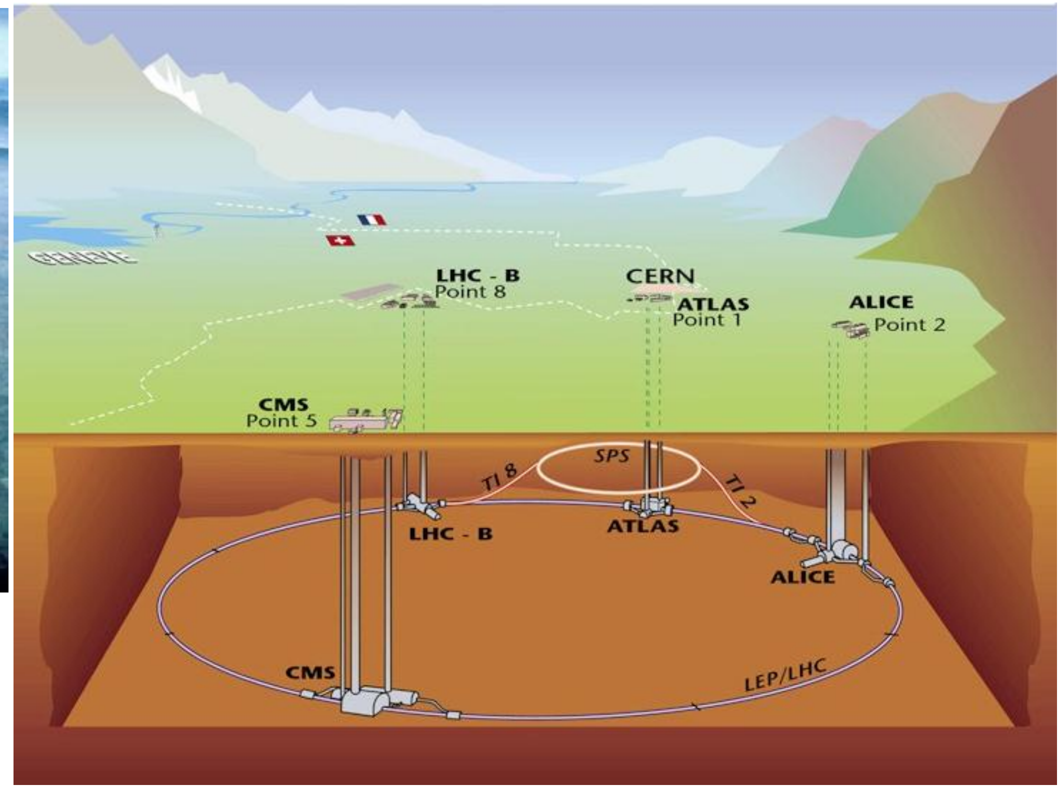
GENEVE
LHC - B
Point 8
CERN
ATLAS
Point 1
ALICE
Point 2
CMS
Point 5
SPS
TI 8
TI 2
LHC - B
ATLAS
ALICE
CMS
LEP/LHC

LHC Hadron Collider beam properties

- Proton-proton LHC center of mass energy 14 TeV. Ecm = 2 Ebeam
- 10^{34} $cm^2 sec^{-1}$ luminosity
- Collision region length sigma ~ 5cm
- Interaction region cross section 100μm
- Event rate > 100,000,000 per second
- Good stability of collision point
- Collision period 25 ns between crossings
- High Radiation fields, especially at forward angles

Fixed target experiment

- Beam energy up to 400 GeV
- beam structure (18 ns bunches at FNAL)
- flat top, up to 10^{13} particles over 2 second spill
- $Ecm = (2m_{target}E_{beam})^{1/2}$
- event rate determined by particles per spill. Can be extremely large.
- radiation fields can be extremely large at target region.
- Target can be gas jet, liquids, metals, active instrumented targets.

Simplest Detector?
Scintillation Counters

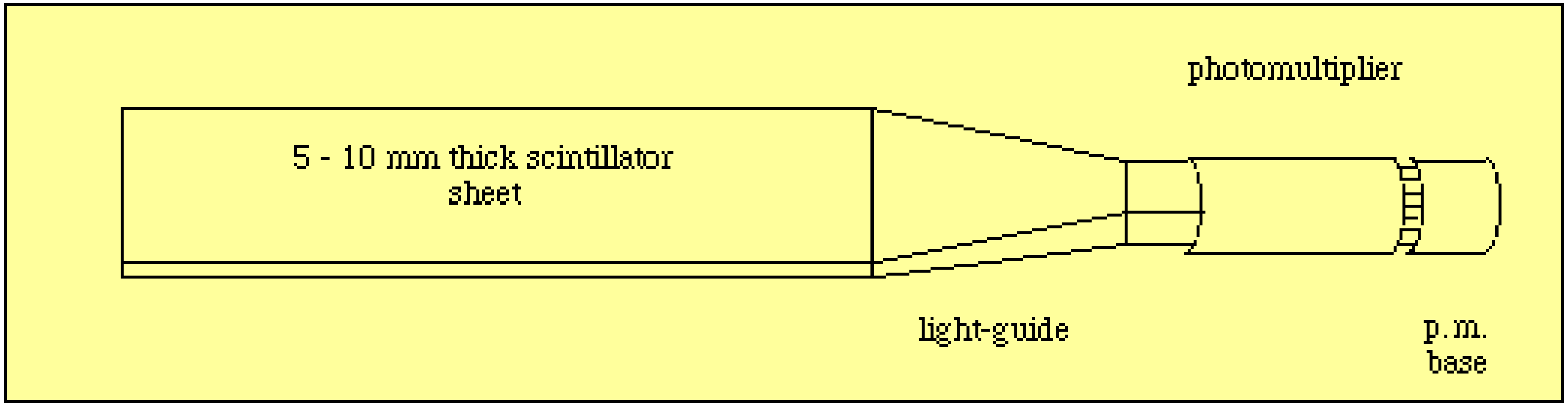

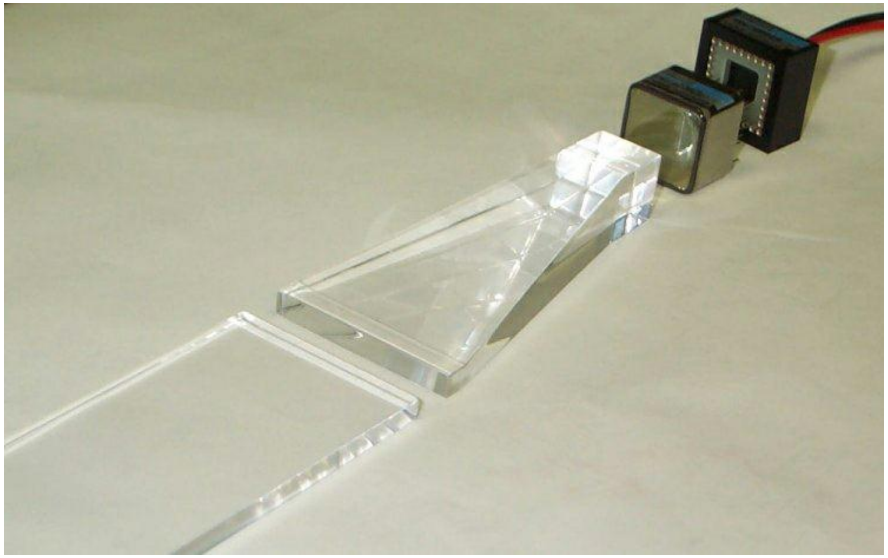

Organic Scintillator

Scintillator plastic very commonly used in HEP. Light production mechanism complicated. To make scintillator, start with scintillator base material, plastic containing benzene rings (polystyrene). The base material is sensitive to ionization energy loss of the particle. Molecules of the base material are excited into vibrational modes. Add Primary Fluor, a chemical that is excited by the vibrational mode of the base molecule and emits UV photon.) (Forster mechanism). Then add secondary fluor that absorbs UV photon, re-emits at a longer wavelength (called Stokes Shift of fluor). The UV photon is typically absorbed and shifted within 1mm of it's creation. The Stokes shift is necessary to prevent re-absorption of the UV photon by the primary fluor, hence improving attenuation length of the light in the material..

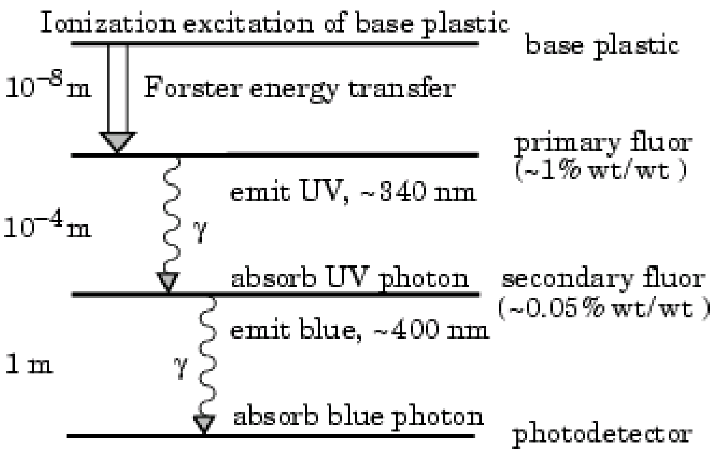

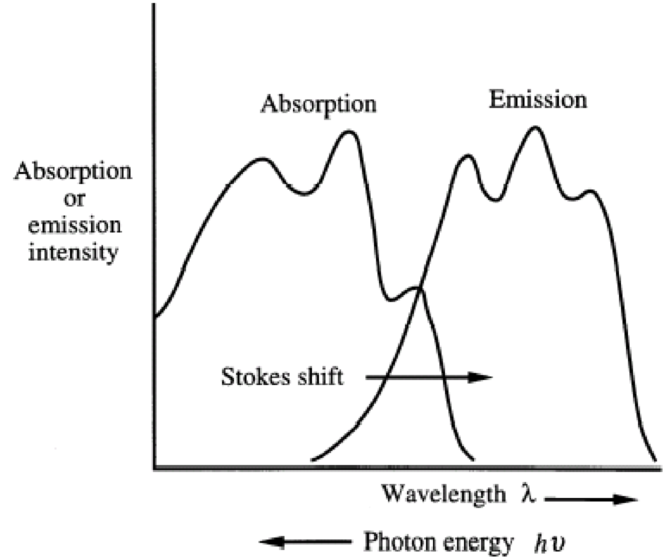

Light Guides and Liouville's Theorem

Liouville's Theorem is that the density of points in phase space is an incompressible fluid. For instance if you squeeze the x variable, you expand the p variable. Photons in a light guide can be treated as points in phase space, with the variables: the transverse coordinate in the light guide; and the photon's angle. Compressing the transverse coordinates too much will cause the photon angle to increase beyond the critical angle for total internal reflection, and the photon will escape from the light guide. Designing good light guides is subtle.

Use of wave-length shifting a way around Liouville's Theorem.

The PMT is often coupled to the scintillator through a light guide

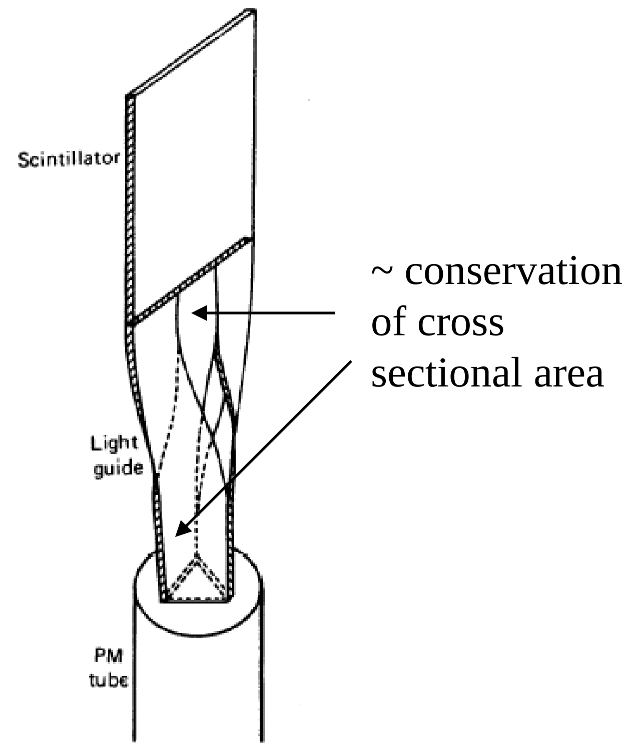

Wavelength shifting

Light emitted by scintillator is absorbed and re-emitted by wavelength shifter in a light guide. The new photon is emitted isotropically. Depending on the design of the light guide, 10-30% of the light can be captured in the light guide and carried to the photo-detector. In this way a very large compression of the density of light can be achieved. The ratio of the cross section of the scintillator to the cross section of the light guide can be quite large.

→cost savings in photocathode area. (CMS HCAL has ~800 cm^2 of photocathode

→Reduce cracks

→Example Tile/Fiber

Optical fiber doped with wavelength shifter acts as light guide.Fiber is placed in a groove in the scintillator, absorbs scintillator light, re-emits it. About 5% of the light is captured in the fiber

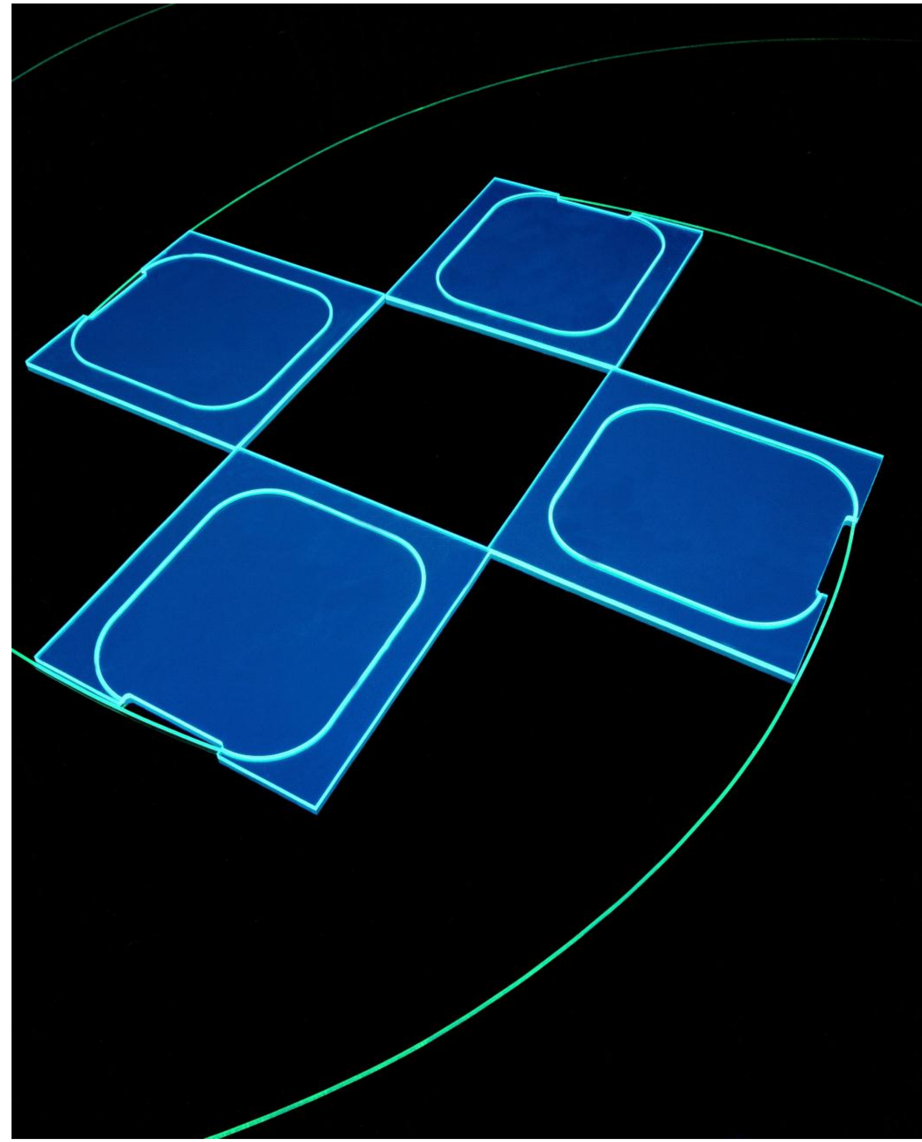

Wavelength Shifters

Another example of wavelength shifting to concentrate light. Calorimeter

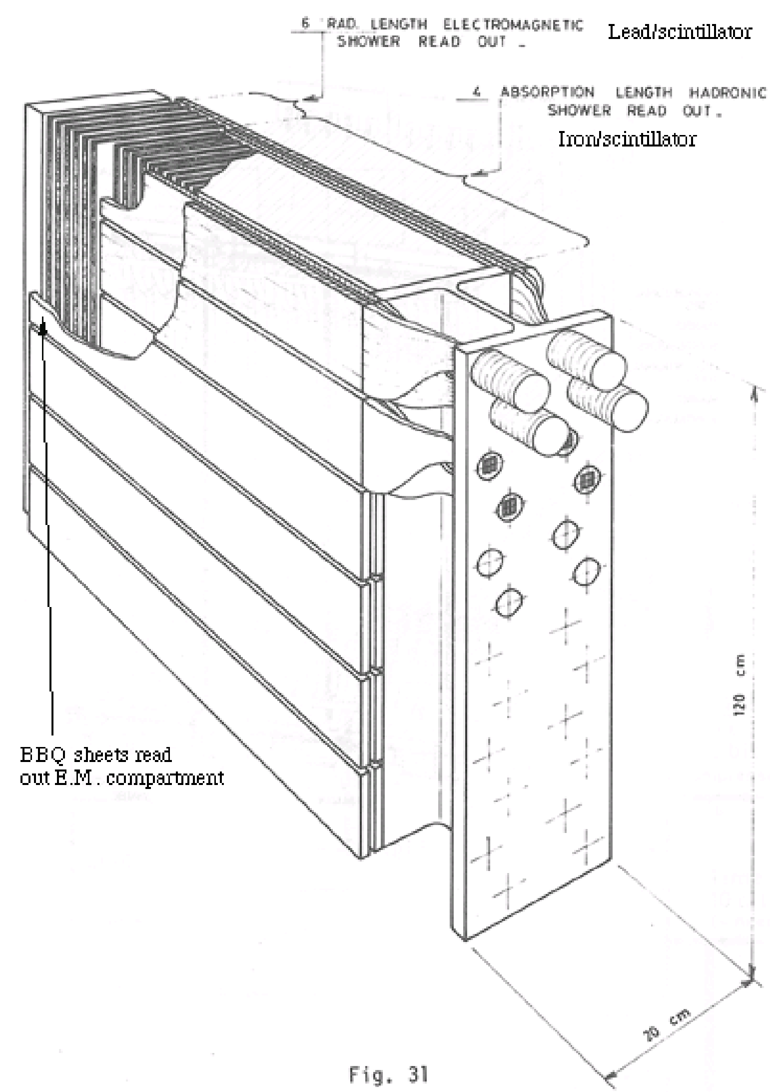

Fig. 31

Photomultiplier

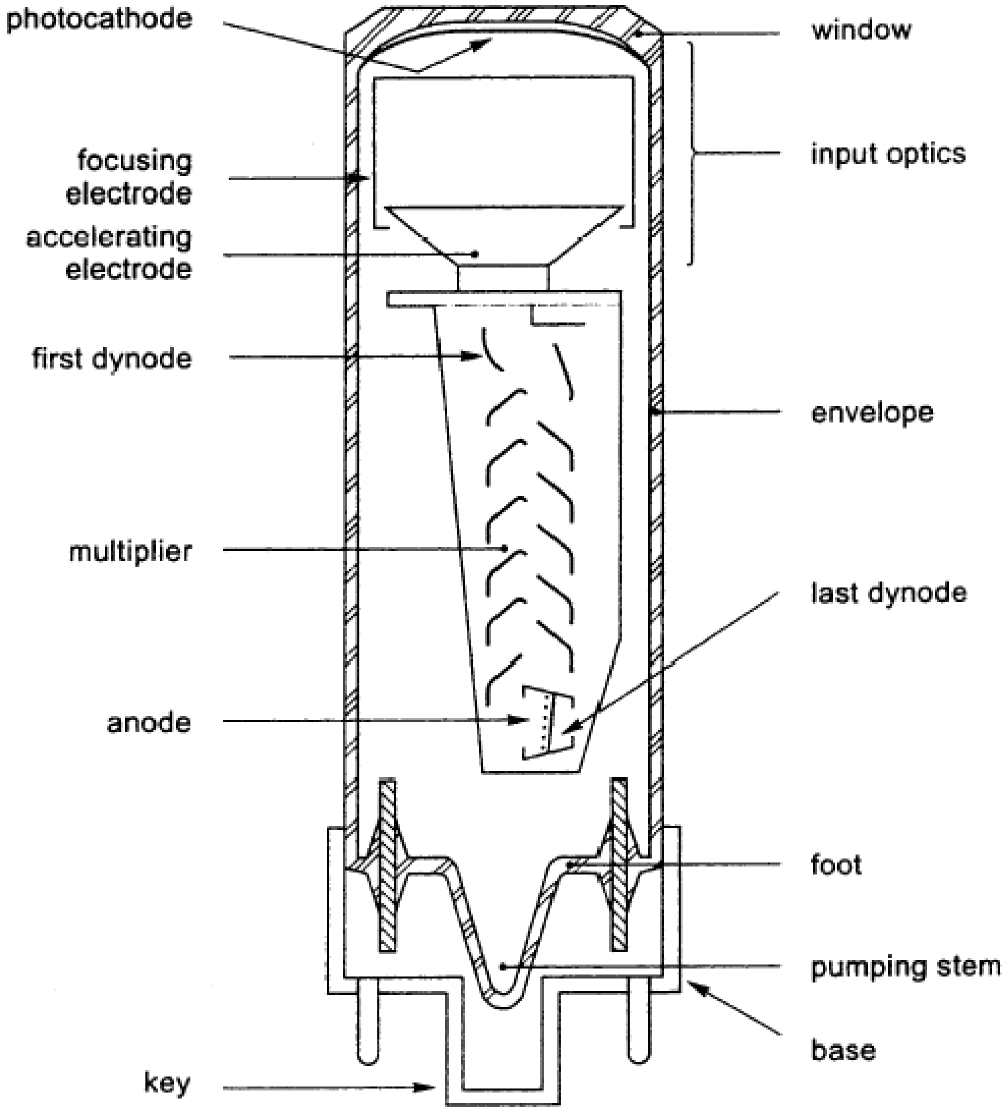

Uses photoelectric effect to convert photon to electron, then electron multiplication. Invented in 1930. Still heavily used.

Photomultipliers

Photomultiplier

Properties:

- Window
- Photocathode
- Quantum Efficiency
- Single pe resolution
- Gain
- Speed
- Noise

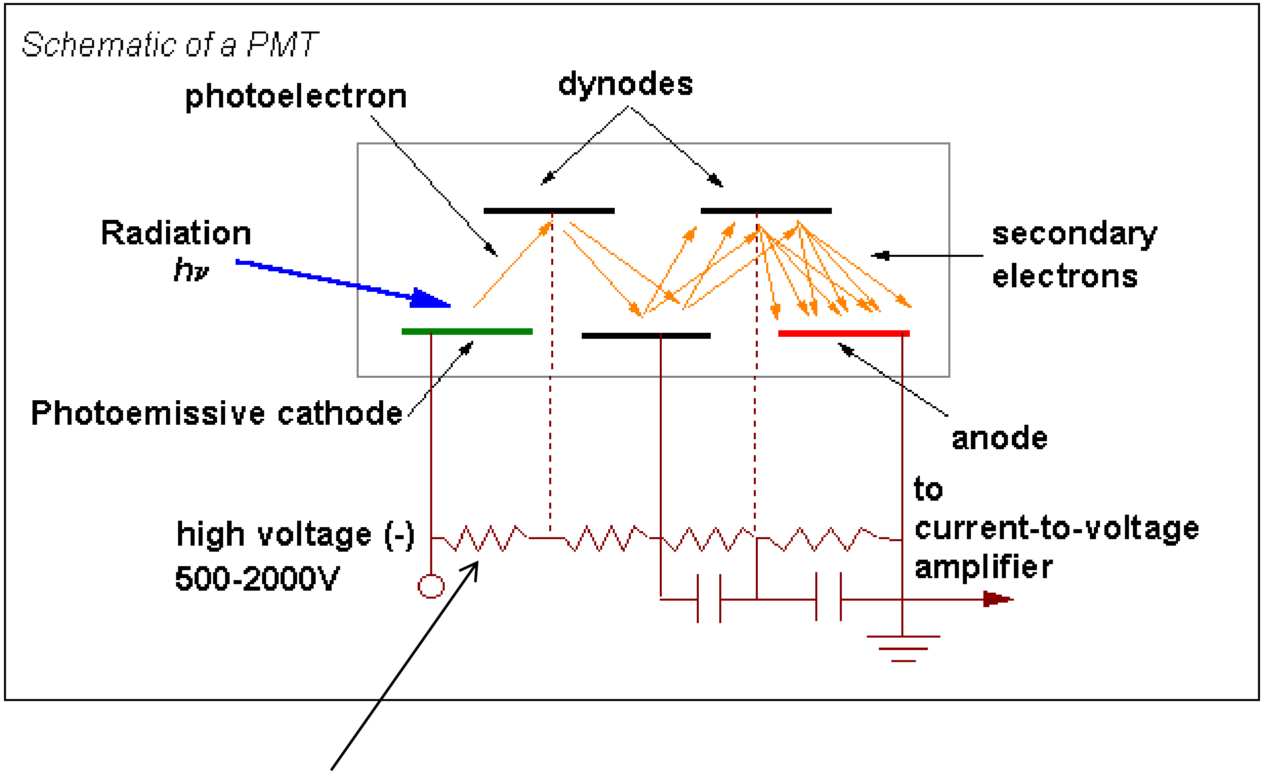

Resistor-divider pmt base

PMT – Photocathodes and windows

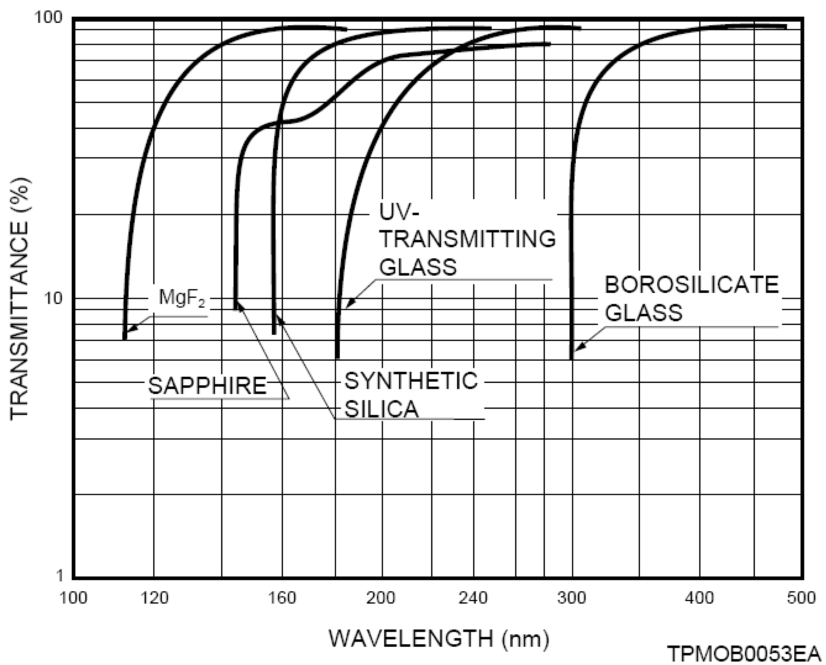

Figure 3-3: Spectral transmittance of window materials

Transmission for types of phototube window

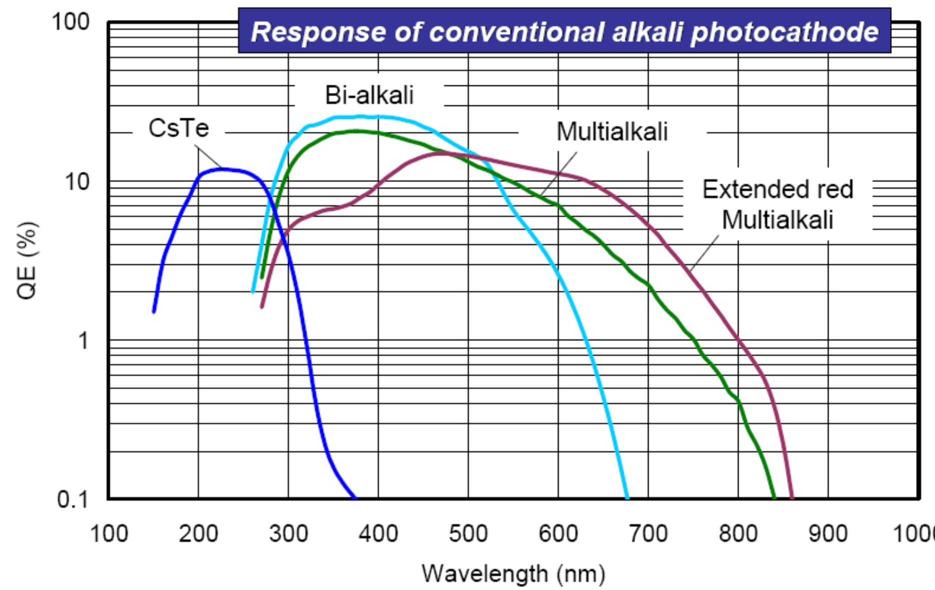

Quantum Efficiency for various types of photocathode material

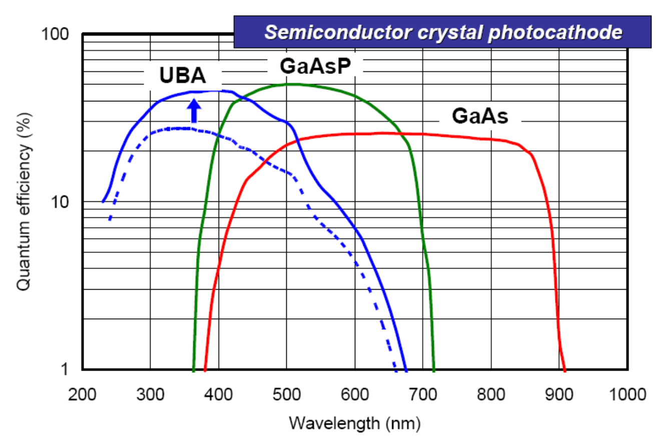

Photomultiplier – secondary emission

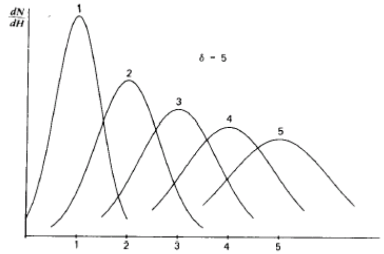

δ = 5

High emission dynodes allow resolution of single photoelectrons

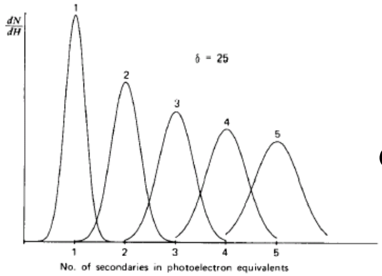

δ = 25

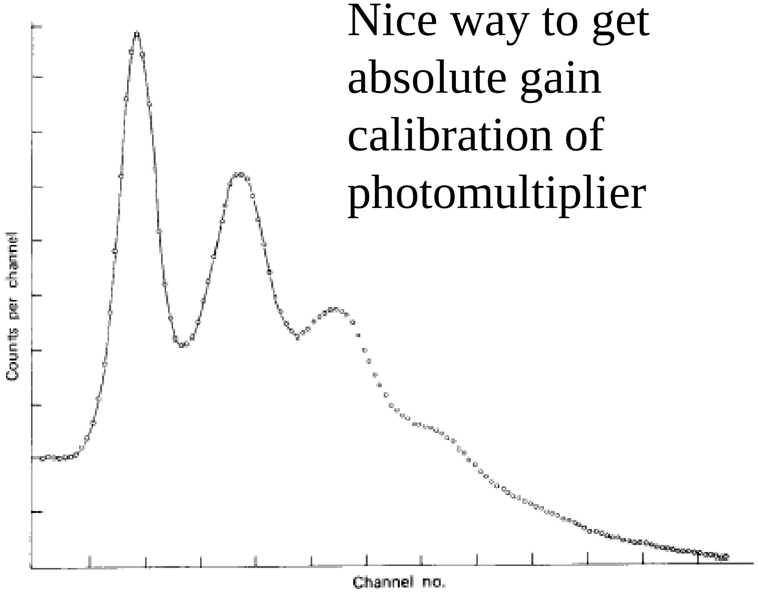

Nice way to get absolute gain calibration of photomultiplier

Secondary emission coefficients of commonly used dynode materials vs. incident electron energy:

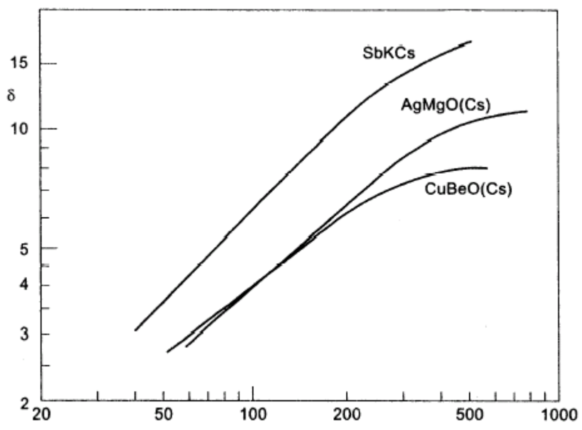

JF Primorsko June 2012

Specialty PMTs

Solar blind small metal package PMT

The R9875U is a small metal package PMT, whose Cs-Te photocathode features excellent solar blind characteristics. This new tube offers high sensitivity in the VUV region, whilst also having a high resistance to shock and vibration. This makes the R9875U ideal for more demanding applications.

Features
- Excellent solar blind characteristics
- High shock and vibration resistance
- High VUV sensitivity
- Small form factor

Applications
- Fire detection
- UV-LIDAR

Specifications
- Spectral range 160 nm to 320 nm
- Low dark current of 10 pA
- High gain of 3.7 x 10^5

Author: Richard Harvey, Hamamatsu Photonics UK

Spectral response

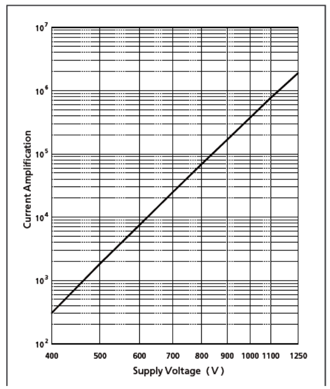

8 x 8 multianode PMTs featuring super bialkali photocathode technology

Hamamatsu Photonics are pleased to introduce the latest product in their successful multianode PMT range. The H10966A-100 and H10966B-100 have a high effective area ratio allowing them to cover a wide area by placing multiple detectors side by side. Coupled with their high quantum efficiency of 35% at 420 nm these detectors are ideal for large area scintillation work.

For ease the H10966A-100 comes with high voltage cable assembly attached for integration into systems.

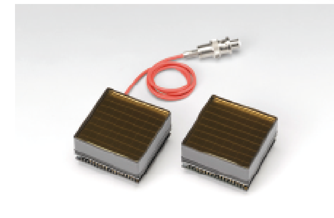

Features
- High QE – up to 35% at peak
- 64 pixels
- Small dead space
- Fast time response

Applications
- High resolution PET
- Gamma camera
- 2-D radiation monitor

Specifications
- 8 x 8 multianode PMT
- 52 mm square
- Spectral range of 300 to 650 nm
- Gain of 3.2 x 10^5

Author: Robin Smith, Hamamatsu Photonics UK

Spectral response

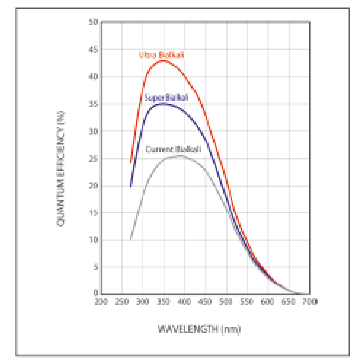

+/- of PMTs

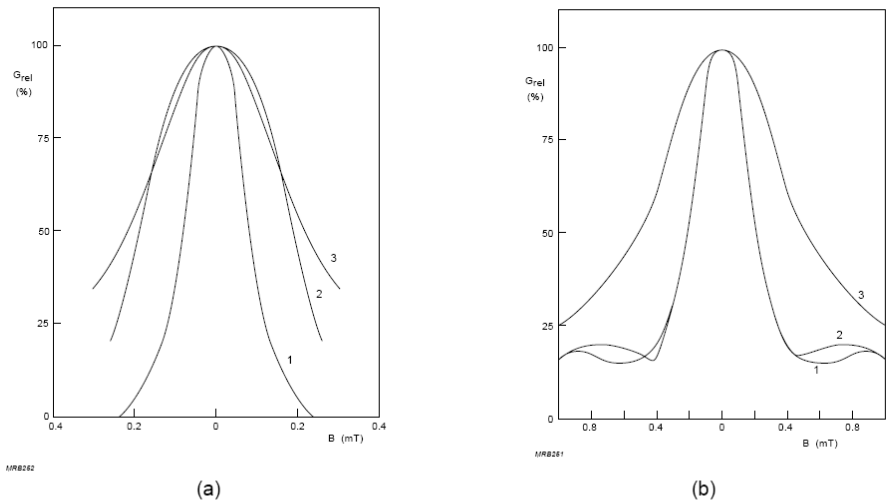

Fig.4.36 Relative gain variation as a function of magnetic field: (a) for a tube with linear focusing dynodes, (b) for a tube with venetian-blind dynodes.
curve 1: field aligned with y-axis (Fig.4.35)
curve 2: field aligned with x-axis
curve 3: field aligned with z-axis

Severe magnetic field gain dependence

Positives

•Large photocathode area possible
•Radiation Hard
•Small temperature dependence
•High Gain (1E5 – 1E7)

Negatives

•High Voltage 1K +
•Large volume
•Magnetic field sensitivity
•Expense (up to $1K per channel)

CDF Time of Flight Counters

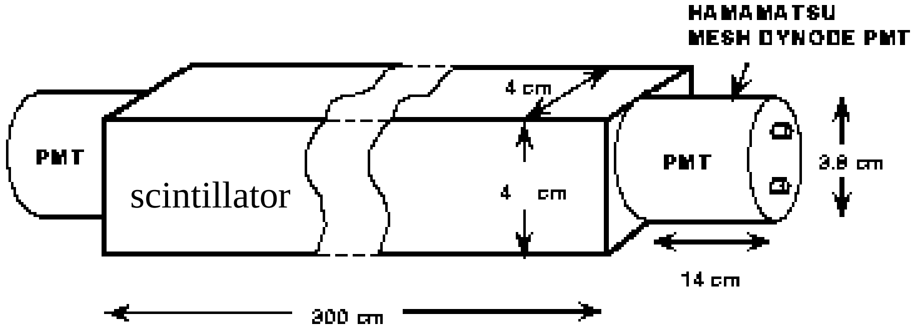

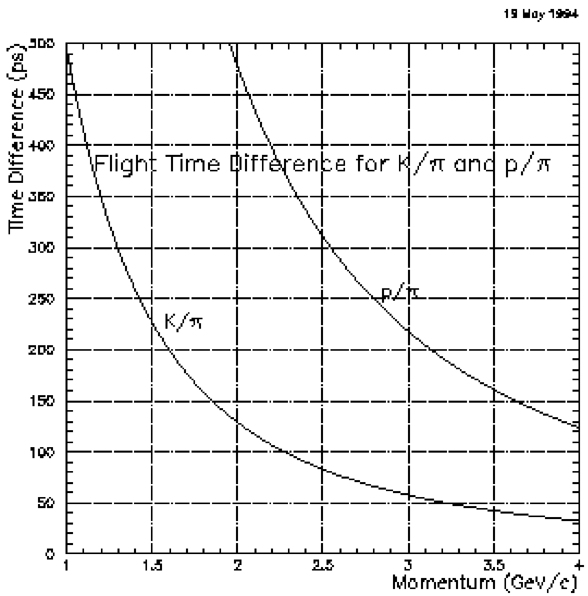

Figure 1: Flight time difference at a radius of 1.4 m (CDT location) versus momentum for π/K and π/p.

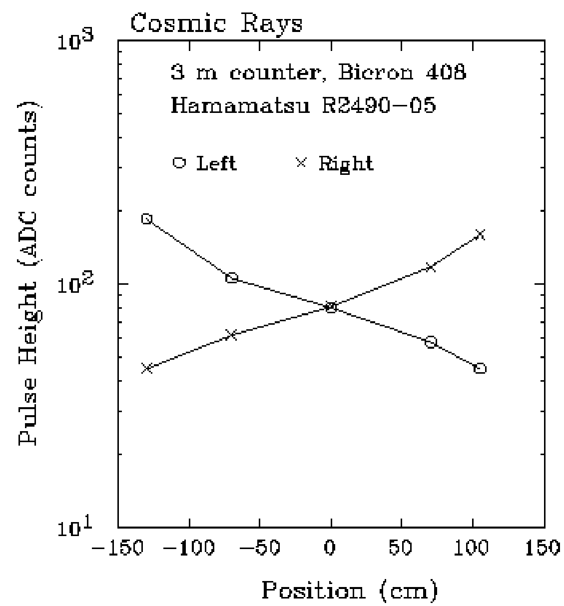

Cosmic ray test. Pulse ht vs position

Note: speed of light in scint ~ 20cm/ns

Discriminators and Time Walk

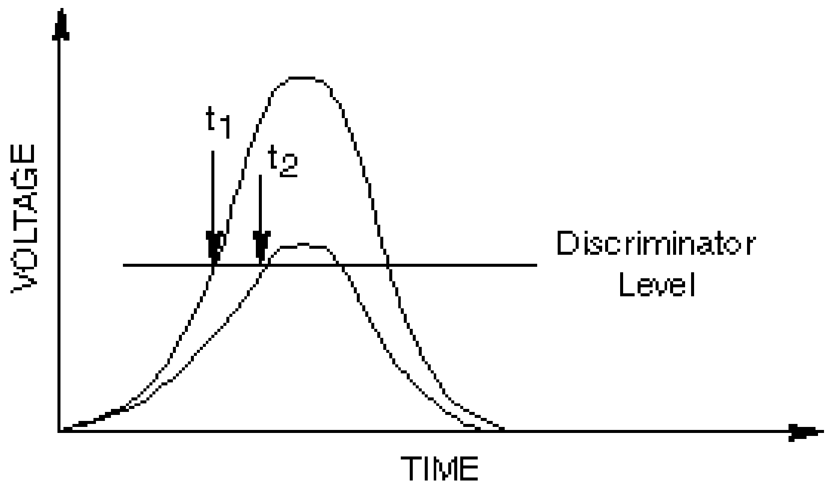

Leading Edge Timing

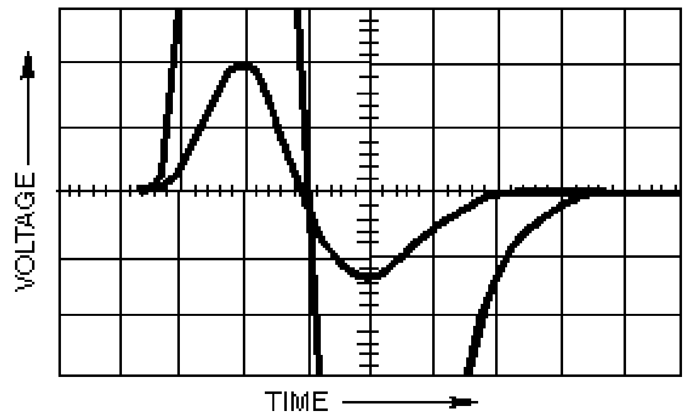

Phototube pulse showing amplitude variation (position, …)

Differentiated signal shows very little shift of zero-crossing time vs amplitude

→ zero-crossing discriminator

Scintillation Counter Problem

Some typical parameters for a plastic scintillation counter are:

energy loss in plastic scintillator:	2MeV/cm
scintillation efficiency of plastic:	1 photon/100 eV
collection efficiency (# photons reaching PMT):	0.1
quantum efficiency of PMT	0.25
gain of phototube	10**6
Pulse length	50 ns

What electrical signal do we get (into 50 ohms) for minimum ionizing particle going through 1 cm thick scintillator counter?

Poisson probability to get n for mean <n> is

$$P(n) = \frac{<n>^n \, e^{-<n>}}{n!}$$

What is probability our counter got zero photoelectrons?

Silicon Track Detector (CMS tracker)

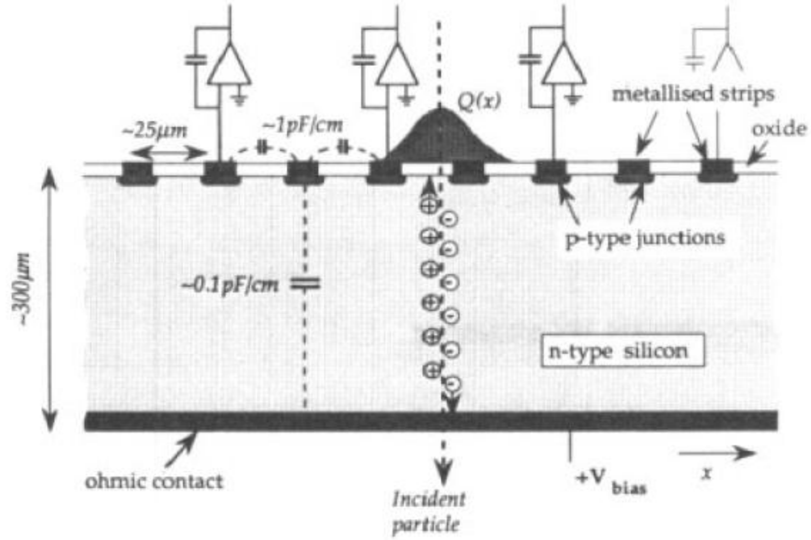

Reverse-biased pn diode.
Gain=1, signal ~ 1000e
Strip pitch ~ 100 microns
Strips 10 – 20 cm long

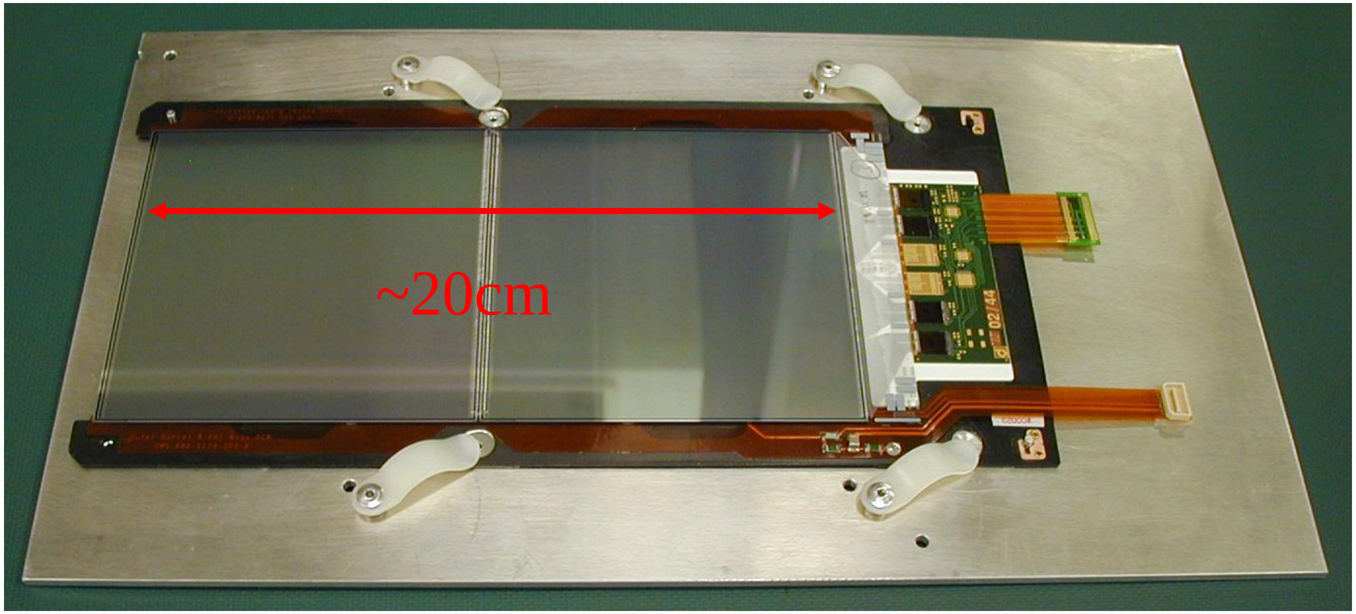

CMS - All Si tracking

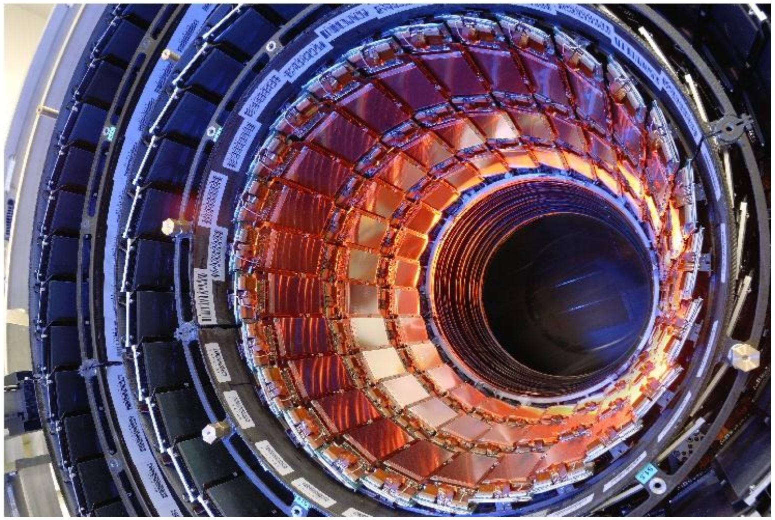

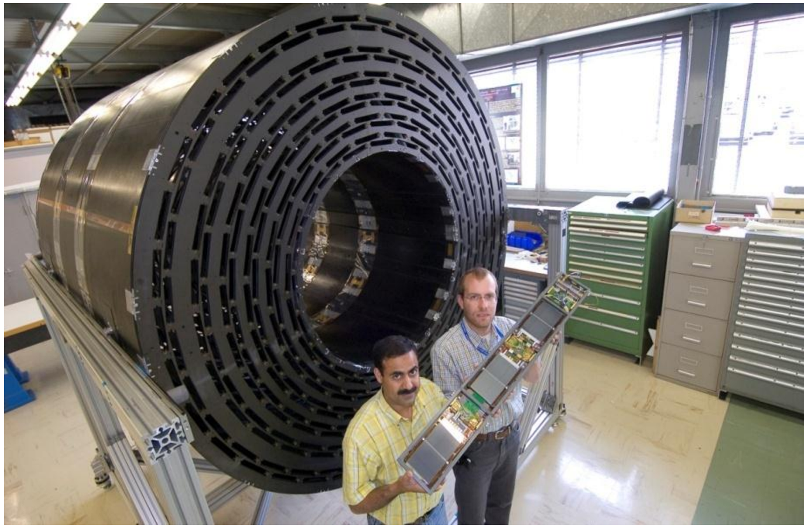

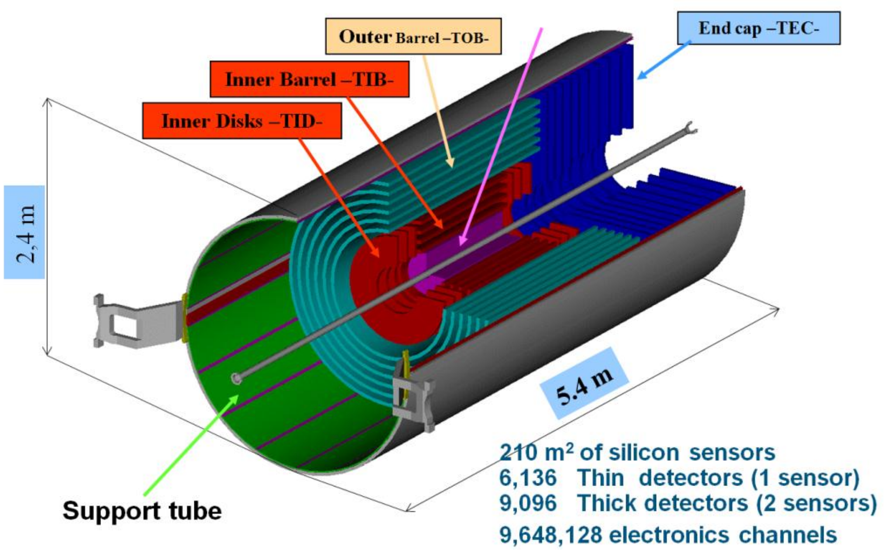

Pixel detector – Same operation as strips

- bump-bonded sensor/readout chip sandwich

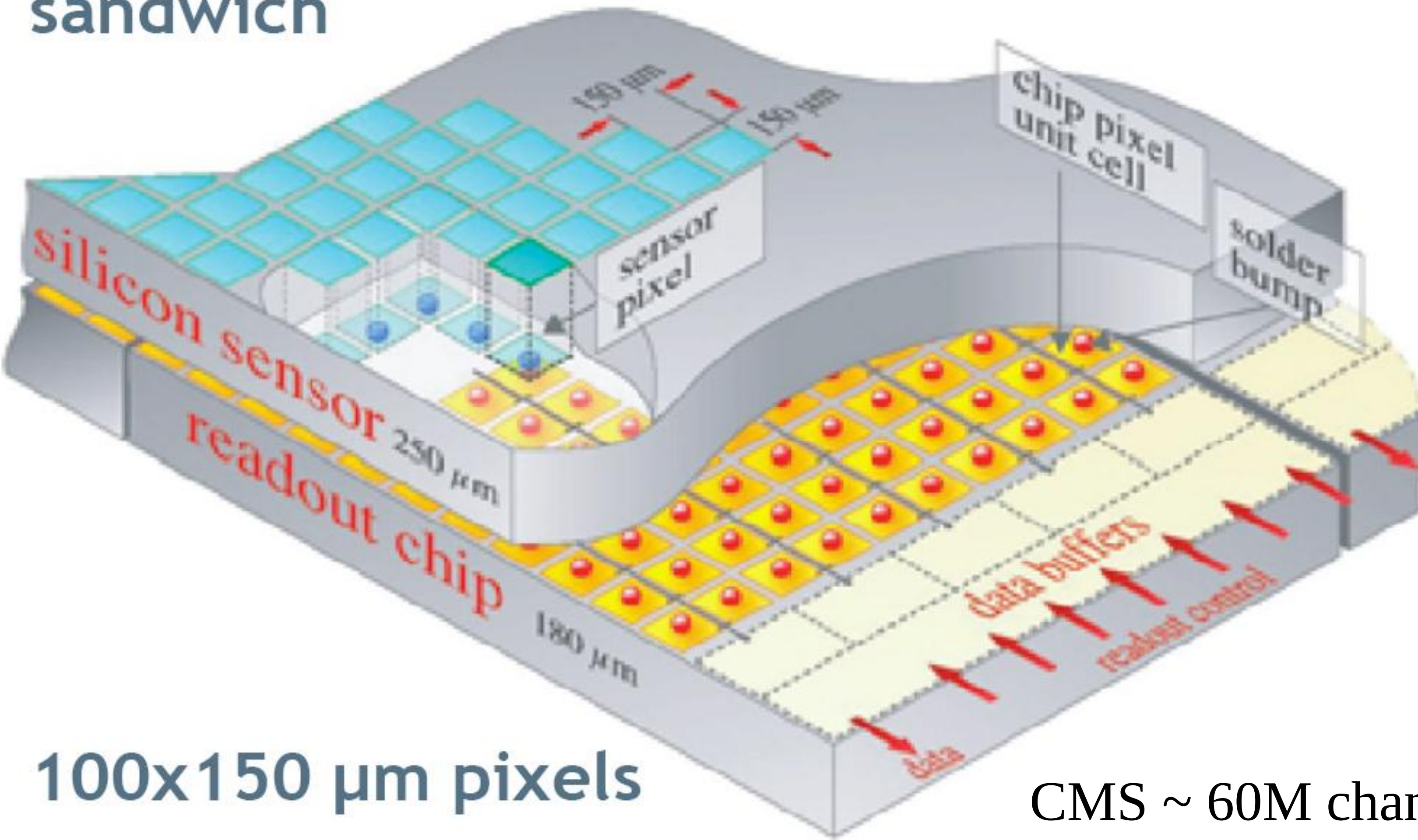

- 100x150 μm pixels

CMS ~ 60M channels

Photodiode: PN junction reverse biased

Photodiode

QE up to 80% +

Gain = 1

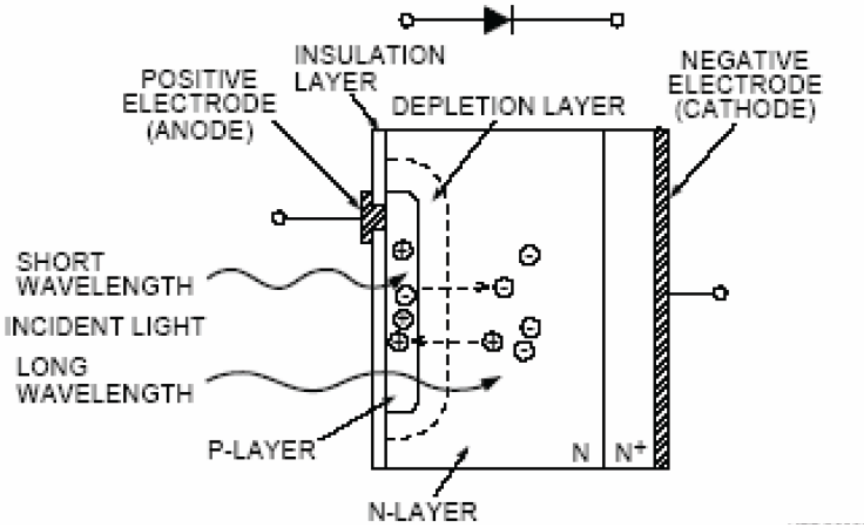

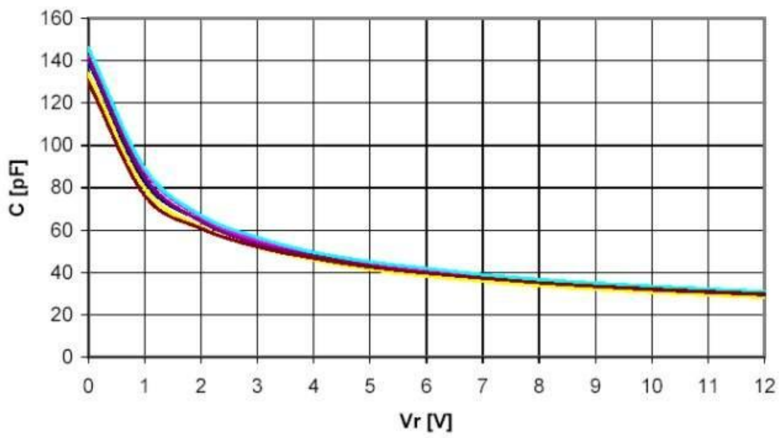

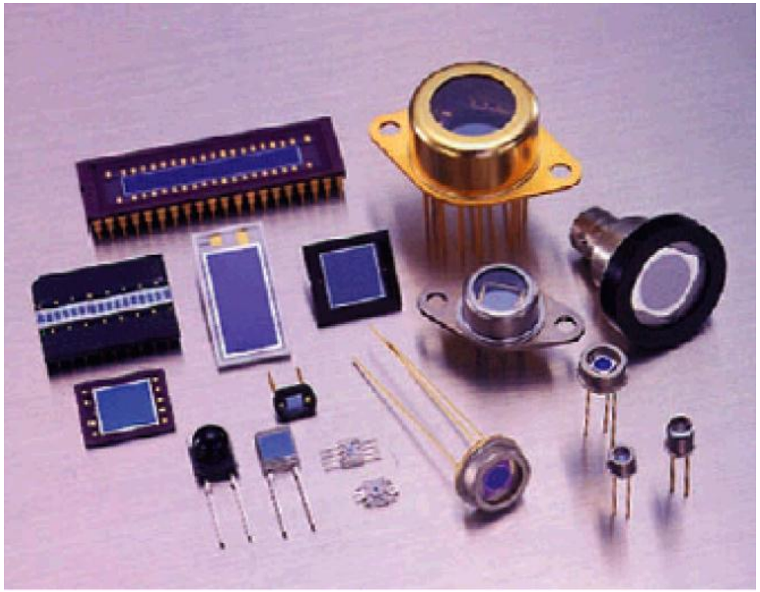

Solid State Photodetector: APD

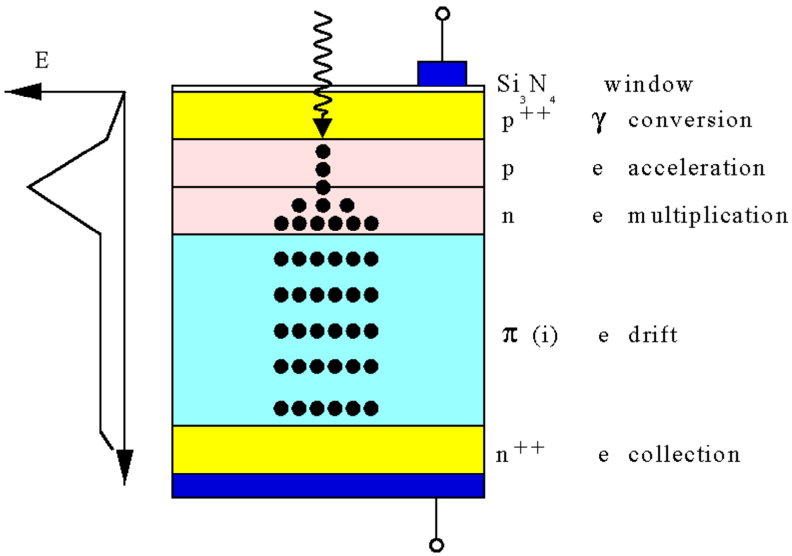

Avalanche photodiodes are photodiodes with built-in high electric field region. With increasing reverse bias voltage, electrons (or holes) are accelerated and can create additional electron-hole pairs through impact ionization → gain.

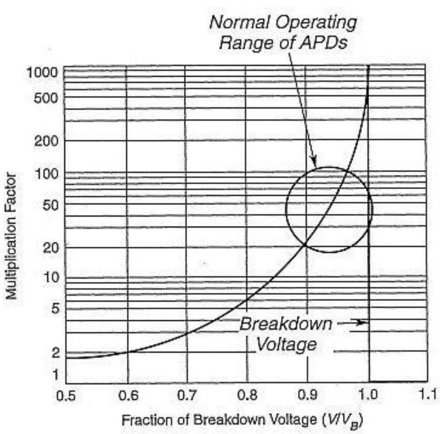

Two 5× 5 mm² APD's/crystal.
Gain – 50.
QE – 80% @ 420 nm.
Temp sensitivity – -2.4%/ °C.

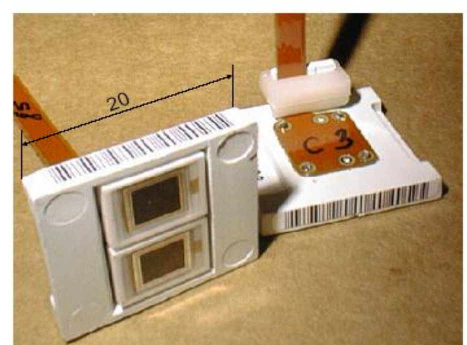

Note: If you reverse bias high enough voltage, avalanche causes geiger breakdown

Silicon Photomultipliers (SIPMs)

Array of Gieger-mode APDs (quench protected) connected to a single output:

Signal = Σ of cells fired

If probability to hit a single cell < 1 => Signal proportional to # photons

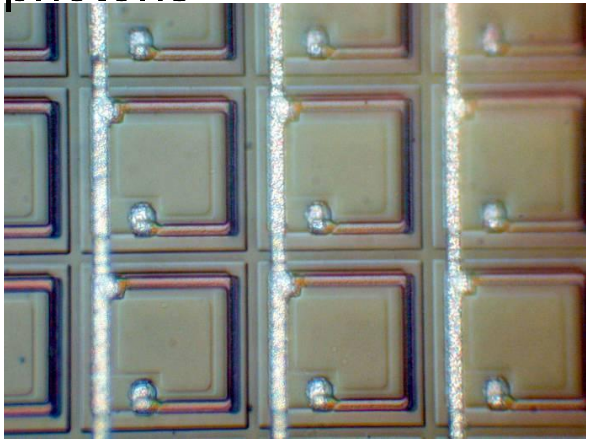

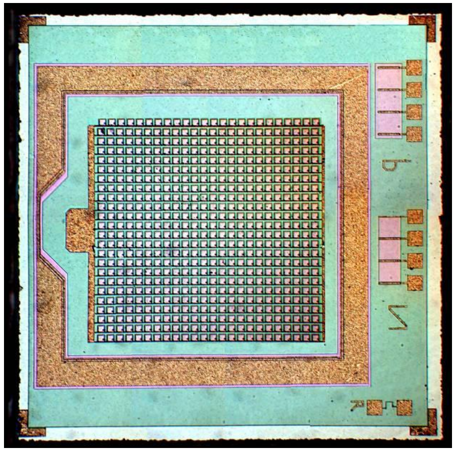

Pixel size:
~10 x 10 μm^2 to ~100 x 100 μm^2

Array size:
0.5 x 0.5 mm^2 to 5 x 5 mm^2

SIPMs (the wave of the future)

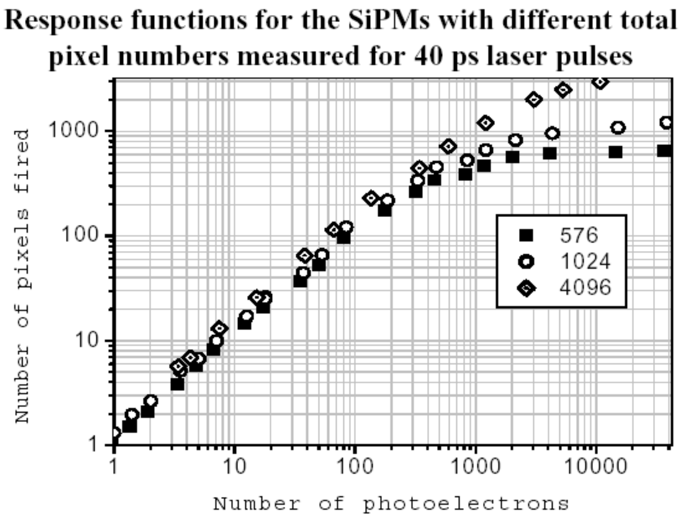

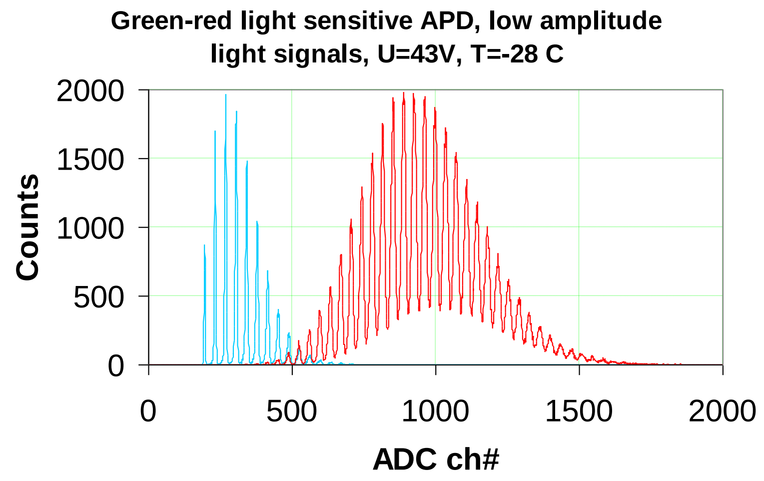

$$N_{firedcells} = N_{total} \cdot \left(1 - e^{-\frac{N_{photon} \cdot PDE}{N_{total}}}\right)$$

SIPM Features

- Photon-counting
- Gain 1E5 – 1E6
- Dynamic range limited by # pixels
- Large temp dependence
- Radiation damage → increase leakage current

HPD – proximity focussed CMS

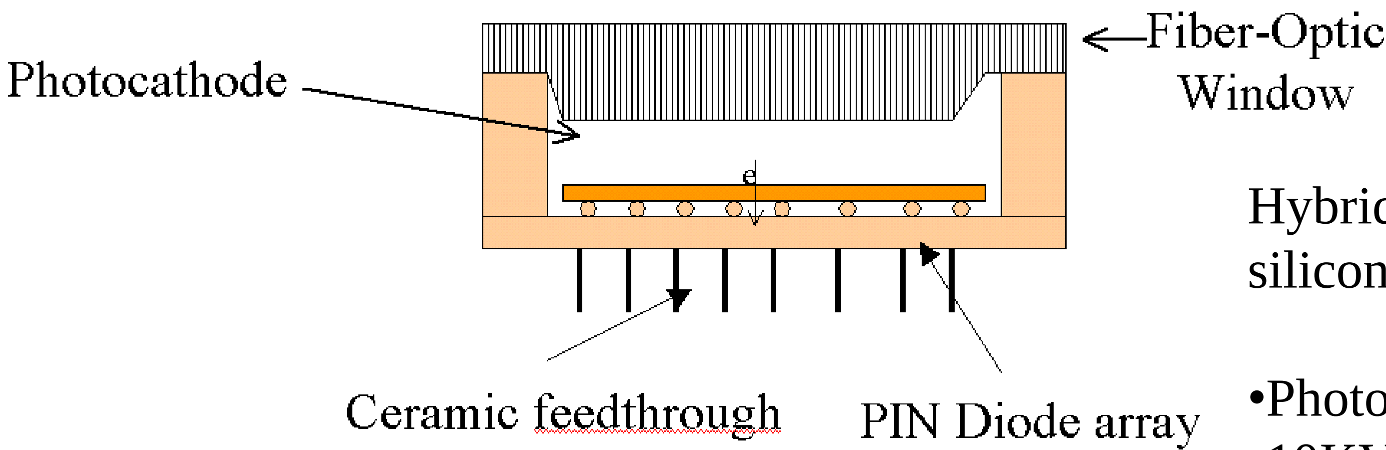

Hybrid between pmt and silicon detector.

- Photocathode → pe
- 10KV accelerates pe
- 3MV/meter E field
- Impact on silicon → gain of 2000
- Can be pixelated
- Can operate in high B field

Diode Structure

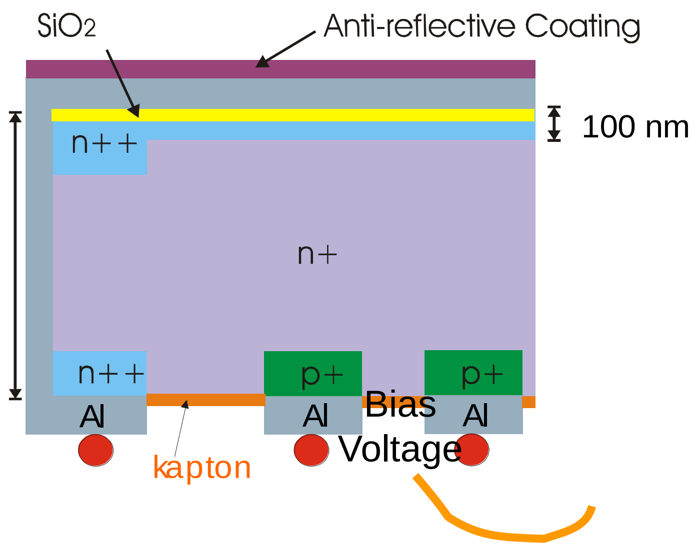

HPD Electrostatic focussed LHCb

- HPDs developed for the LHCb RICH
- 80 mm diameter tube has 1024 pixels
  each ~ 2.5×2.5 mm² at the photocathode
  Uses a silicon sensor with 32×32 pixel array, bump-bonded to a readout chip which can read out the signals fast enough for the LHC (25 ns)

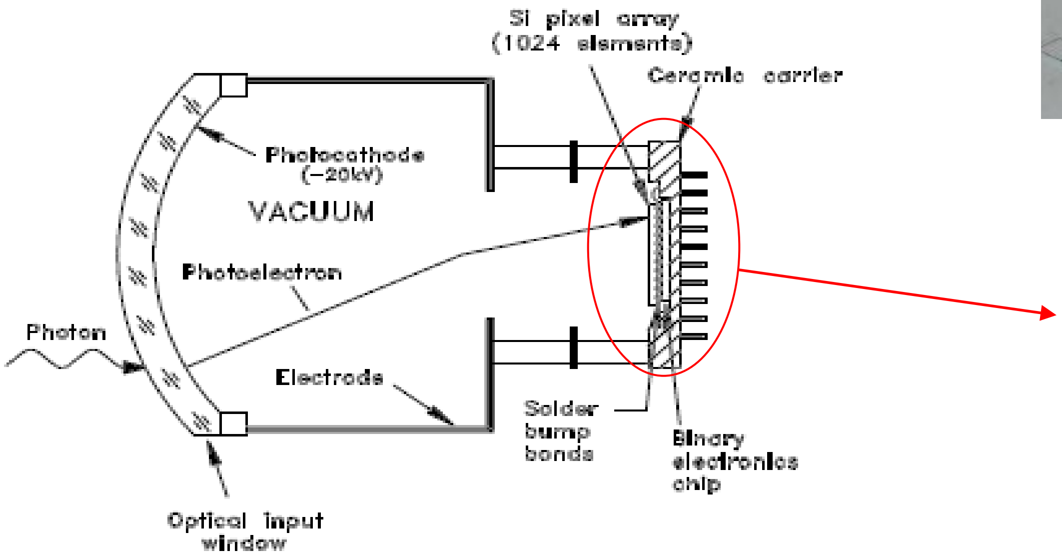

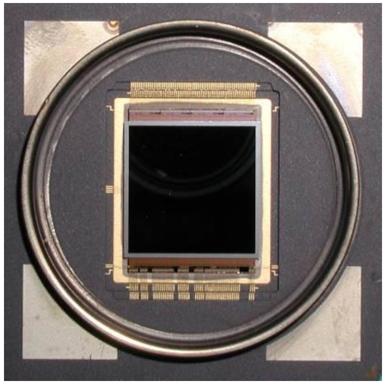

Wire Chamber

A wire chamber is a gas tight container with a wire inside.

The gas is the medium that gets ionized by a passing charged particle.

The wire helps define an electric field and “collects” ionization.

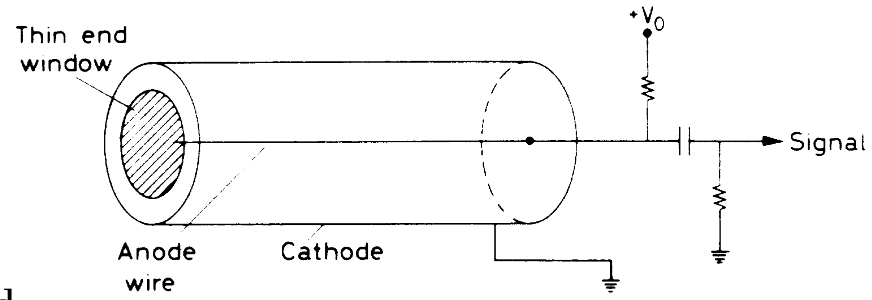

Typical cylindrical wire chamber has:

a wire (anode) held at +V

outside of cylinder (cathode) held at ground

Charged particle passing through cylinder creates ions

movement of ions creates a voltage or current pulse

signal pulse travels down wire to “outside world”

usually to preamplifier

Location of charged particle is measured relative to wire

Drift Chambers

CDF Central tracker
drift chamber

“open” low mass geometry. Cathode formed by field shaping wires

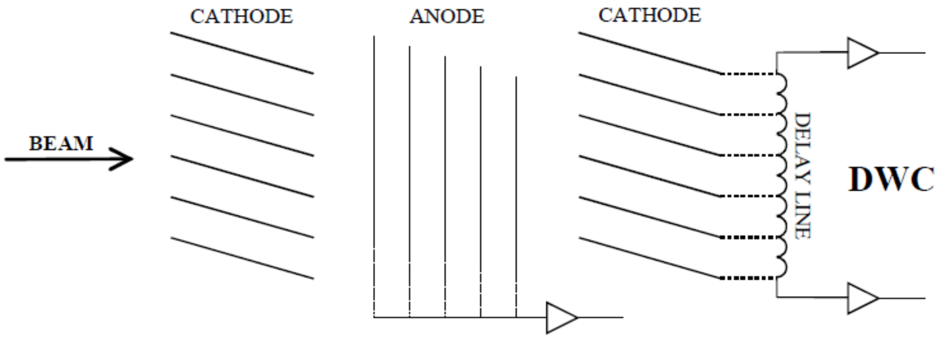

CERN standard
testbeam wire chamber

Cerenkov Effect

- From Relativity, nothing can go faster than the speed of light *c* (in vacuum)
- However, due to the refractive index *n* of a material, a particle *can* go faster than the *local* speed of light in the medium $c_p = c/n$
- Analogous to sonic shock wave when airplane travels faster than speed of sound in medium

Cerenkov Effect

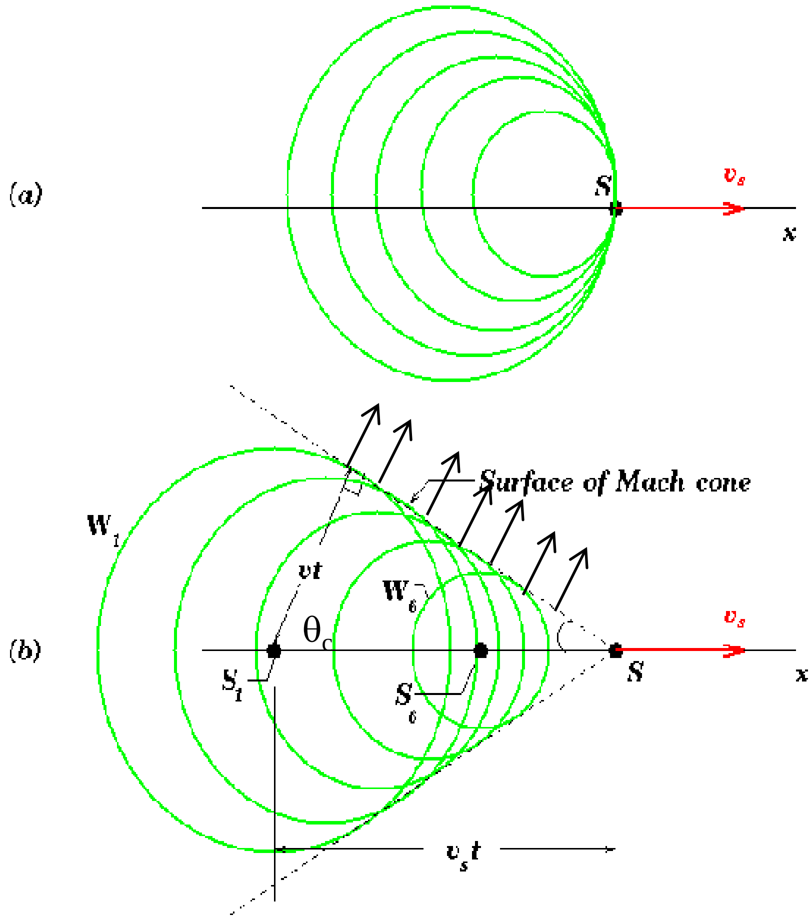

Cerenkov effect same as supersonic shockwave. When particle moves at speed faster than speed of light in medium (1/n), generates Cerenkov radiation. Characteristic angle

$\cos\theta_c = 1/\beta n$ for $\beta > 1/n$

Threshold Cerenkov Counters

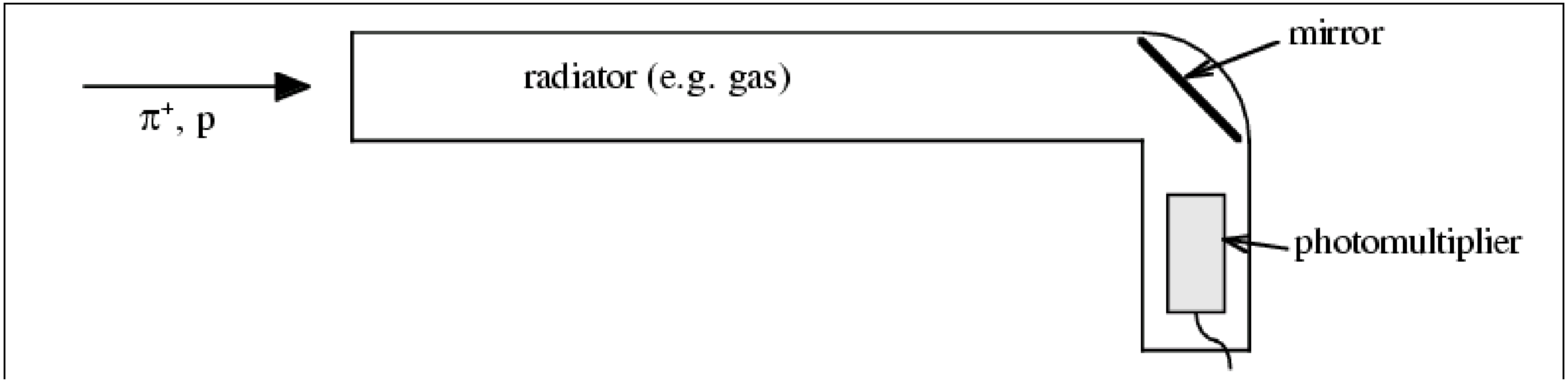

$$(n-1) = (n_0 - 1) \cdot \frac{P}{P_0}$$

Approximation of Lorentz – Lorenz Law

$(n^2 - 1)/(n^2 + 2) = (R/M)\rho$

Refractive indices vary in the range of 1 to 2.

Material	n	γ_{Th}
glass	1.46 to 1.75	1.22 to 1.37
scintillator	1.4 to 1.6	1.3 to 1.4
water	1.33	1.52
silica aerogel	$1 + (2 \text{ to } 10 \times 10^{-2})$	2 to 5
pentane (at S.T.P.)	$1 + 1.7 \times 10^{-3}$	17
carbon dioxide (at S.T.P.)	$1 + 4.3 \times 10^{-4}$	34
helium	$1 + 3.3 \times 10^{-5}$	123

Aerogel Cerenkov Radiator

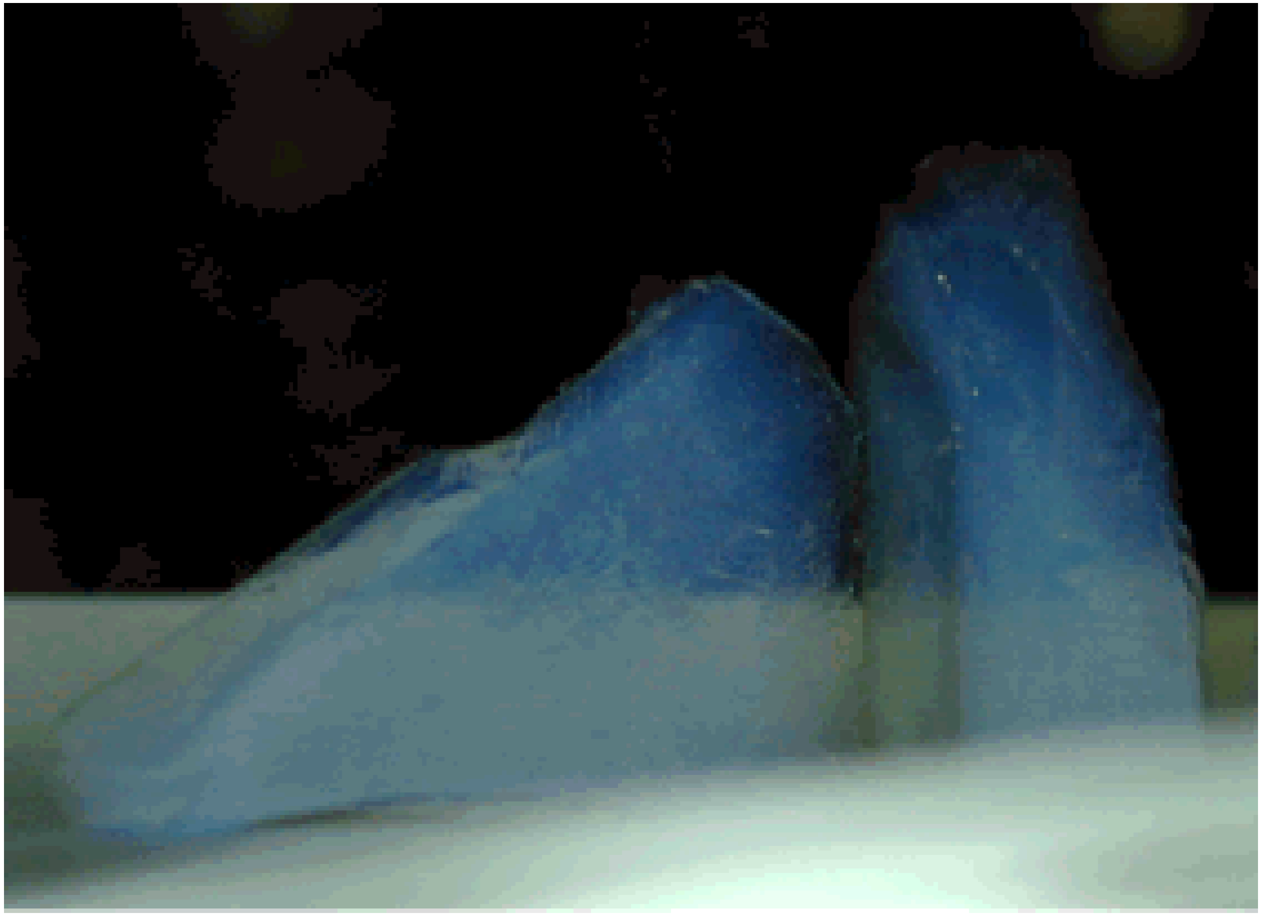

Aerogel is solid silica gel. Densities from 0.003 to 0.35 g/cc.

Index of refraction n from 1.00063 to 1.14

Threshold Cerenkov Counters

Cerenkov radiator gas (~10 meters long)

Mylar or Foil Window

Gas Pressure Control

Photomultiplier

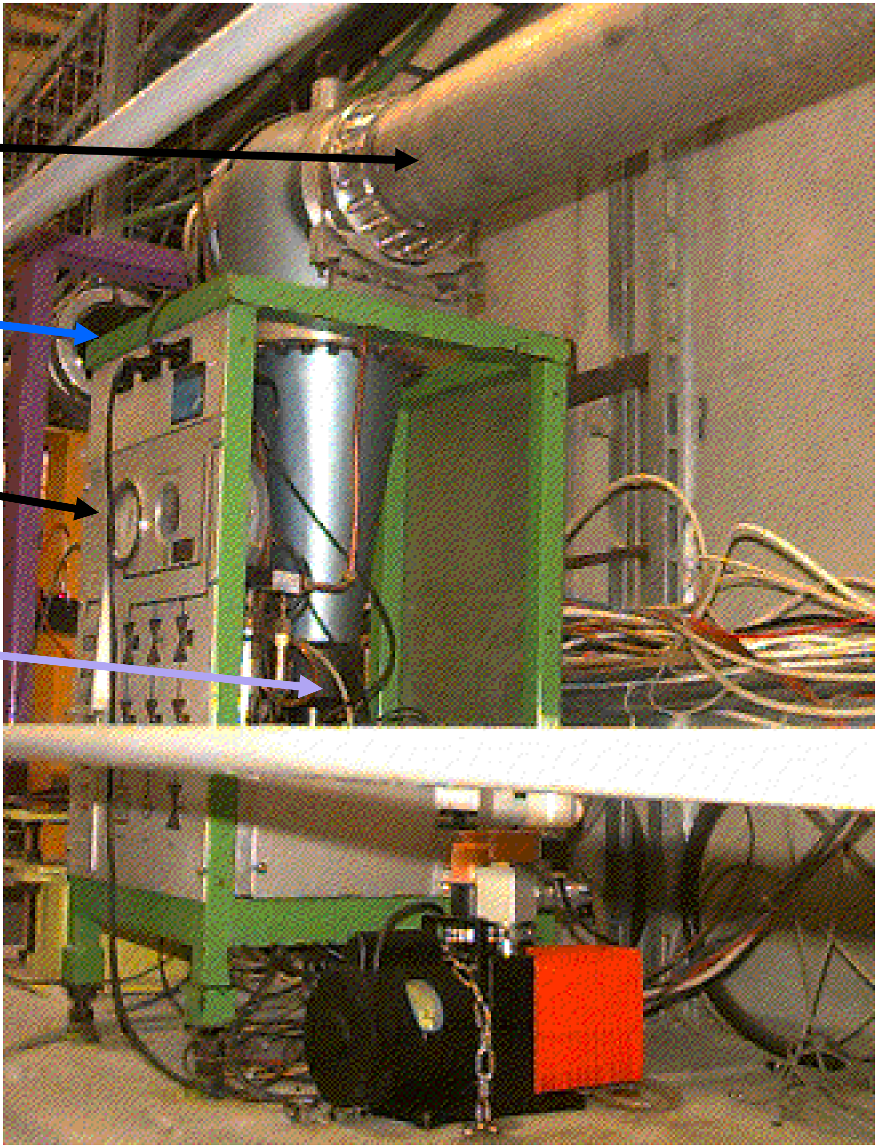

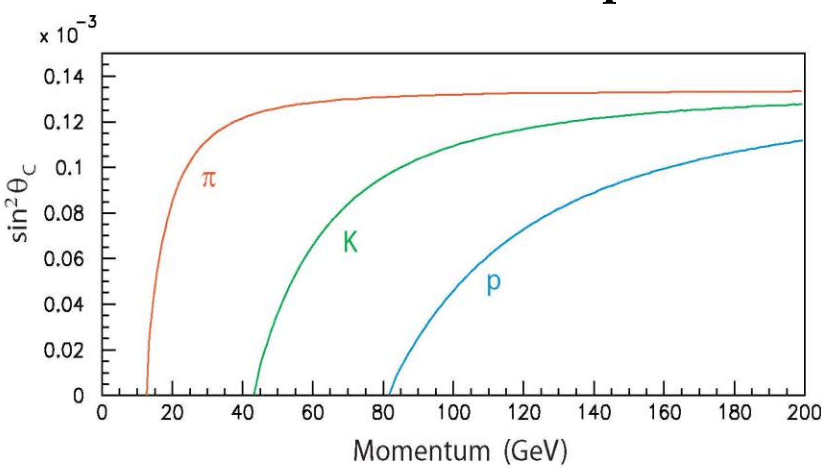

Threshold Cerenkov

π/k separation as a function the particle momentum.

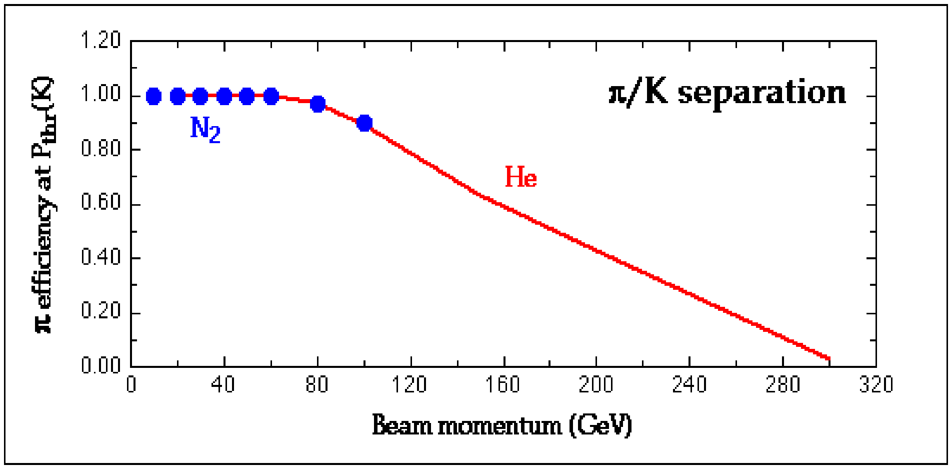

For counter with A = 100, L = 10 meters

$$n = 1 + k \frac{\rho}{\rho_{ref}}$$

Index of refraction for gas vs density

ß = v/c = p/E ~ 1 - $M^2/(2*p^2)$

In a gas with pressure P, the light velocity is given by v = c/n, where n is the refractive index.

n is a function of the pressure of the gas. For a given threshold pressure Pth, p/E = c/n(Pth). This threshold pressure is given by

$$Pth = (1/2k) * M^2/p^2$$

With k the gas constant

- **k = 3.22 10^{-5} for Helium,**
- **k = 2.99 10^{-4} for Nitrogen.**

Cerenkov Efficiency

Photons are emitted at an angle

$Ø^2 = 2kP - M^2/p^2$

and the number of photoelectrons N emitted over a length L (in cm) is approximately

$N = A\,L\,Ø^2$

$N_{pe} = \dfrac{\alpha^2 L}{r_e m_e c^2} \int \varepsilon \sin^2 \theta_C \, dE$, where $\dfrac{\alpha^2}{r_e m_e c^2} = 370\ \mathrm{cm^{-1}eV^{-1}}$

with A depending on quantum efficiencies, inefficiencies of the optical system and so forth. Typical values of A are 100.

$N \sim 100\,L\,(2kP - M^2/p^2)$

The efficiency of the counter is then given by

$Eff = 1 - e^{-N}$

Threshold Cerenkov Problem

Recall $N = A L Ø^2$

Assume A = 100 and L = 10 meters. P beam = 50 GeV.

The counter is filled with nitrogen gas.

What is the threshold pressure for 50 GeV kaons?

What is the pion efficiency at this pressure?

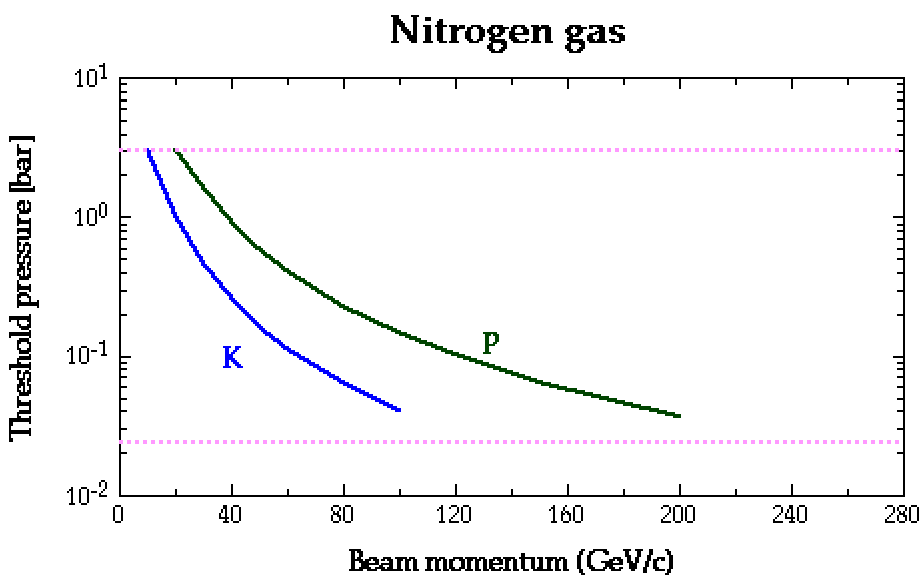

Differential Cerenkov Counter

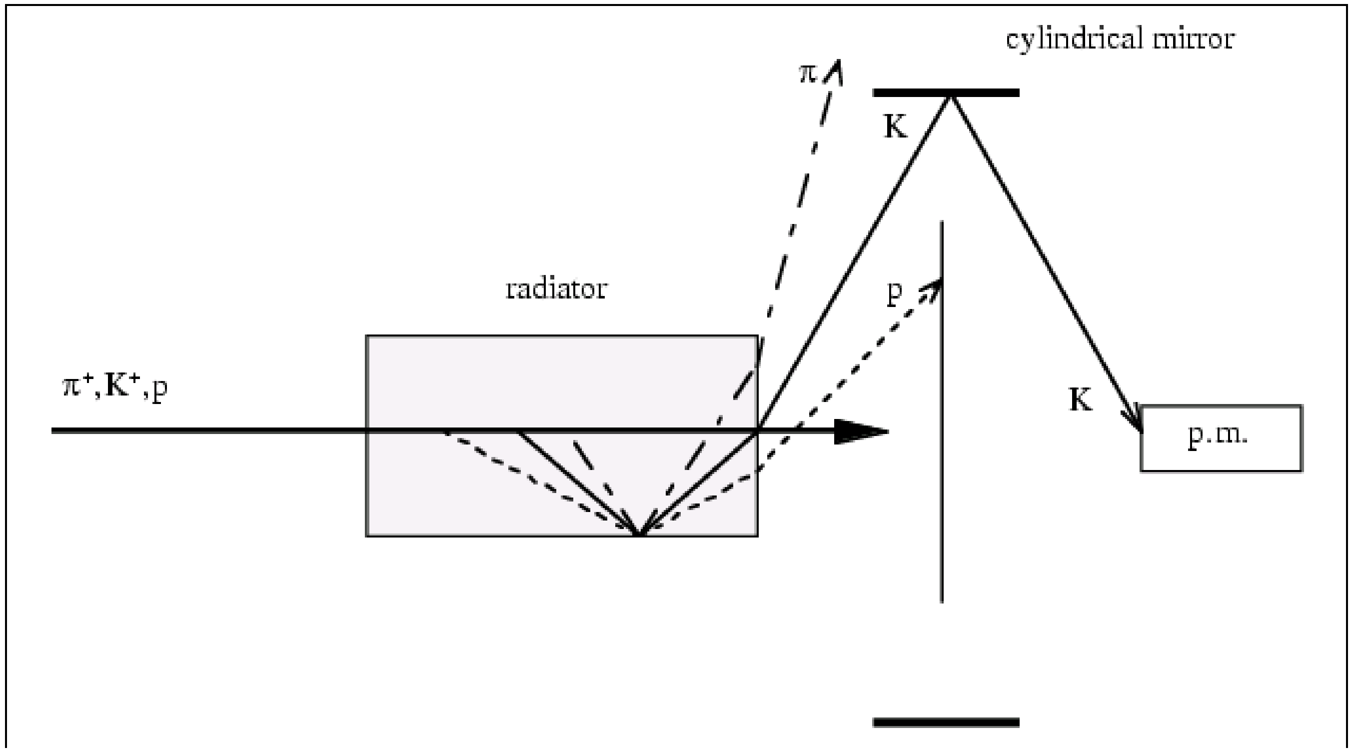

A Differential Cherenkov detector only gives a signal for particles with a certain range of β (corresponding, for a given momentum, to a given range in mass).

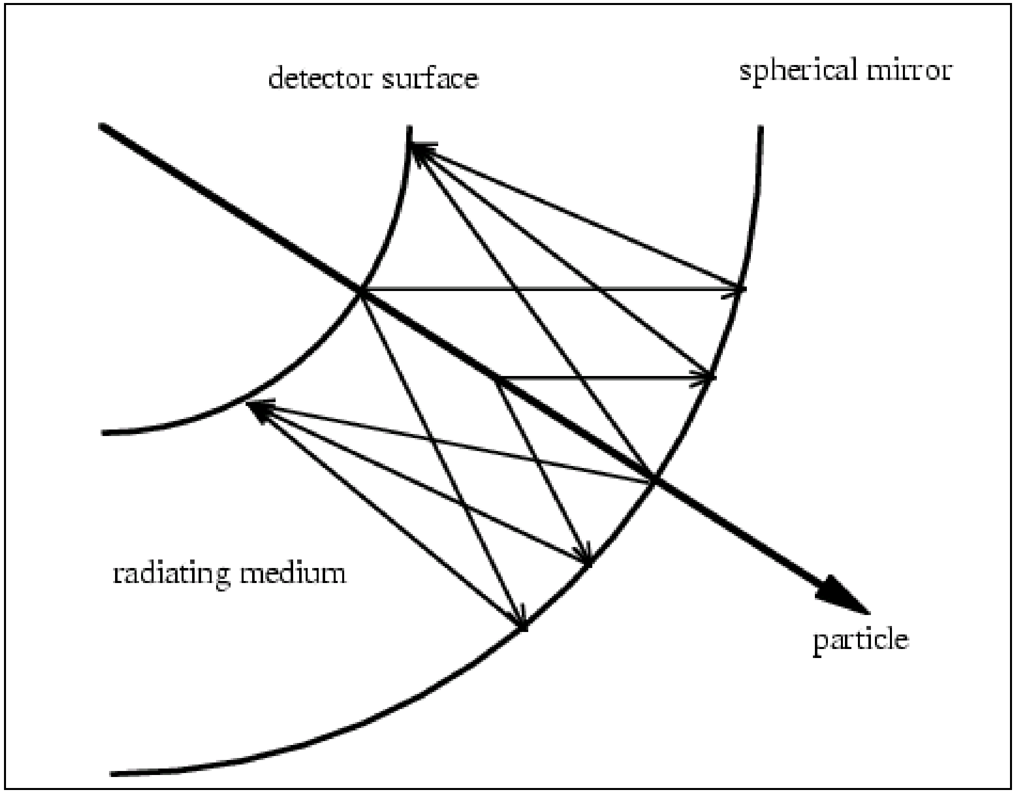

Cerenkov light emitted in cone with half-angle θ_c

RICH counters have optics designed to preserve angles of the photons, so measure β

Photon detector is often a multiwire proportional chamber with UV sensitive gas added (TMAE tetrakis dimethylamine ethylene; TEA triethylamine)

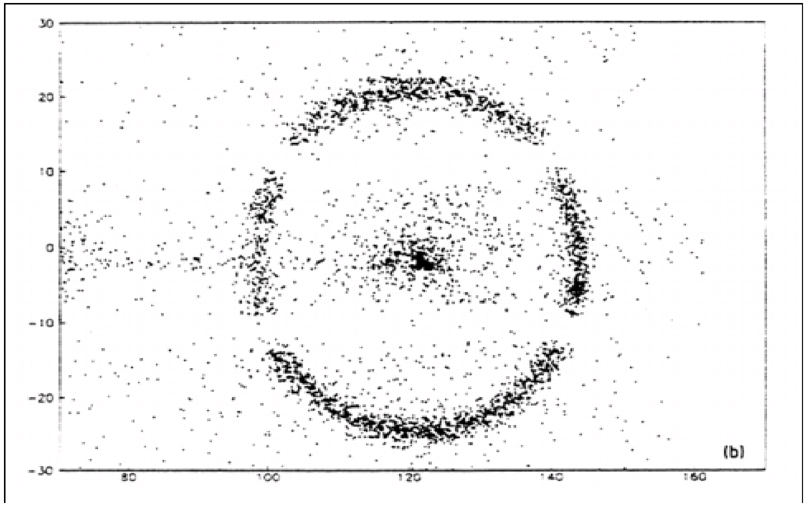

Test beam exposure of RICH to 10 GeV pions. Ring and direct ionization are seen. ~ 27 hits/pion. Gas chamber readout

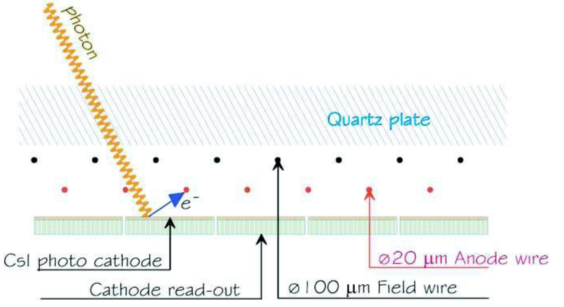

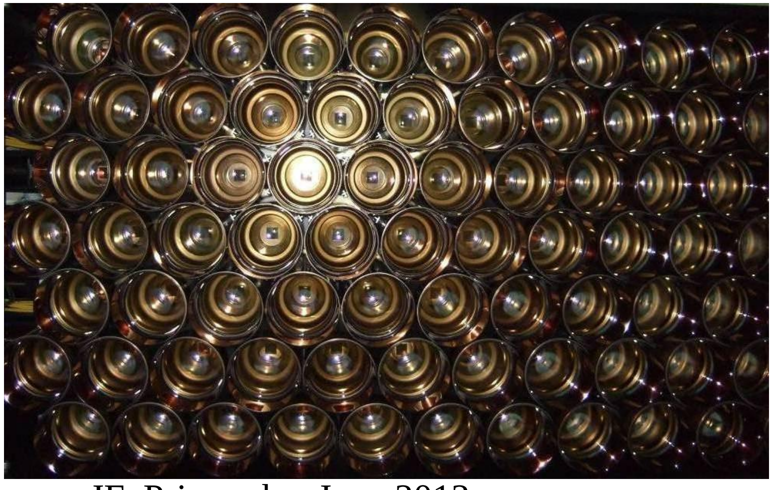

LHCB pixelated HPD readout

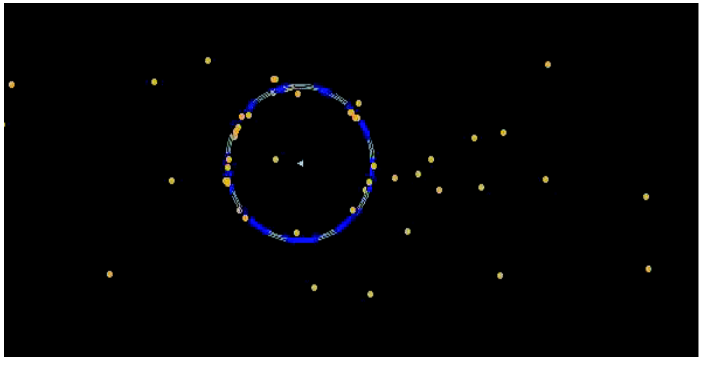

Antiproton production mechanism

$p\,p \rightarrow p\,\bar{p}\,p\,p$ with $\bar{p}$ = anti-proton

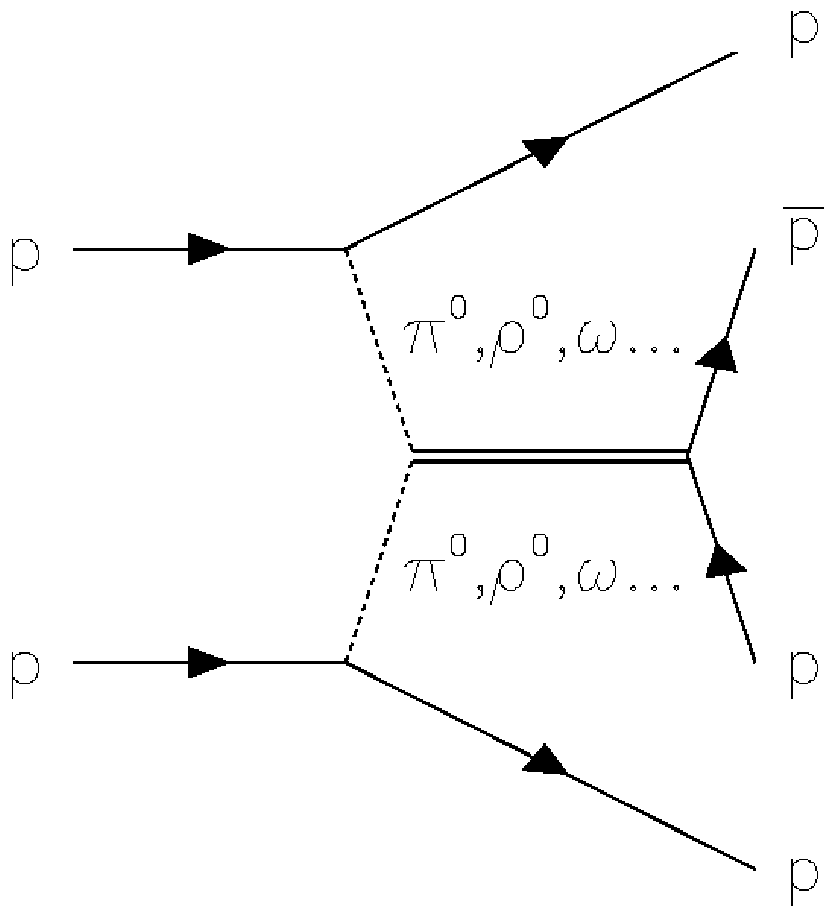

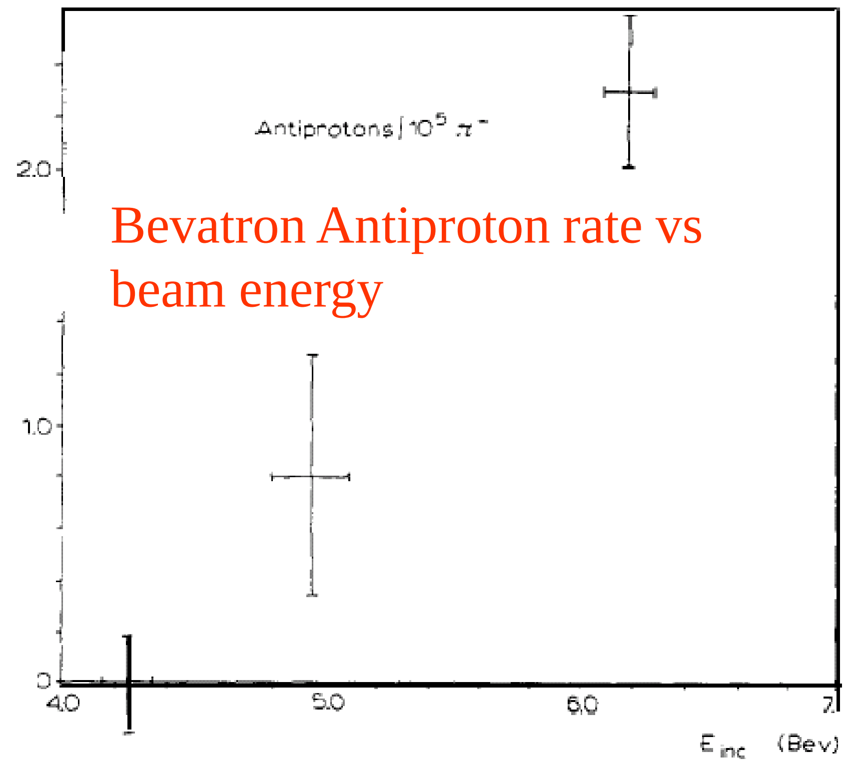

Bevatron Antiproton rate vs beam energy

$$(p_b+p_t)^2 = (E_b+m_p,\ \mathbf{p}_b)^2 = m_b^2+m_t^2+2m_tE_b = 2m_p^2+2m_pE_b = (4m_p)^2$$

$E_b = 7m_p = 6.6$ GeV

Chamberlain Discovery of Antiproton

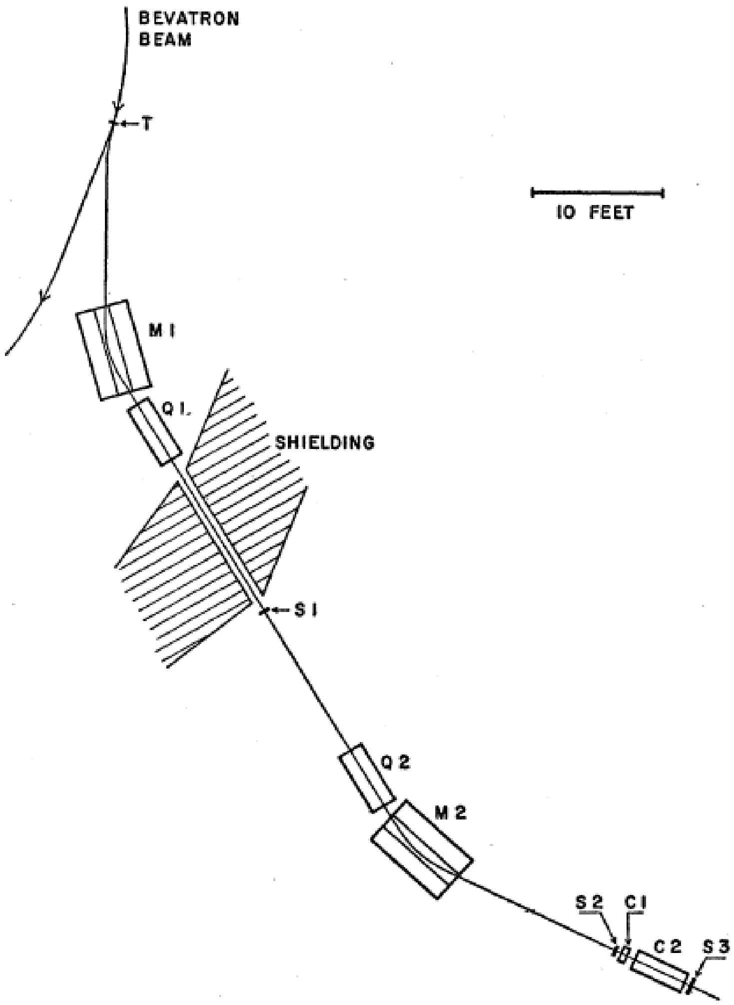

FIG. 1. Diagram of experimental arrangement. For details see Table I.

Bevatron protons energy = 6.2 GeV

Momentum selection to v/c = 0.78

C1 is veto cerenkov counter, set to have threshold at β = 0.78

C2 is differential cerenkov, 0.75< β <0.78

S1, S2 TOF counters separated by 40 ft.

Chamberlain Discovery of Antiproton

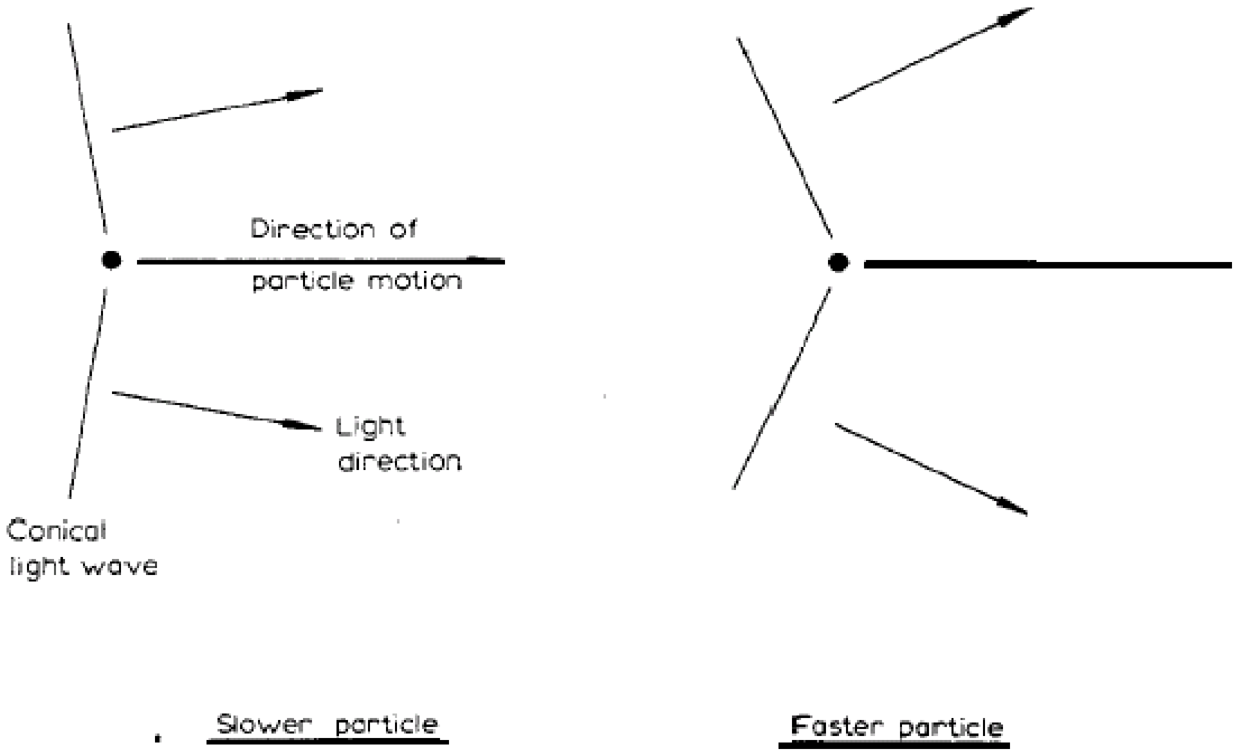

Fig. 5. Diagram of Čerenkov radiation. The angle of emission of Čerenkov light depends on the speed of the charged particle.

Chamberlain Discovery of Antiproton

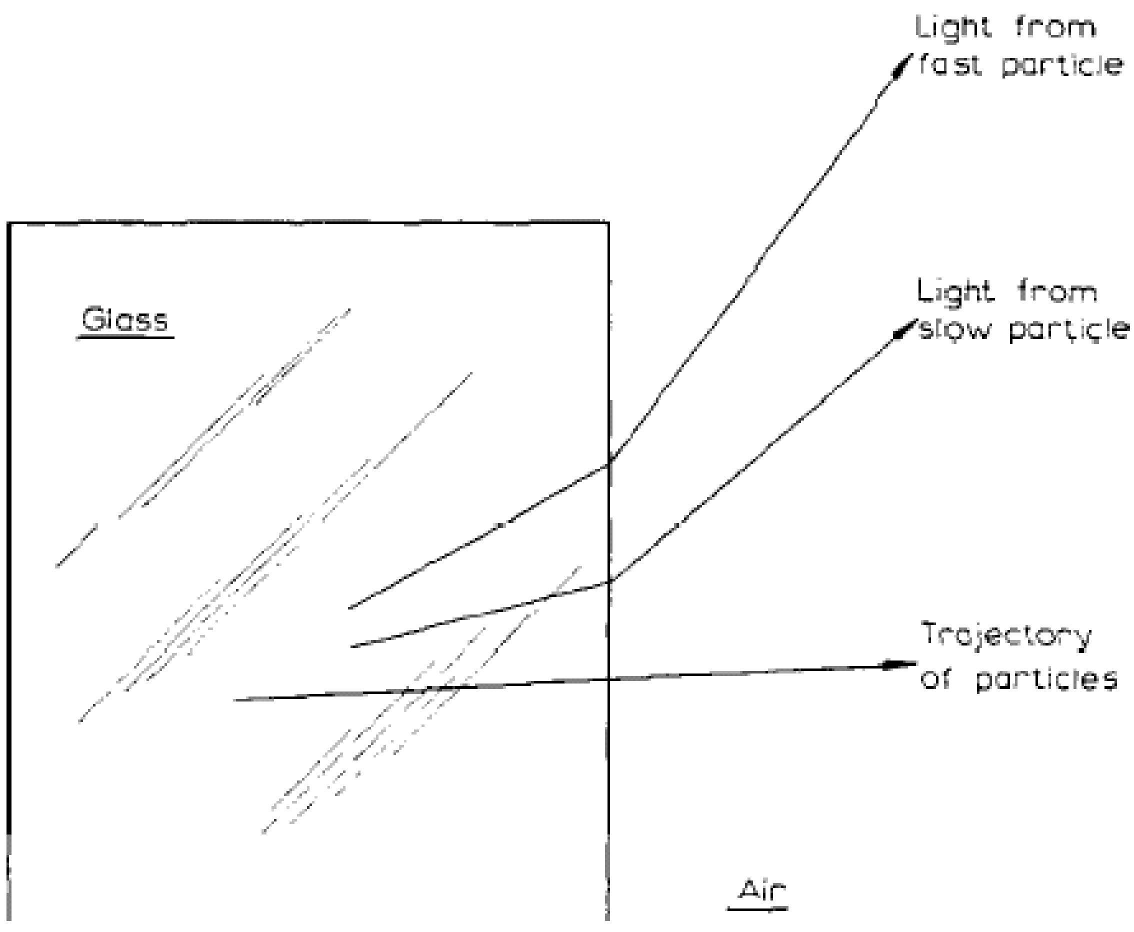

Fig. 6. Refraction of Čerenkov radiation at the interface between glass and air.

Chamberlain Discovery of Antiproton

1959 O. CHAMBERLAIN

C2

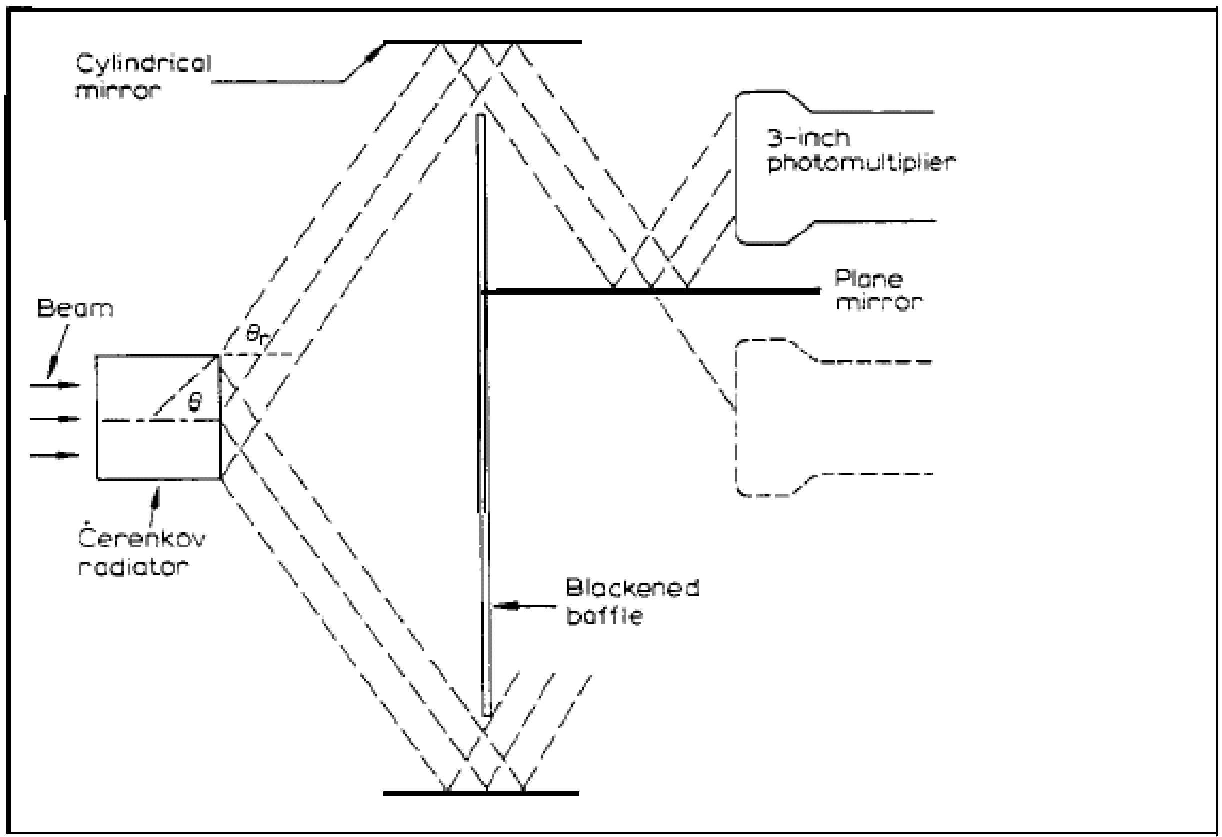

Velocity-selecting Cerenkov counter (C2)

Fig. 7. View of the velocity-selecting Čerenkov counter.

Chamberlain Discovery of Antiproton – time of flight

1954: Data run took 7 hours, 60 anti-protons

Pion = S1*S2*C1*$\overline{\text{C2}}$*S3

Pbar =S1*S2*$\overline{\text{C1}}$*C2*S3

S1 and S2 separated by 12 meters:

Pion δ(t) = 40 ns

Pbar δ(t) = 51 ns

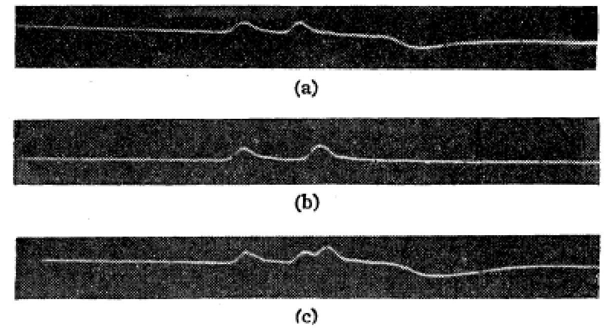

FIG. 2. Oscilloscope traces showing from left to right pulses from *S1*, *S2*, and *C1*. (a) meson, (b) antiproton, (c) accidental event.

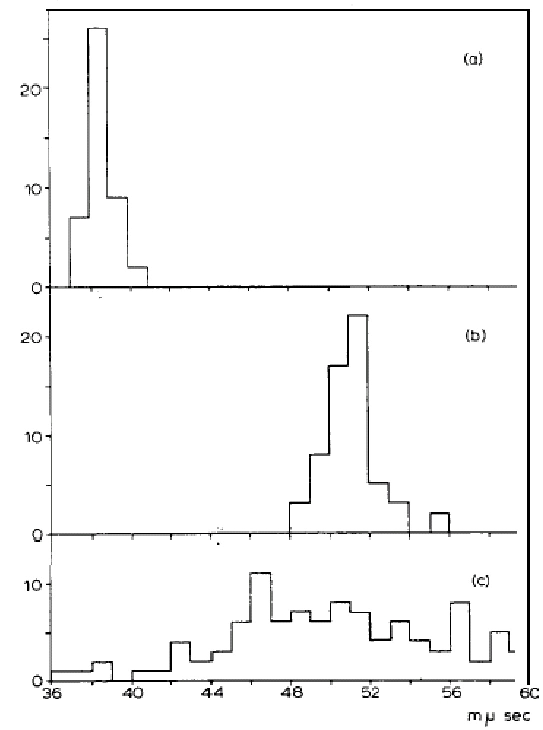

Fig. 10. *(a)* Histogram of times of flight for mesons; *(b)* histogram of times of flight for antiprotons; *(c)* apparent flight times for accidental coincidences.

CMS HCAL testbeam at CERN

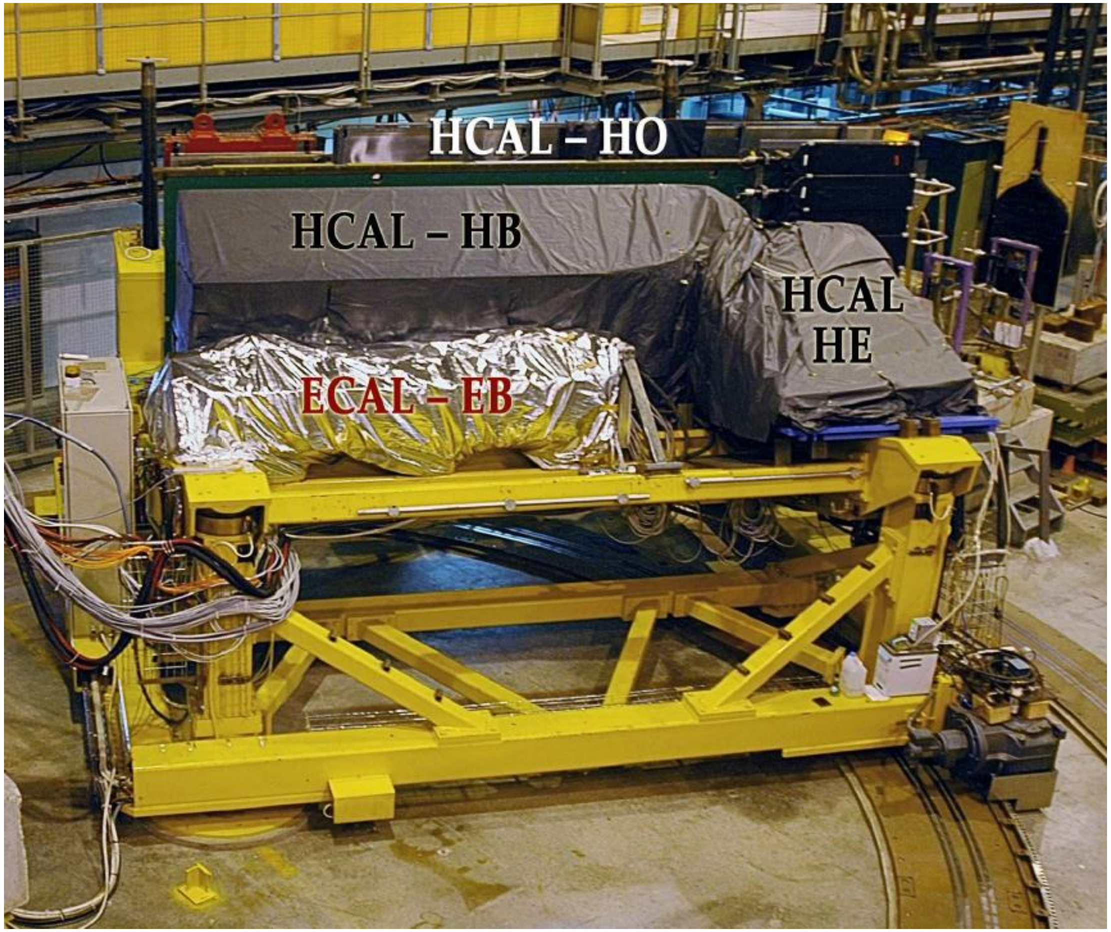

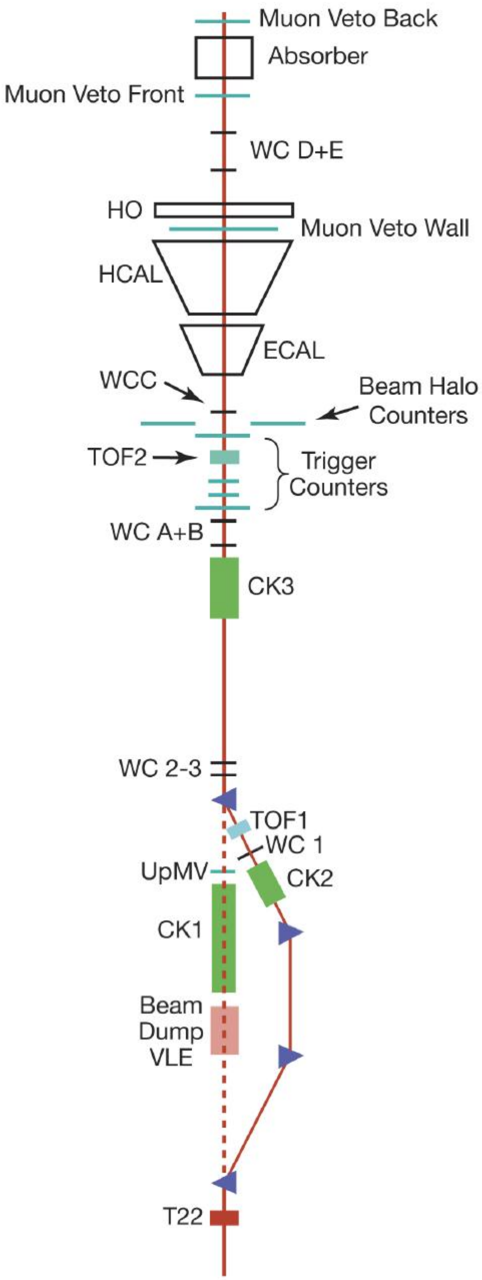

Effect of mass in testbeam

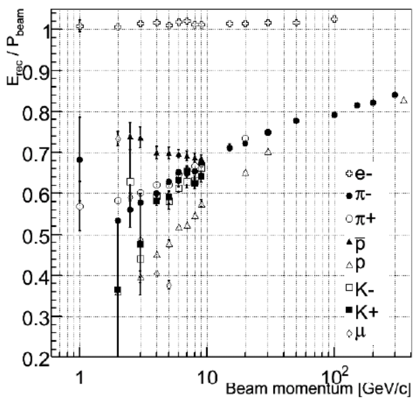

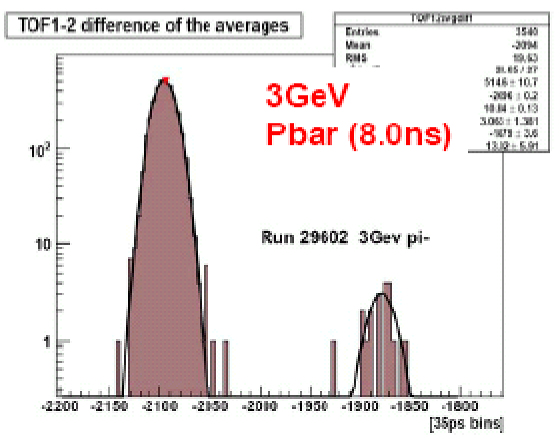

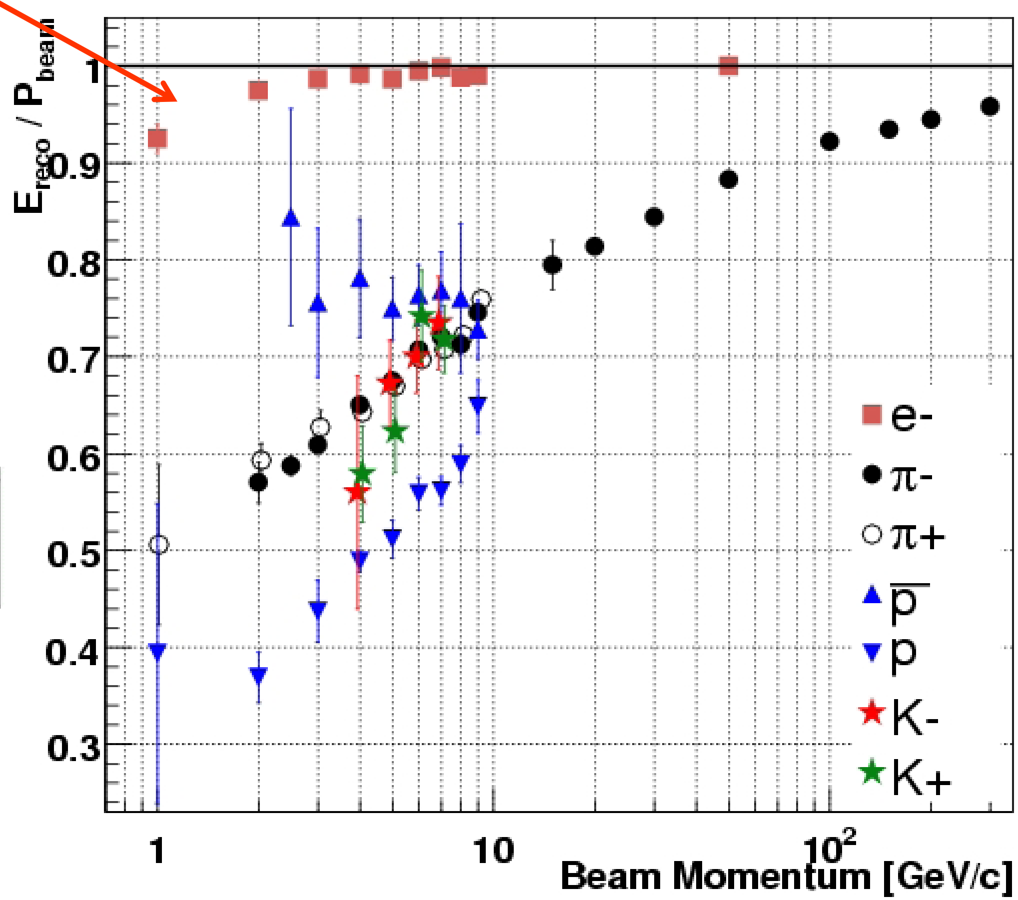

Each point would have been Nobel prize! (in 1950's)

Calorimetry

Calorimeter Technique:

Calorimeters are used to measure the energy of particles.

A destructive process where the particle interacts with the calorimeter (showers). The energy of the secondary shower particles measured.

Calorimeter usually divided into active and passive parts:

Active: responsible for generation of signal (e.g. ionization, light)

Passive: responsible for creating the "shower"

Many choices for the "active" material

inorganic crystals (PbWO4 CMS)

plastic scintillator (CDF, CMS)

liquid scintillator (CCFR)

Noble liquids (argon D0, Atlas)

gas (similar gases as used by wire proportional chambers, CDF Run I)

glass (leaded or doped with scintillator, KTEV)

Many choices for the "passive" material

marble, iron, steel, lead, depleted uranium

Energy Deposition and Showering

Key to calorimetry is the showering process.

In a shower the original particle interacts with the passive material creating many lower energy particles.

The low energy particles deposit energy (via ionization) in the active material.

The amount of ionization (or light) is proportional to the number of amount of energy deposited in the calorimeter.

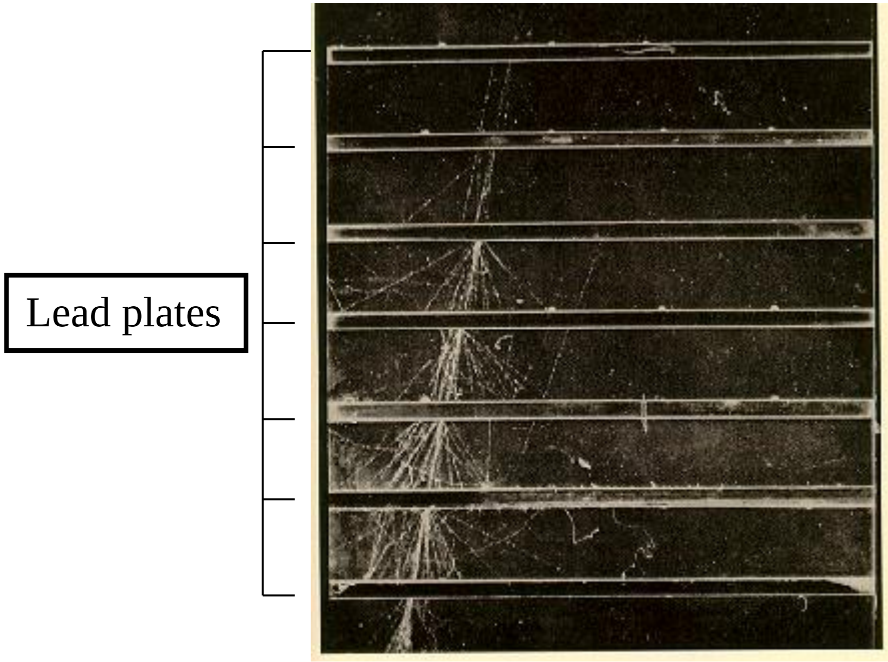

Cloud chamber photo of an electromagnetic shower. A high energy electron initiates the shower. The electron radiates photons via bremsstrahlung when it goes through the first lead plate. The photons are converted to electrons and positrons by the lead and they in turn create new photons. This process continues until the photons are no longer energetic enough to undergo pair production.

Hadronic showers are more complicated than EM showers

- Strong and weak interactions are involved in the hadronic shower process

Energy resolution of hadronic calorimeter usually worse than EM calorimeter

- neutrinos leak energy out of calorimeter
- muons will not usually be absorbed by calorimeter (unlikely to bremsstrahlung)
- long lived particles (K_s, K_L, Λ) may escape calorimeter before decaying (or interacting)

MC simulation of hadronic (proton) and EM shower (photon). Hadronic showers typically have larger lateral spread compared with EM showers.

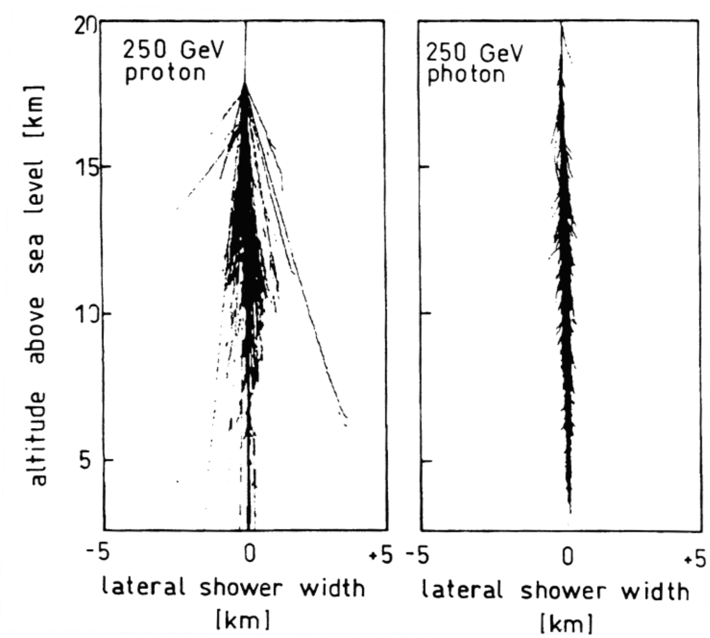

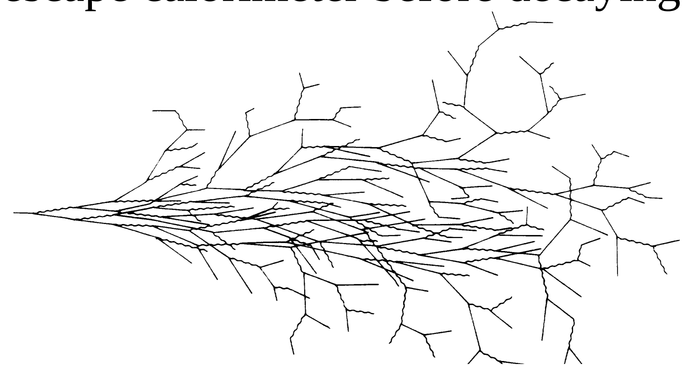

EM shower

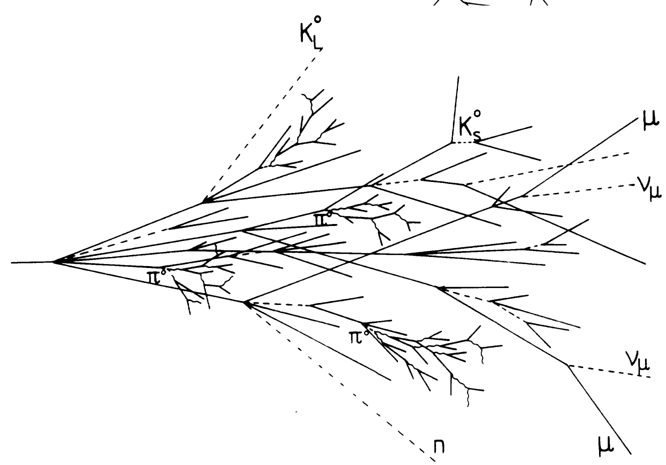

Hadronic shower

Hadron Shower

200 GeV π p Interaction

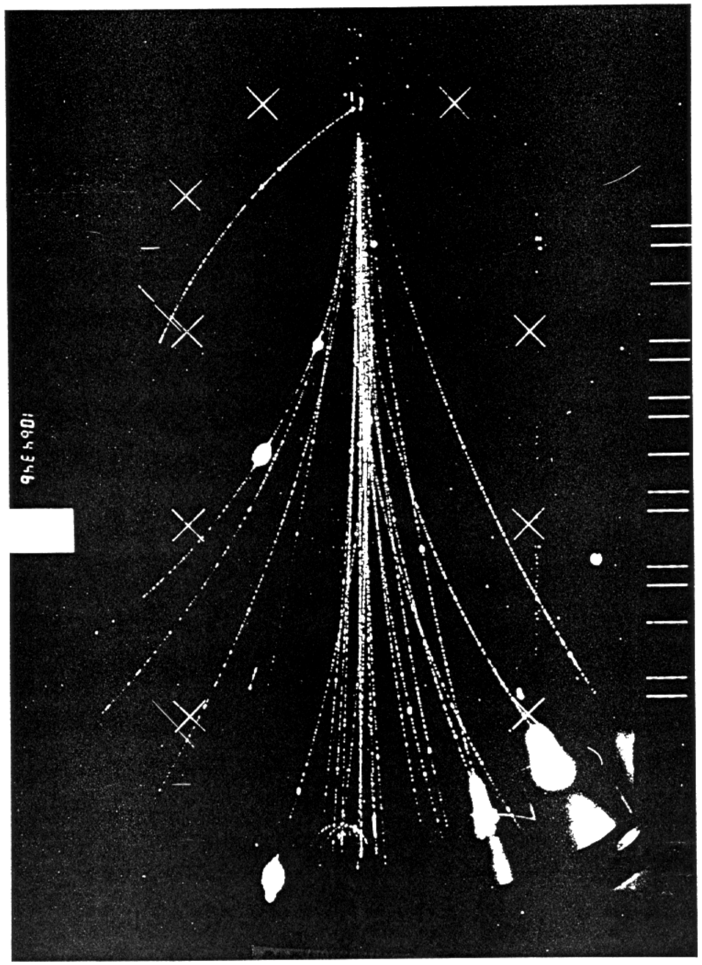

π^+, π^-, π^0

$\langle p_T \rangle_h \sim 0.4\, GeV$

Note large multiplicity
And small angle production
→ limited P_T

Sampling Calorimeters

Sampling calorimeters have active and passive material interleaved.

A few typical examples of SC's and their active material are given below.

a) Scintillator
b) Scintillator with wave shifter readout
c) liquid argon with ionization chamber readout
d) Gas with MWPC readout

For a)-d) the passive material could be lead or iron.

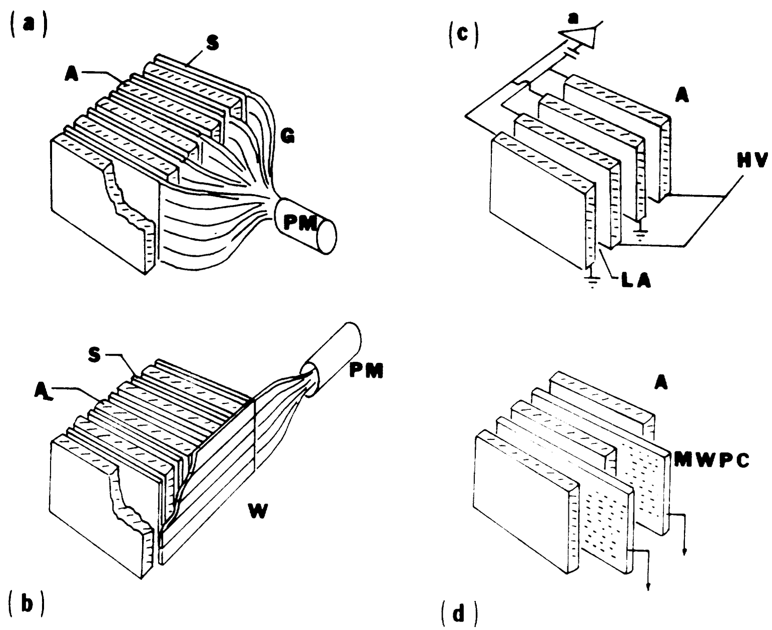

Energy Resolution

$$\frac{\sigma_E}{E} = \frac{(7.5-25)\%}{\sqrt{E}} \quad \textbf{EM}$$

$$\frac{\sigma_E}{E} = \frac{(35-80)\%}{\sqrt{E}} \quad \textbf{hadronic}$$

Material Properties

	R_L(cm)	E_c (MeV)	λ_a(cm)
Lead	0.56	7.4	17.2
Iron	1.76	20.7	16.8
Tungsten	0.35	8.0	9.6

λ_a= nuclear absorption length

Crystal Calorimeters: fully active

These calorimeters have only active elements (e. g. crystals) that combine a short radiation length with large light output.

	NaI(Tl)	CsI(Tl)	CsI	BGO	$PbWO_4$
Density (g/cm^3)	3.67	4.51	4.51	7.13	8.28
X_0 (cm)	2.59	1.85	1.85	1.12	0.89
R_M (cm)	4.8	3.8	3.5	2.3	2.2
Decay time (ns)	230	680	6	60	5
slow component			35	300	15
Emission peak (nm)	410	560	420	480	440
slow component			310		
Light yield γ/MeV	4×10^4	5×10^4	4×10^4	8×10^3	1.5×10^2
Photoelectron yield	1	0.45	0.056	0.09	0.013
relative to NaI					
Rad. hardness (Gy)	1	10	10^3	1	10^5

CMS Crystal ECAL

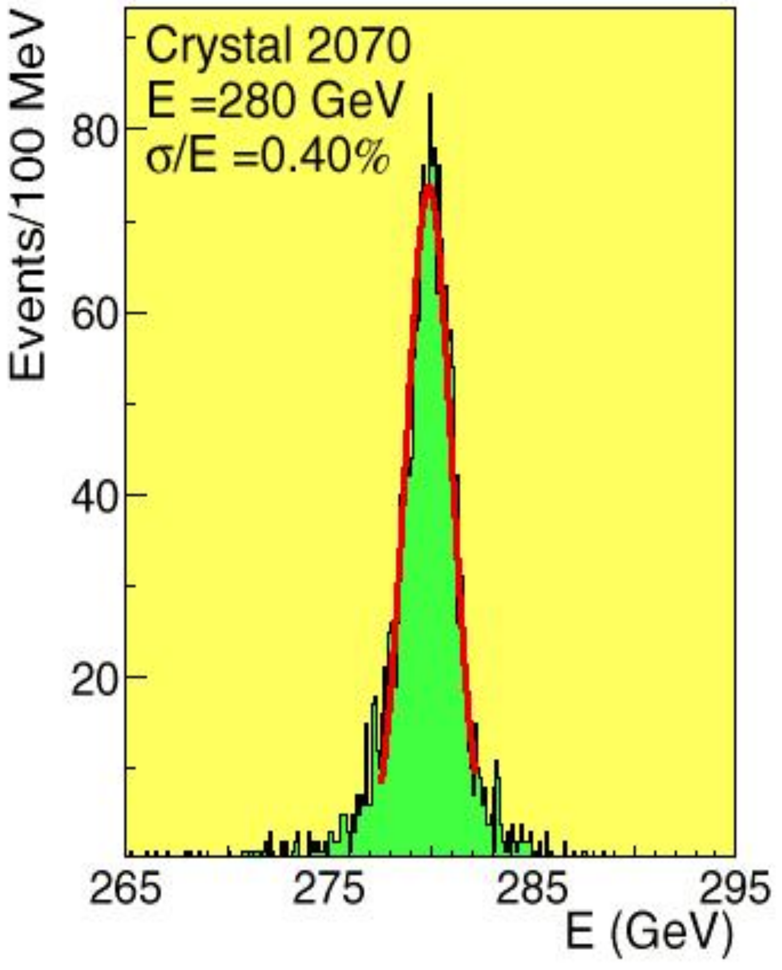

Two APDs 5 x 5 mm surface mounted in a supporting structure (capsule) glued at the rear of the crystal

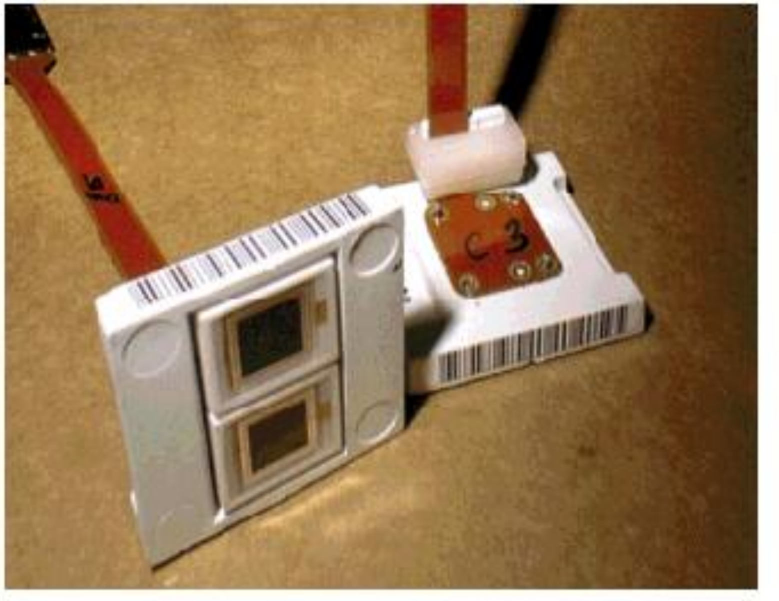

$PbWO_4$ crystal, APD readout

Energy Resolution - Xtals

e.g. PbWO4 – CMS

fully active devices have no sampling fluctuations. However, there is noise and photon statistics, and collection non-uniformity.

dE/E ~ 0.7 % at 100 GeV

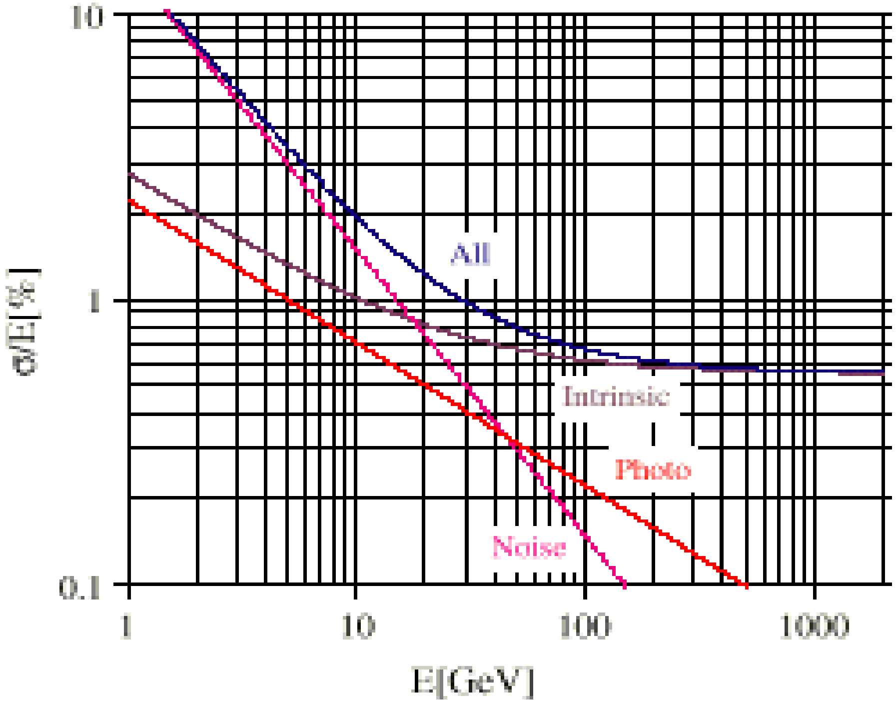

Fig. 1.3: Different contributions to the energy resolution of the $PbWO_4$ calorimeter.

Calculate: Seeing muon in calorimeter

- Pmt gain 10**6
- Quantum efficiency 15%
- Calorimeter thickness 800 gms/cm**2
- Light yield 100 photon/GeV at tube
- ADC sensitivity 25 pc/count
- Pedestal width 2 counts

- What does muon look like

H_20 Cerenkov Cal Super-Kamiokande

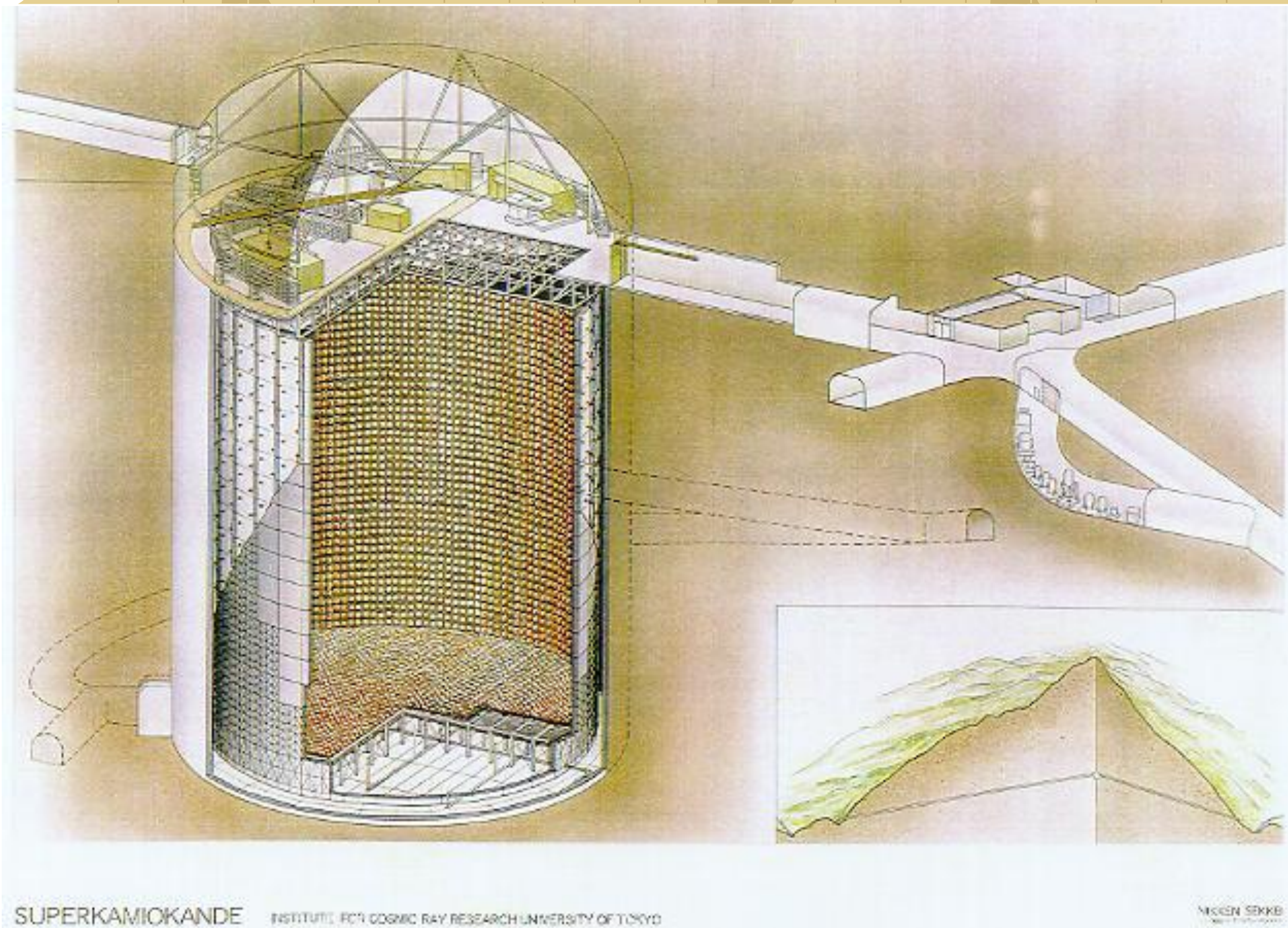

Properties of Super-K

- A Large Water Cerenkov Detector for Cosmic Particles
- Ring imaging Cerenkov and Cerenkov Calorimeter
- Size: Cylinder of 41.4m (Height) x 39,9m (Diameter)
- Weight: 50,000 tons of pure Water
- Number of Photomultipier Tubes: 11,200

Super Kamiokande 9000 tubes installed

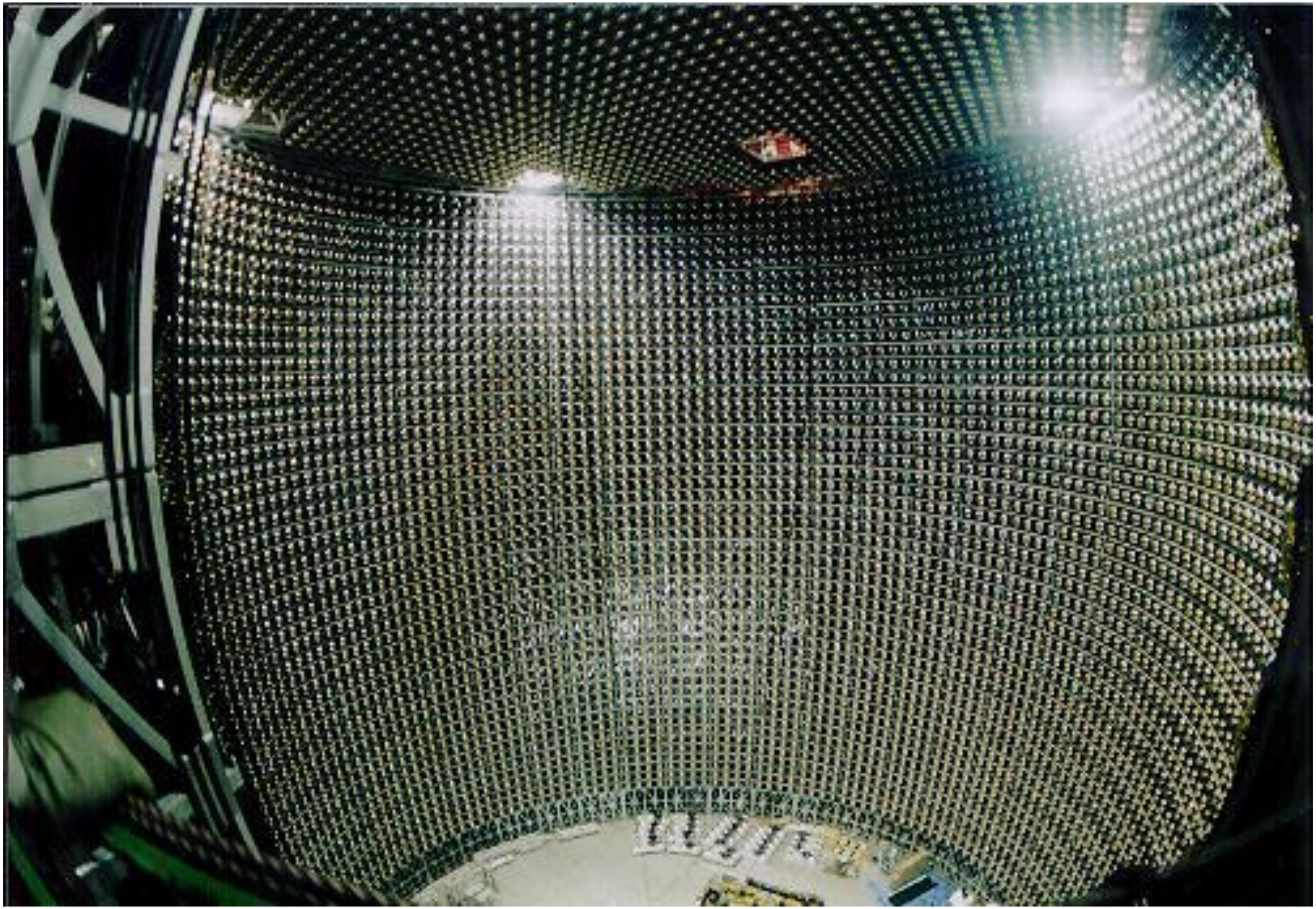

Super Kamiokande ½ full of water

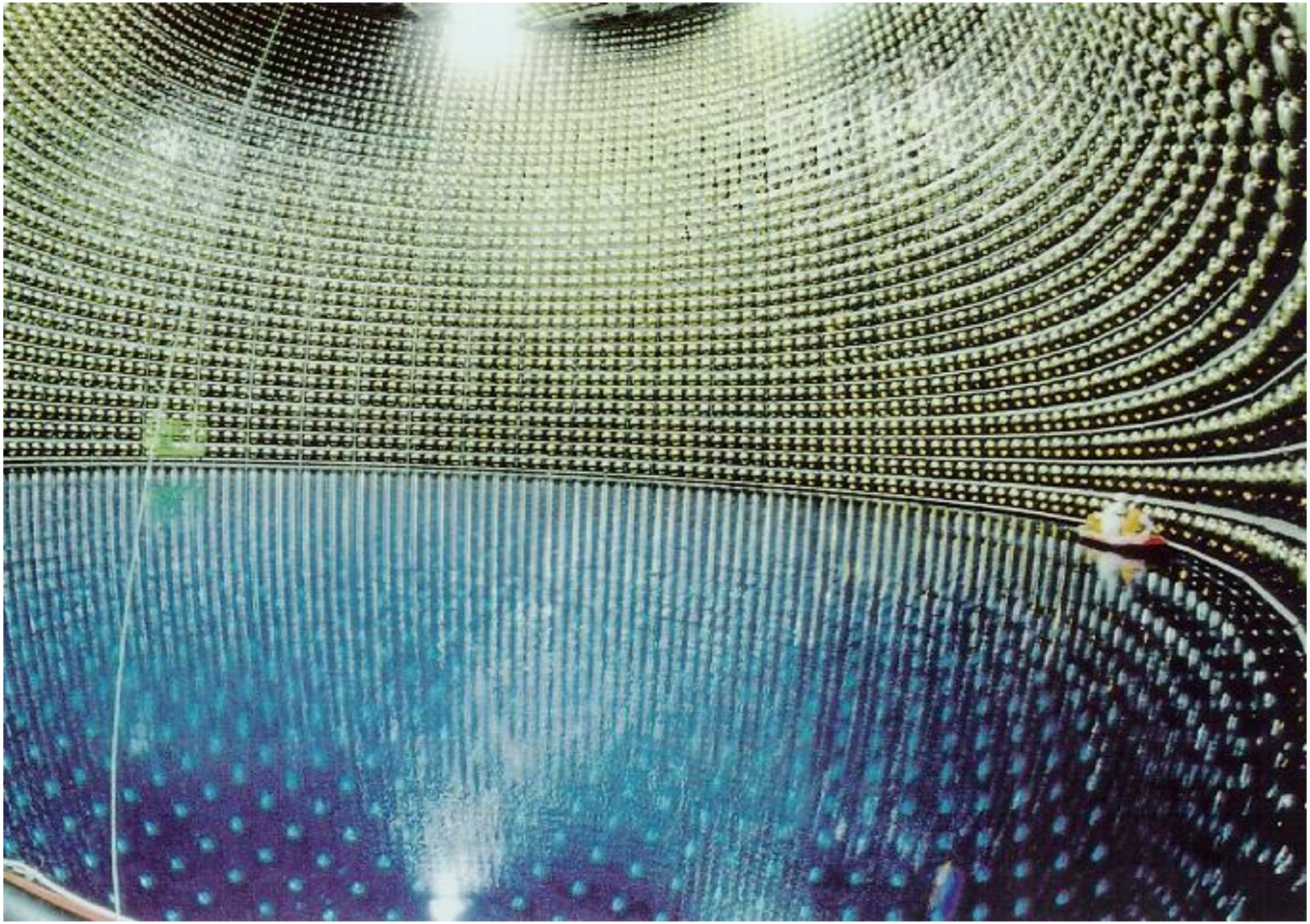

Super-K neutrino interaction

Measurements:

- **Cerenkov ring. Centroid gives direction of particle.**
- **Nr phototubes gives energy of particle**
- **Time difference between photube hits gives coordinates inside of detector**
- **Shape of cerenkov ring determines species of particle**
- **For water, n = 1.33**

  For β=1 cosθ=1/1.33, θ=41°

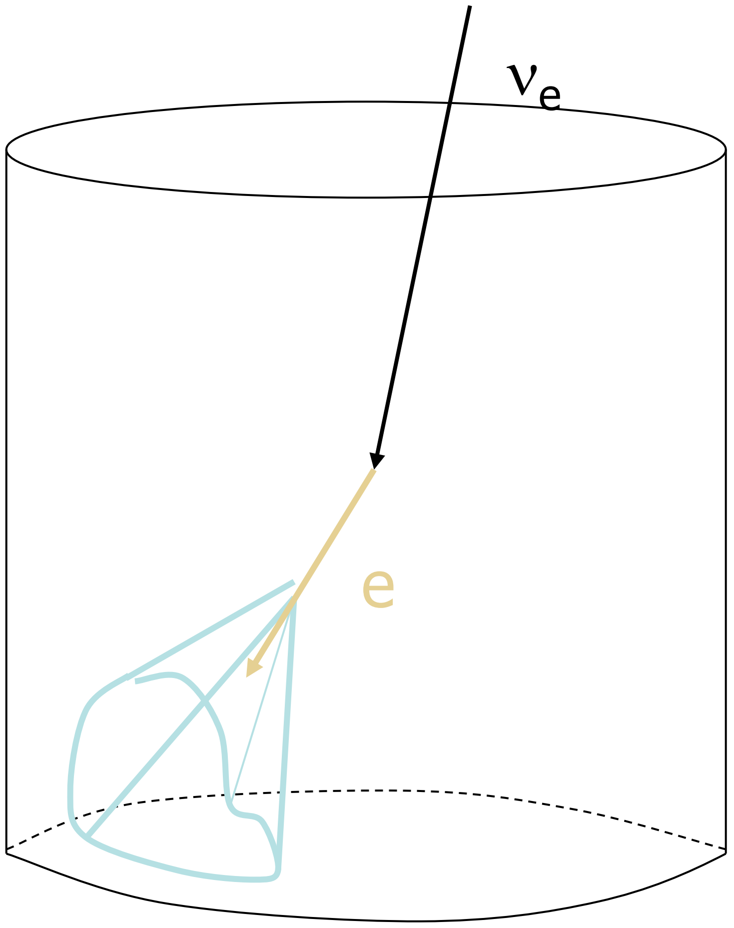

Super-K Electron Detection

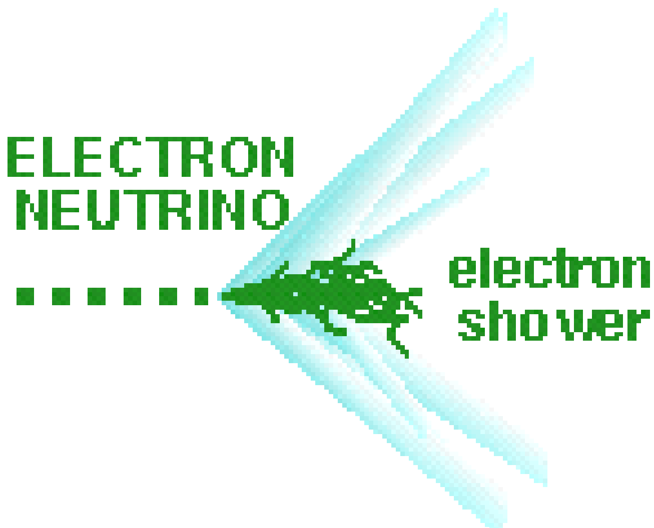

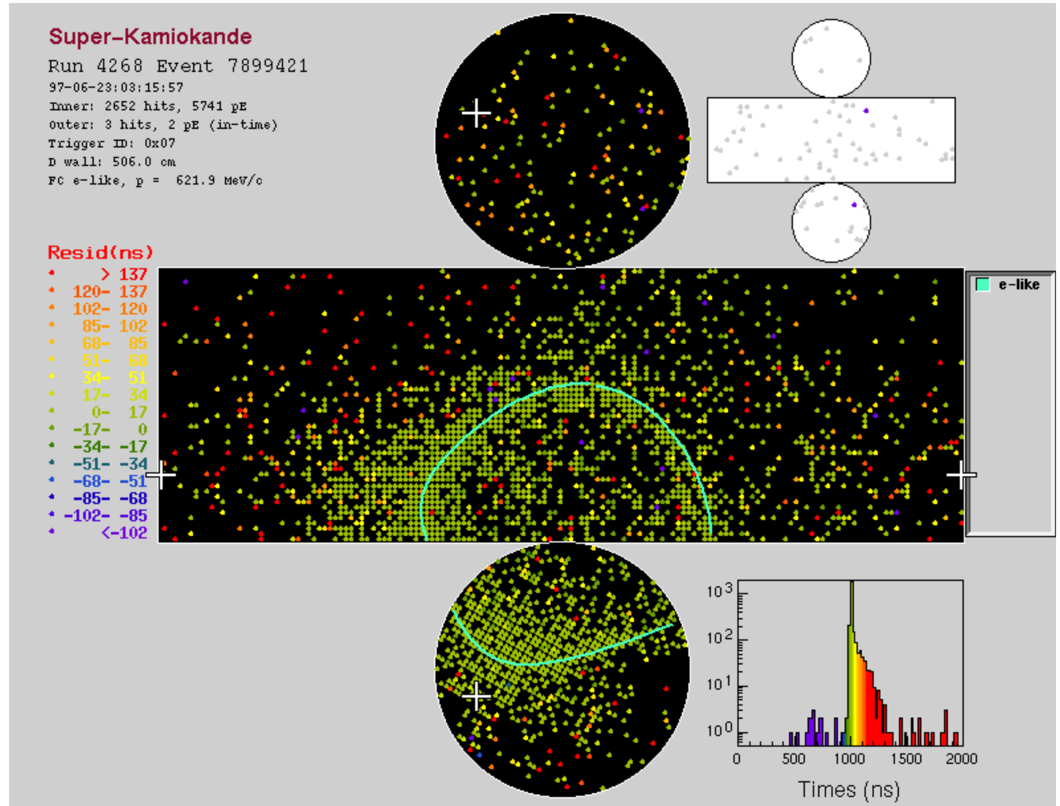

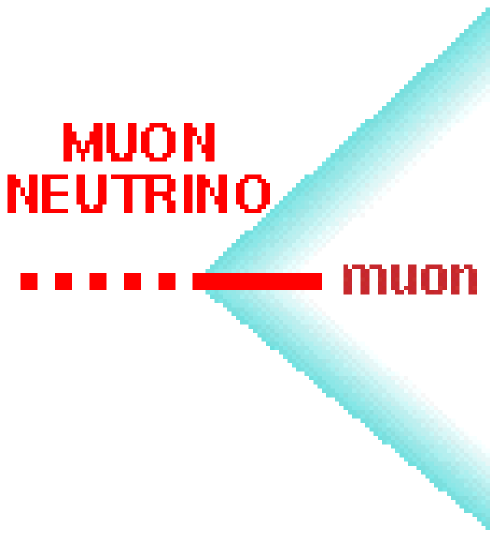
MUON
NEUTRINO
muon

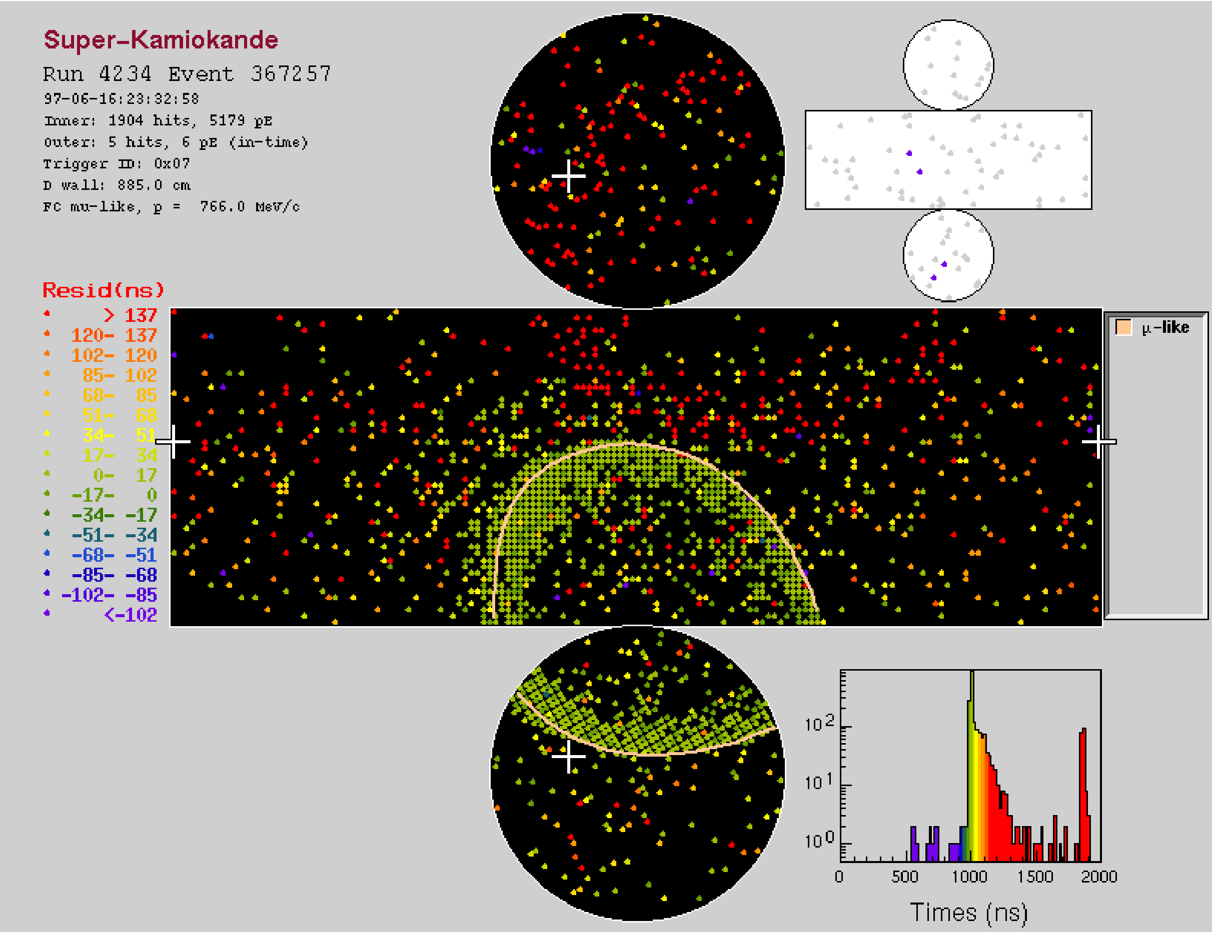
Super-Kamiokande
Run 4234 Event 367257
97-06-16:23:32:58
Inner: 1904 hits, 5179 pE
Outer: 5 hits, 6 pE (in-time)
Trigger ID: 0x07
D wall: 885.0 cm
FC mu-like, p = 766.0 MeV/c
Resid(ns)
> 137
120- 137
102- 120
85- 102
68- 85
51- 68
34- 51
17- 34
0- 17
-17- 0
-34- -17
-51- -34
-68- -51
-85- -68
-102- -85
<-102
μ-like
10^2
10^1
10^0
0
500
1000
1500
2000
Times (ns)

Super-K Detects Sun

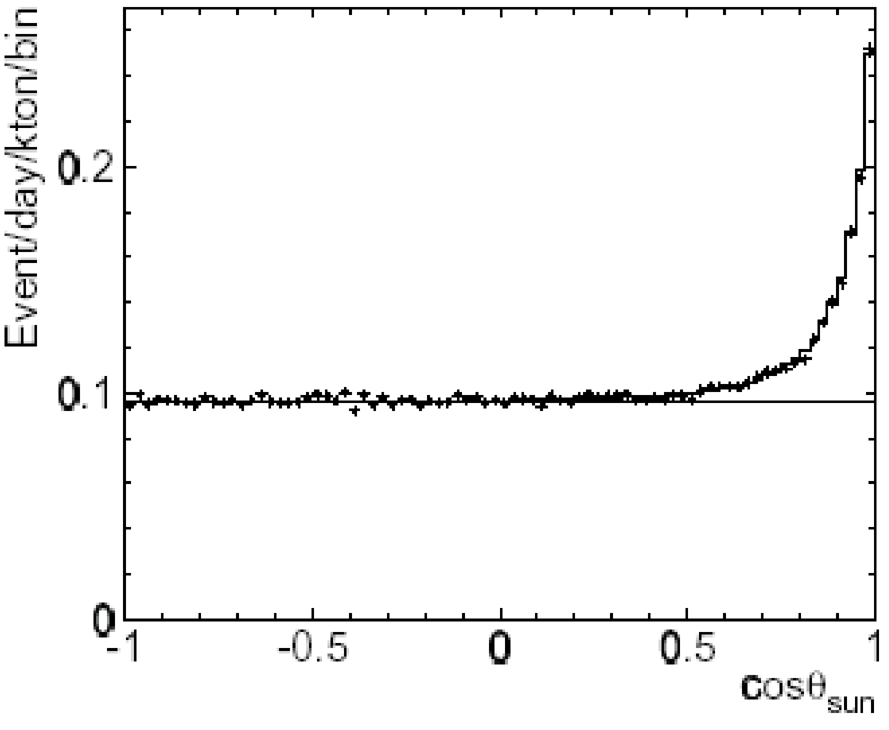

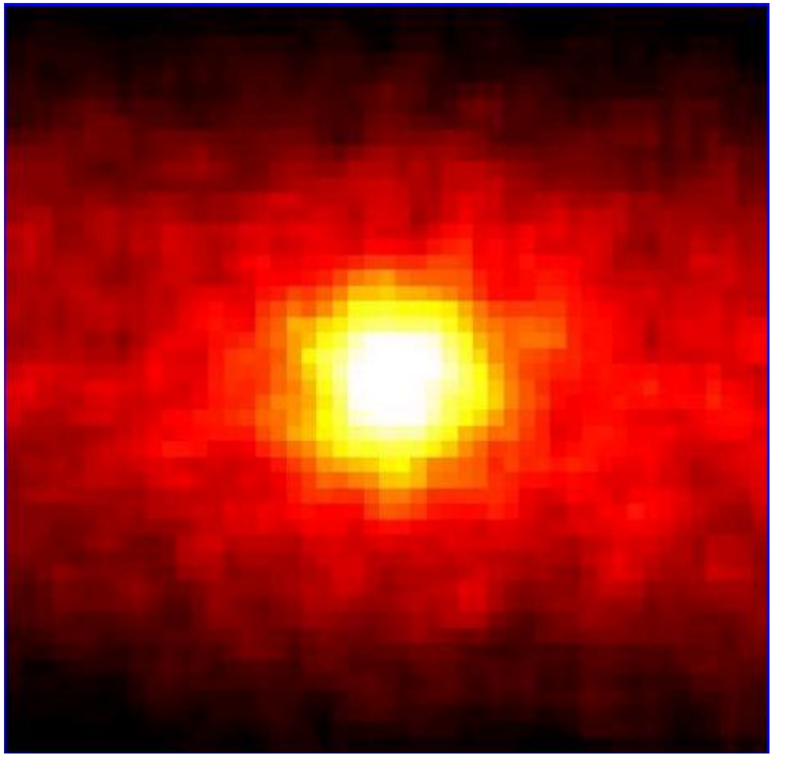

Amanda, IceCube at the South Pole

Calorimetry in Ice

- Absorption length ~100 m
- Scattering length ~25 m
- Light is isotropized well before it is absorbed.
- To first order, sampling is insensitive to geometric position or PMT orientation.
- Current arrays sample a very small fraction of the total Cerenkov light…

  Total PMT area/ detector surface area

  ~ 10^{-5} for AMANDA and IceCube.
- PMTs on a string… ~20 m spacing between PMTs

  String spacing… ~100 m spacing between strings.
- String spacing determines energy threshold.

Ice Cube

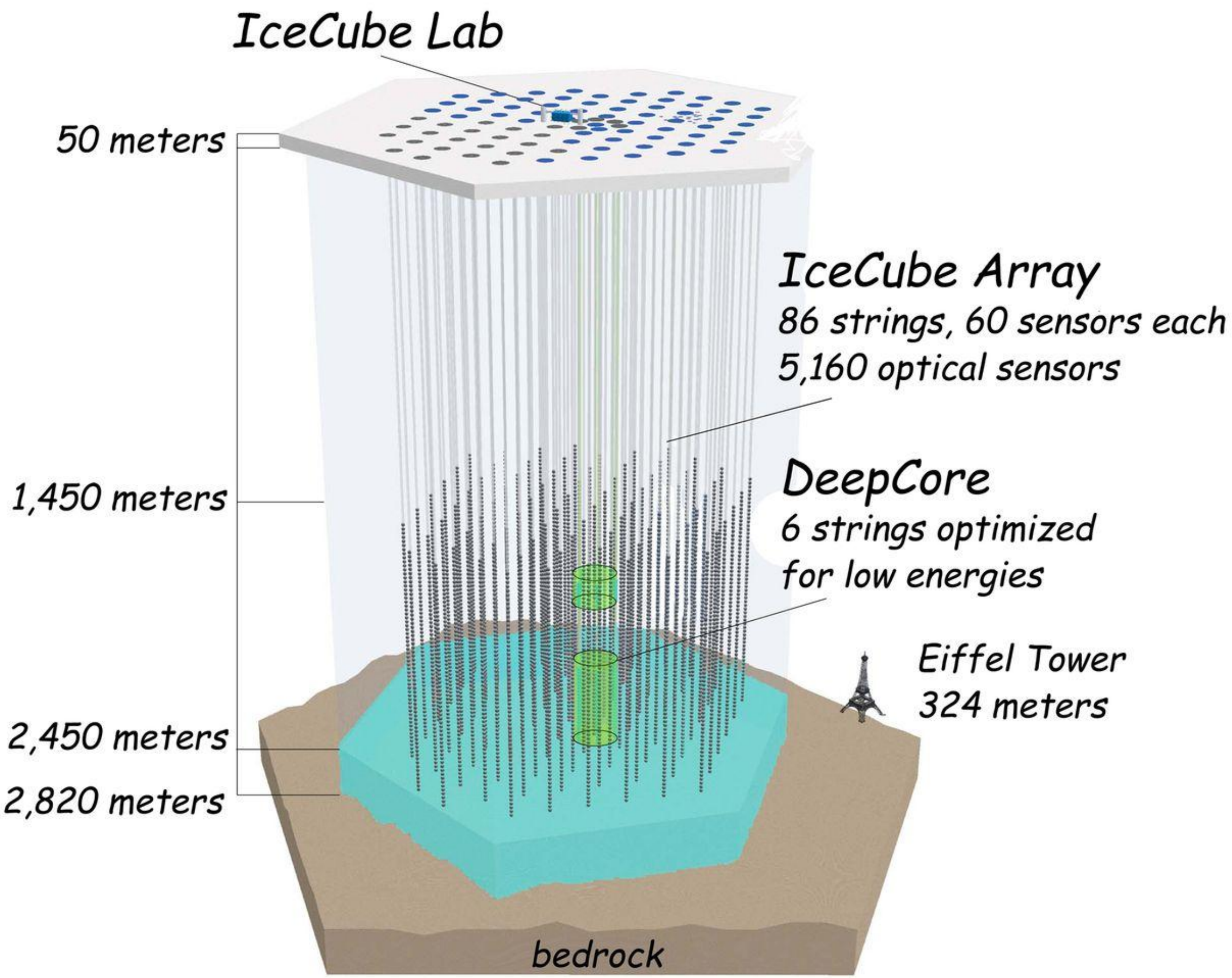
IceCube Lab
50 meters
IceCube Array
86 strings, 60 sensors each
5,160 optical sensors
1,450 meters
DeepCore
6 strings optimized
for low energies
Eiffel Tower
324 meters
2,450 meters
2,820 meters
bedrock

IceCube Optics Module design

Design parameters:

- Time resolution:≤ 5 nsec (system level)
- Dynamic range: 200 photoelectrons/10 nsec
- Integrated dynamic range: > 2000 photoelectrons
- Digitization depth: 4 μsec.
- Noise rate in situ: ≤ 500 Hz (Ice is dark)
- Calibration functions built-in.

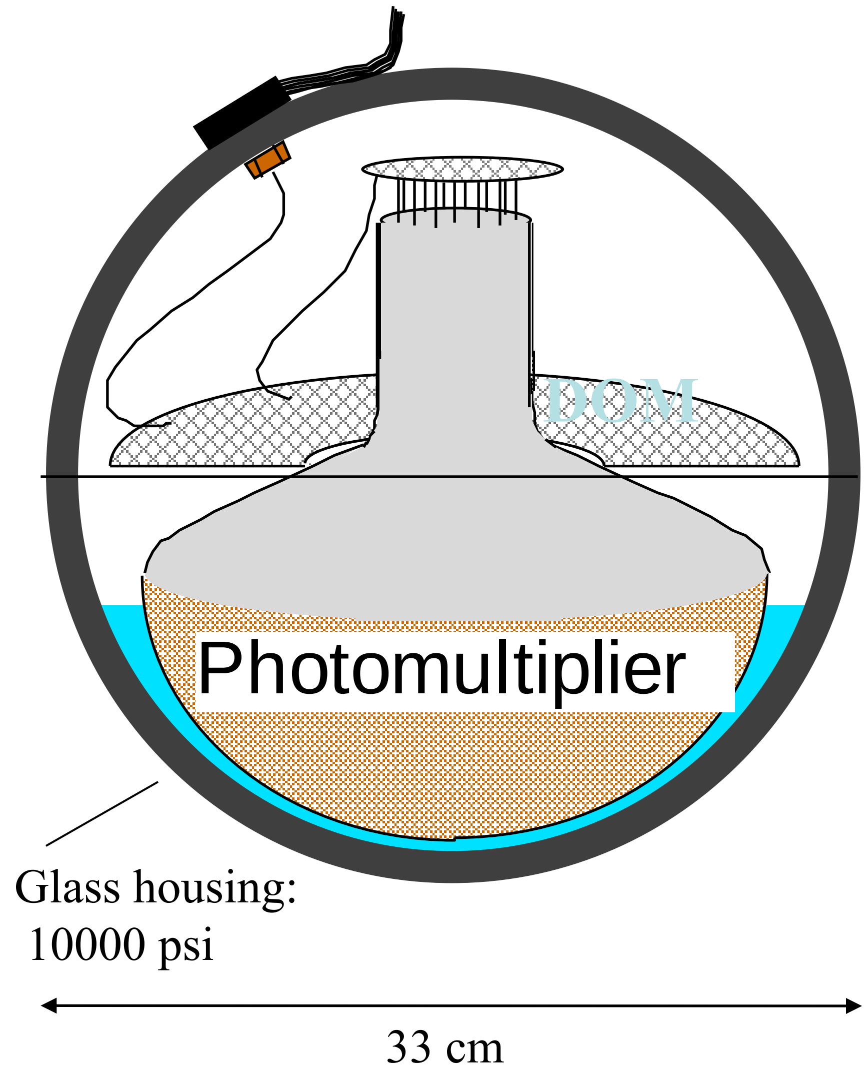

IceCube Muon events

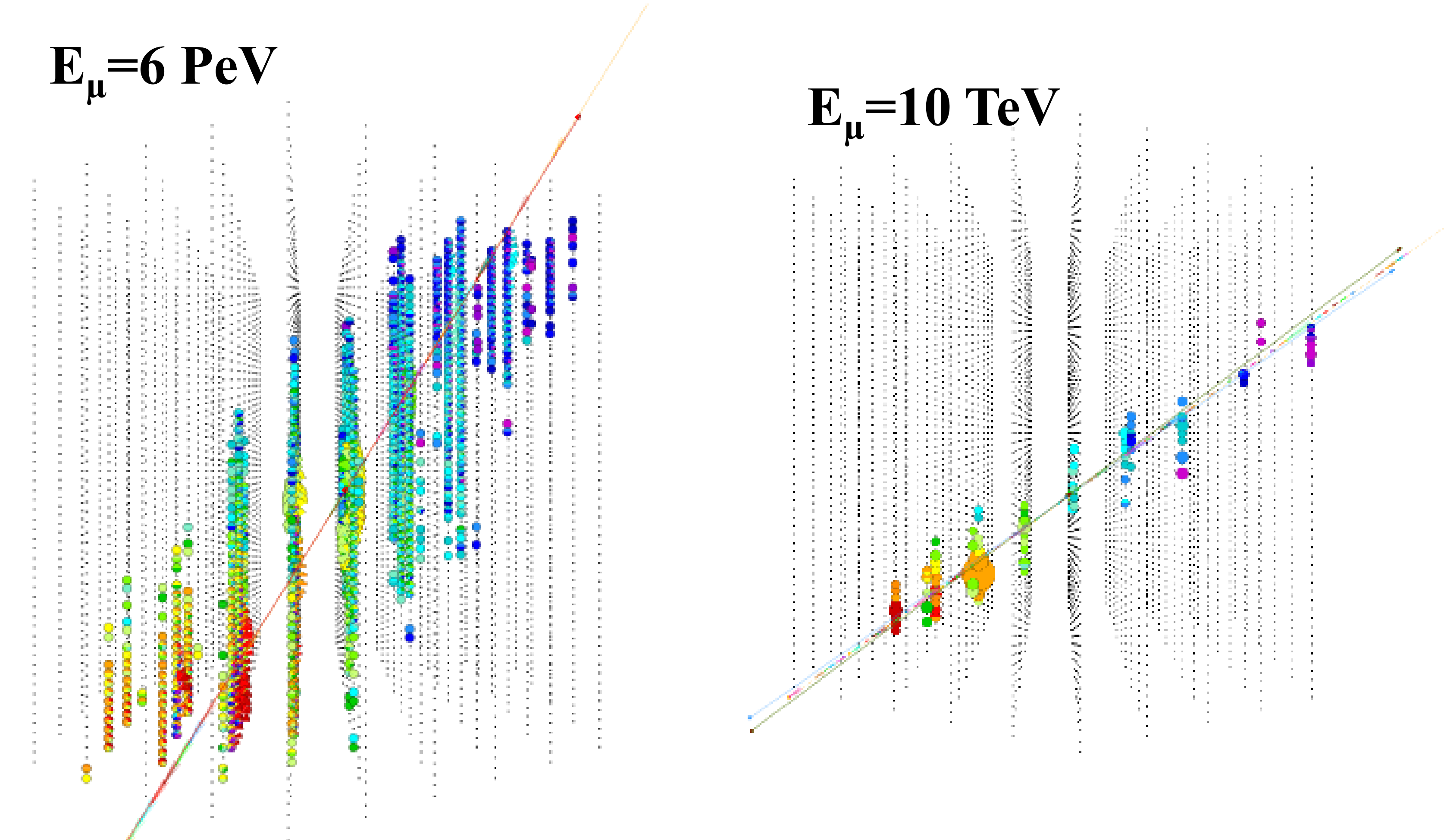

Measure energy by counting the number of fired PMT.
(This is a very simple but robust method) Arrival time color coded.

Fixed target experiment NuTeV

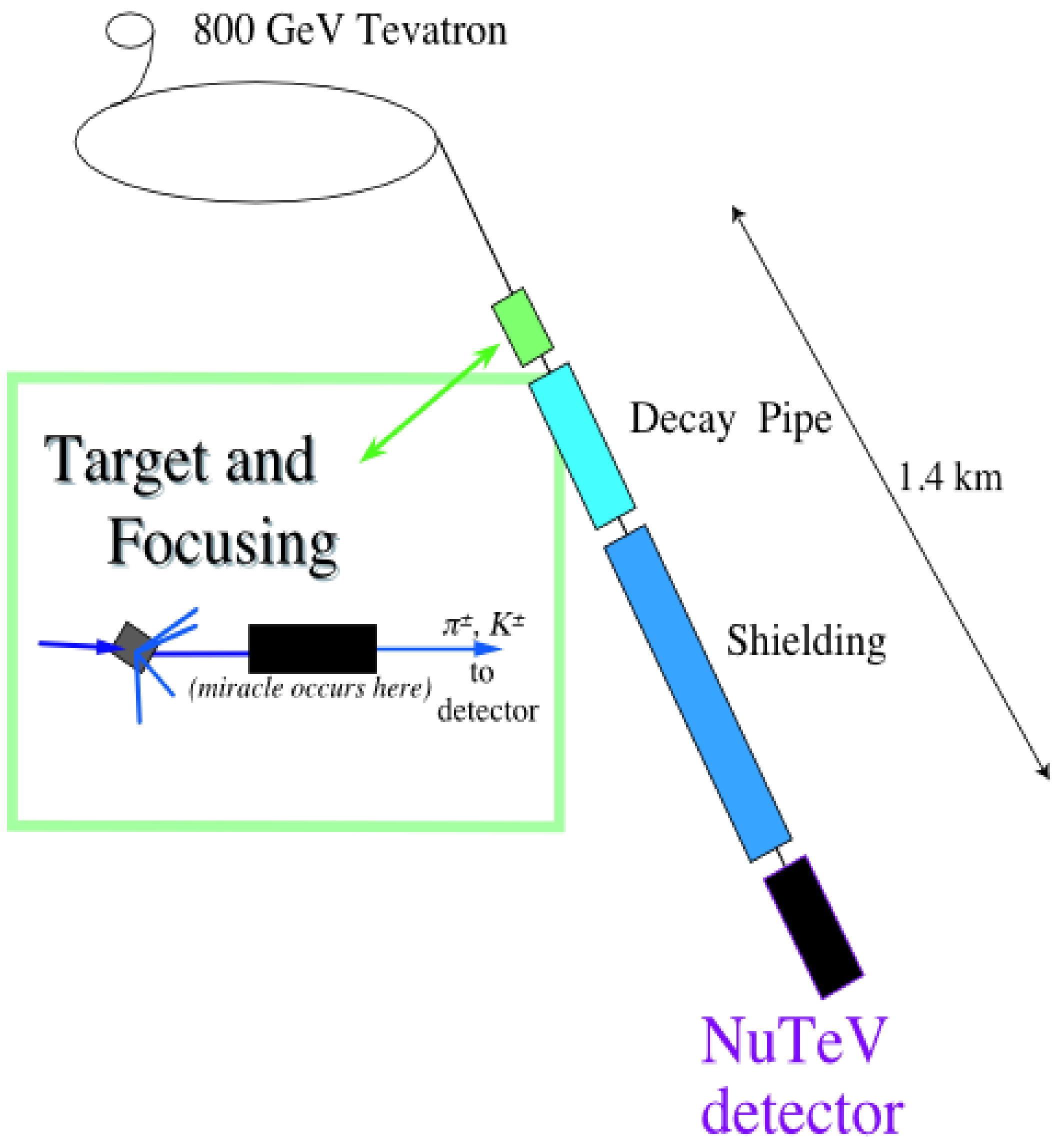

Deep Inelastic Scattering at NuTeV

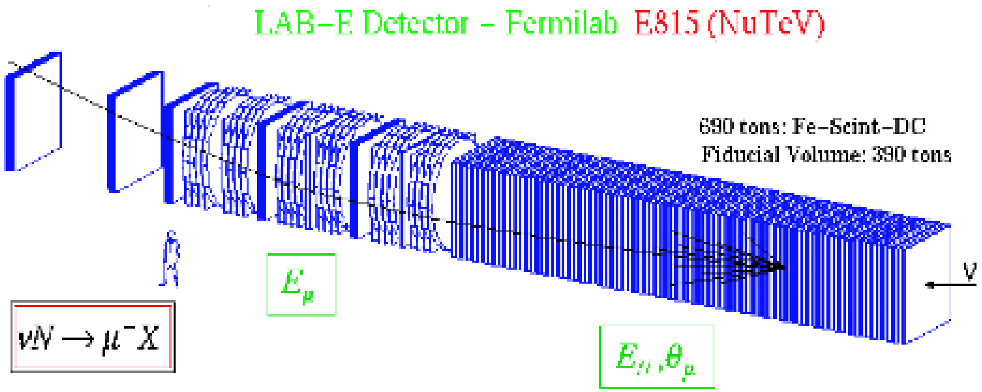

- Target/Calorimeter:
  - 168 Fe plates (3m X 3m X 5.1cm)
  - 84 liquid scintillation counters (every 10.2cm steel)
    To trigger the detector
    To measure the visible energy
    To determine the longitudinal event vertex
    To ascertain the event length
  - 42 drift chambers (every 20.4cm steel)
    To establish transverse vertex of event
- Toroidal Spectrometer:
  15kG field ($P_T = 2.4\,GeV/c$)

NuTeV Detector Details

Target/Calorimeter:

- ≤ 168 Fe plates (3m × 3m × 5.1cm)
- ≤ 84 liquid scintillation counters
  - Trigger the detector
  - Visible energy
  - Neutrino interaction point
  - Event length
- ≤ 42 drift chambers
  - Localized transverse shower position

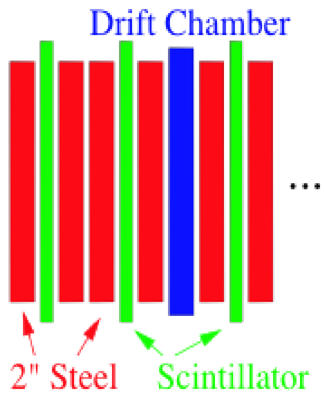

Toroidal Spectrometer:

- ≤ 11 kG field ($P_T = 2.4\,GeV/c$)

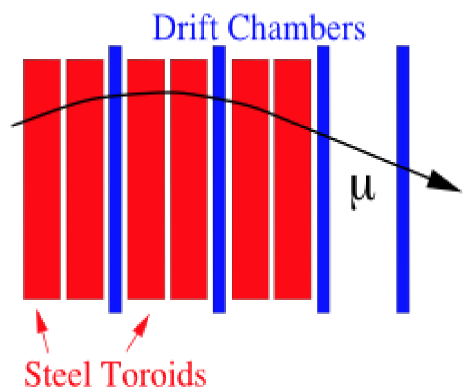

Continuous Test Beam: every beam spill

- ≤ Hadron, muon and electron beams
  - Map toroid and calorimeter response
- ≤ Understand Behavior of Hadronic Showers

NuTeV Scintillation Counter Detail

3 meter square, and an inch thick. 84 in target/calorimeter. plastic boxes, filled with scintillation oil, waveshifter bars,and with a photomultiplier tube looking in at each corner.

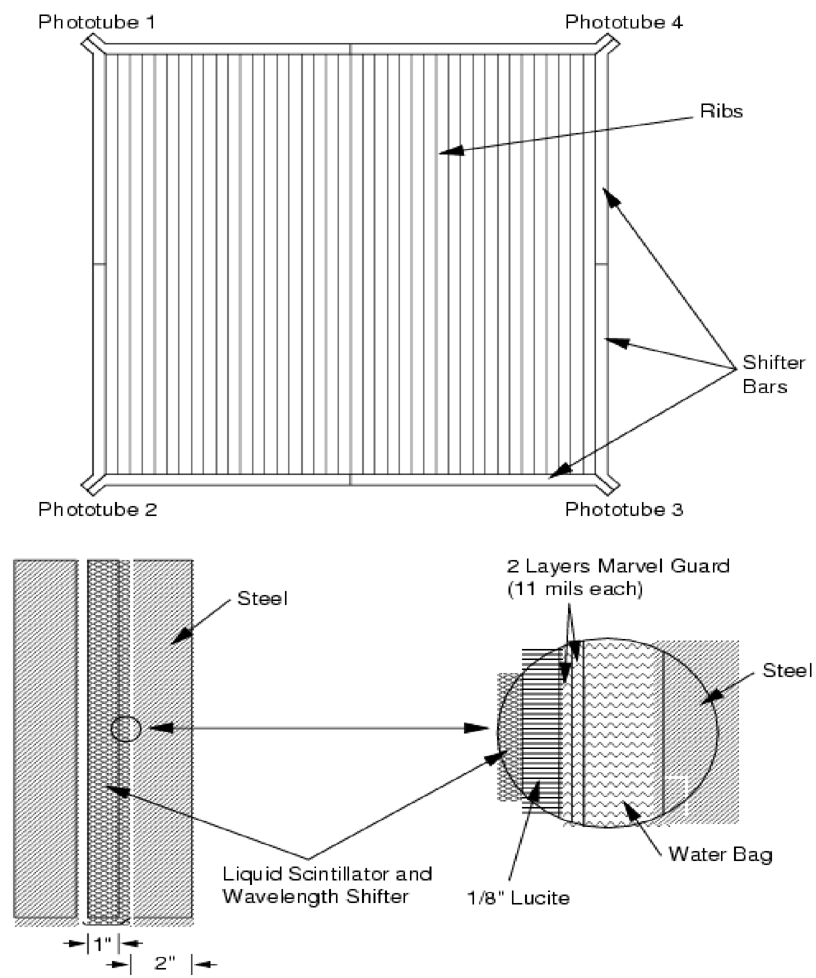

NuTeV Scintillator Counter

NuTeV Detector Hall

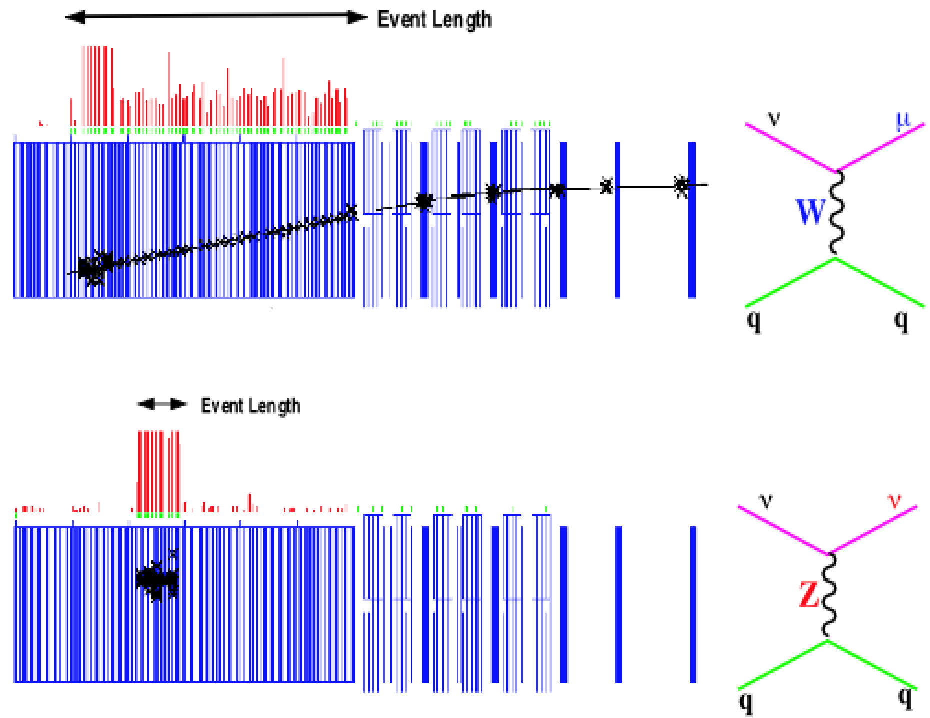

Statistical separation of NC and CC events based solely on "event length":

$$R_{\mathrm{exp}} = \frac{\text{SHORT events}}{\text{LONG events}} = \frac{\mathrm{L} \sum \mathrm{Lcut}}{\mathrm{L} > \mathrm{Lcut}} = \frac{\text{NC candidates}}{\text{CC candidates}}$$

(measure this ratio in both $\int$ and $\bar{\int}$ modes)

Generic Collider Detector: Functional Schematic

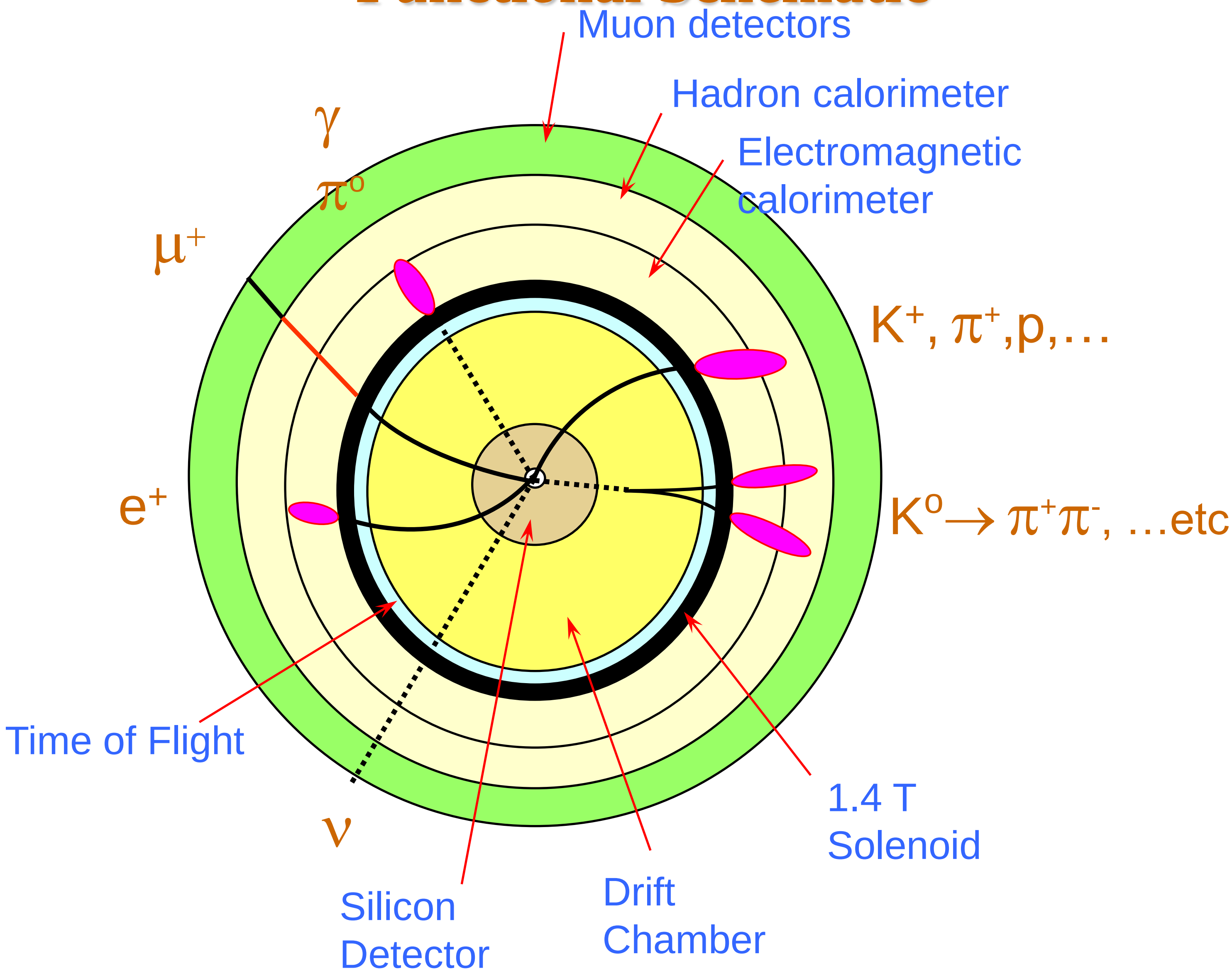

Collider Experiments:CMS

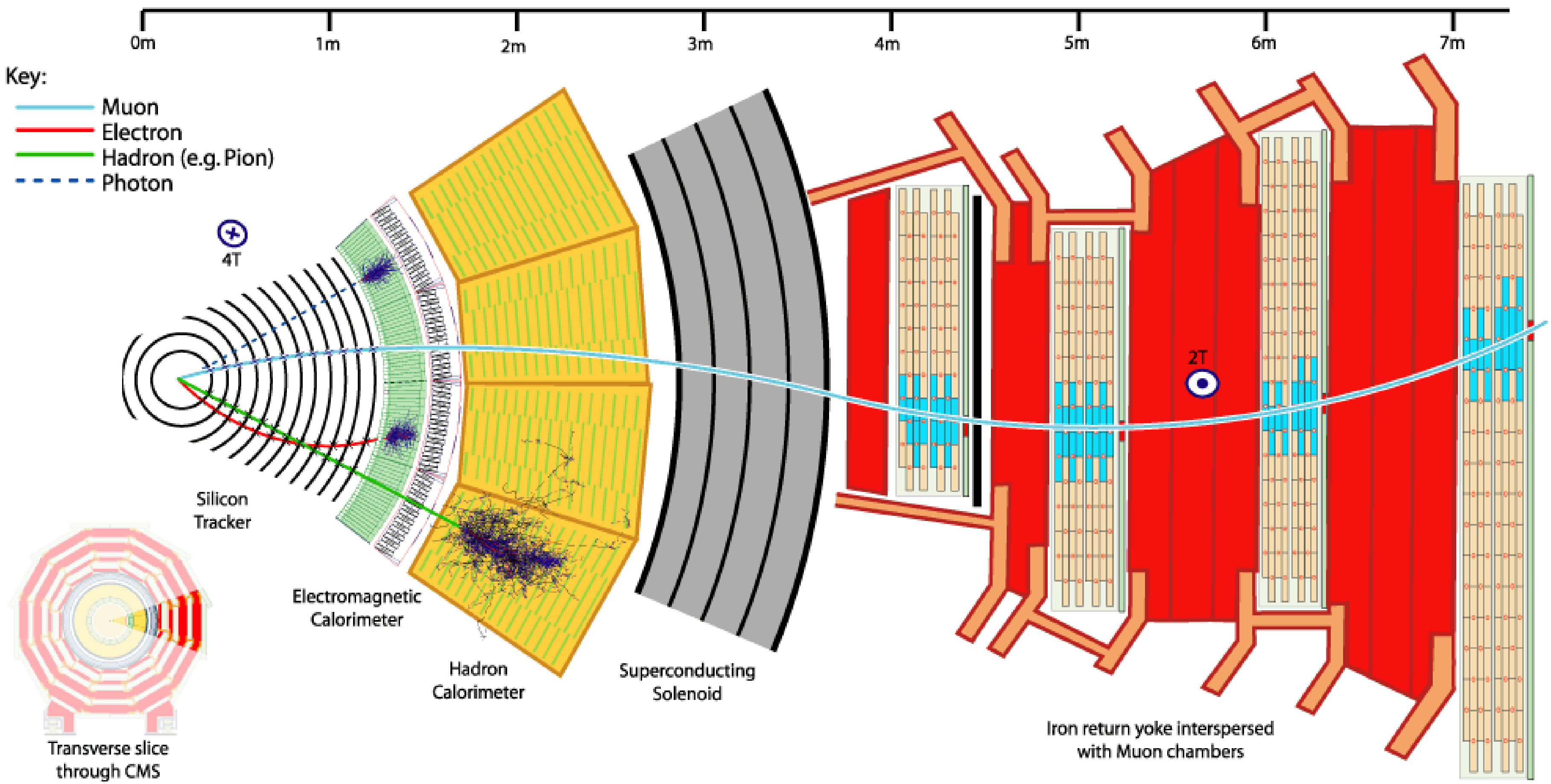

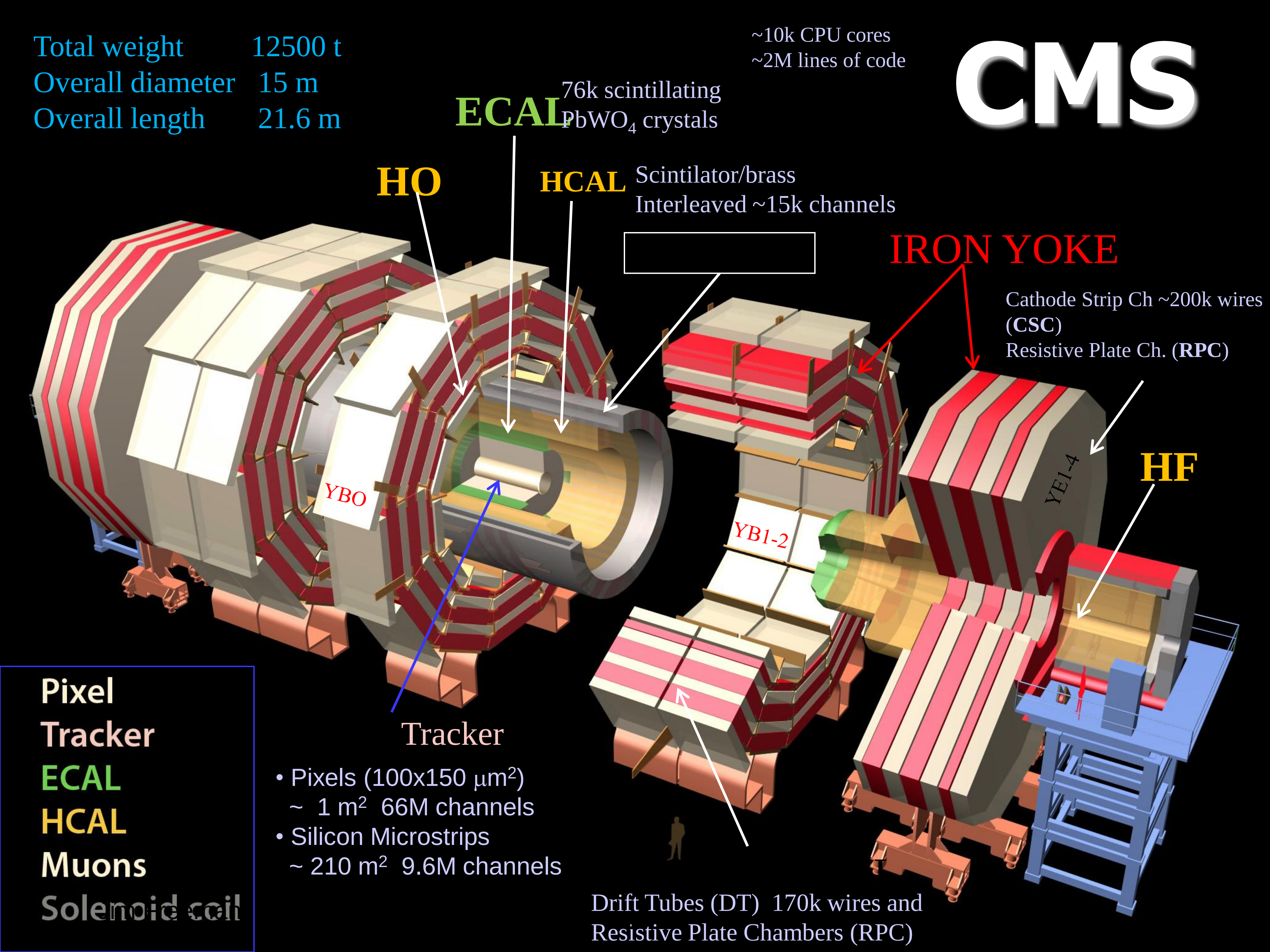
Total weight 12500 t
Overall diameter 15 m
Overall length 21.6 m
~10k CPU cores
~2M lines of code
CMS
ECAL
76k scintillating
$PbWO_4$ crystals
HO
HCAL
Scintilator/brass
Interleaved ~15k channels
IRON YOKE
Cathode Strip Ch ~200k wires
(CSC)
Resistive Plate Ch. (RPC)
YBO
YB1-2
YE1-4
HF
Pixel
Tracker
ECAL
HCAL
Muons
Solenoid coil
Tracker
• Pixels (100x150 μm^2)
~ 1 m^2 66M channels
• Silicon Microstrips
~ 210 m^2 9.6M channels
Drift Tubes (DT) 170k wires and
Resistive Plate Chambers (RPC)


November 2006

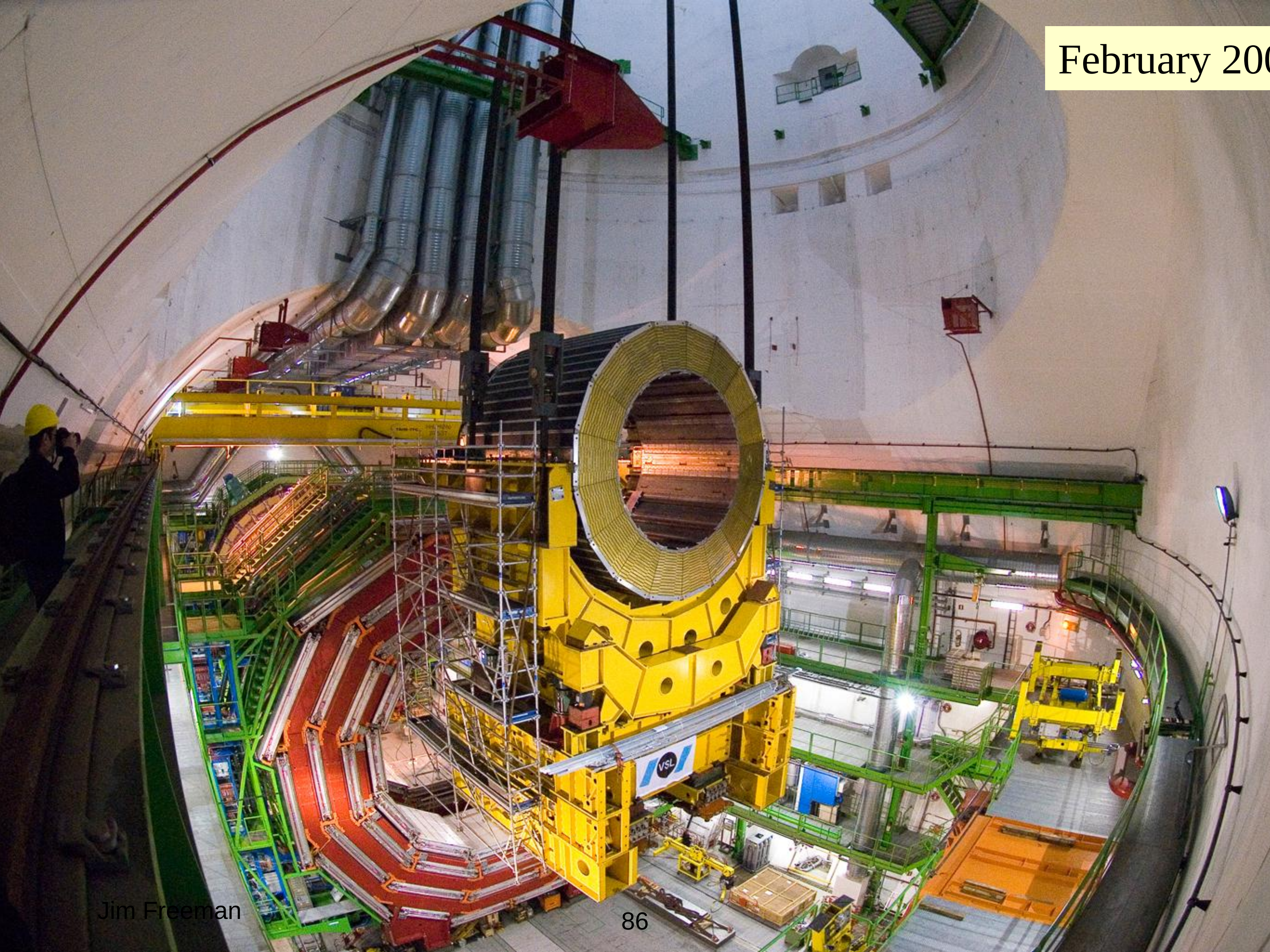

February 200

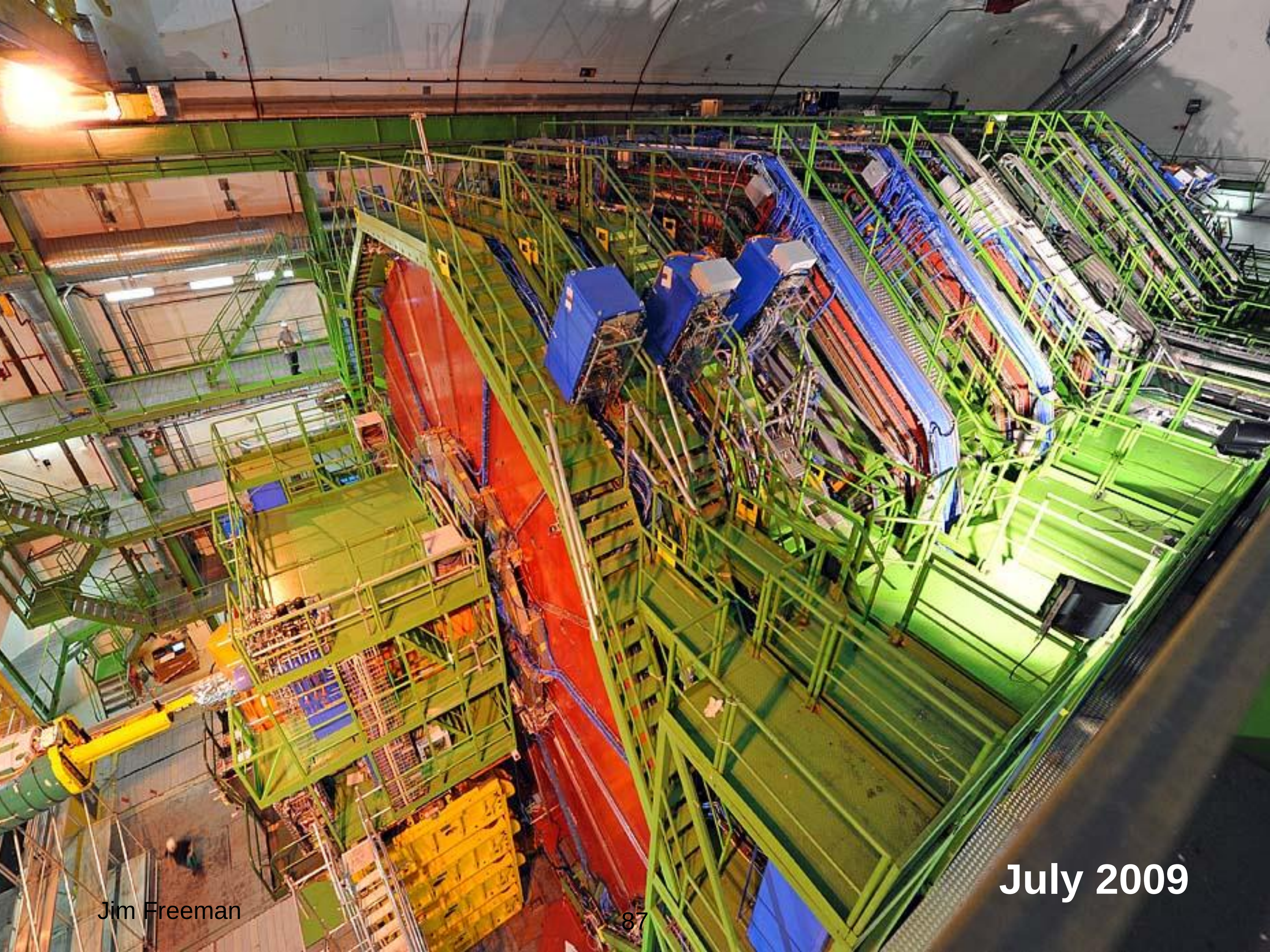

July 2009

Supersymmetry

- Gluinos and squarks are strongly produced (cross sections as high as a few pb for masses as high as 1 TeV
    - they decay through cascades to the Lightest SUSY Particle (LSP) $\tilde{\chi}_1^0$
    - combination of jets, leptons, E_T^{miss}

Look for deviation from SM

multijets and E_T^{miss}

Always 2 LSP if R parity is conserved

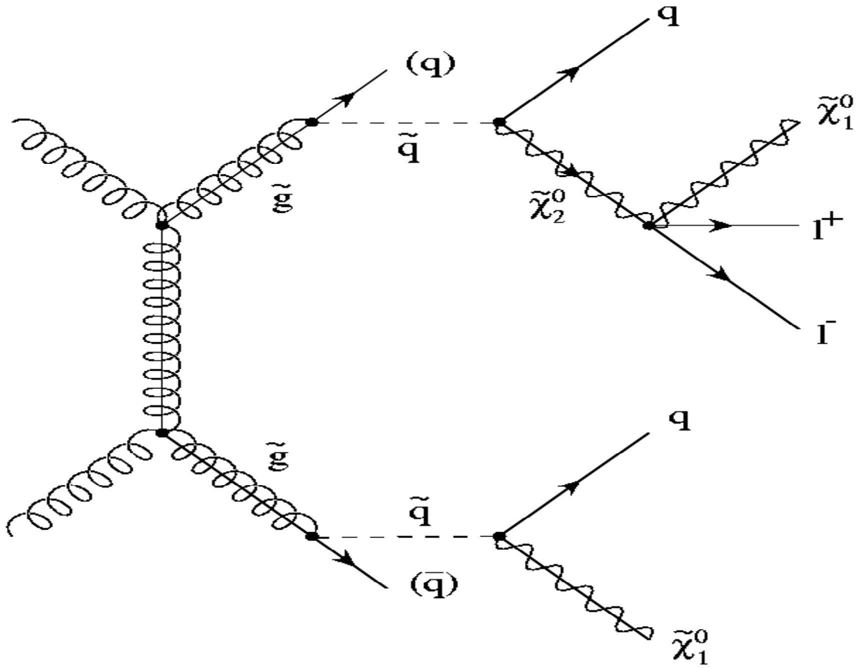

- A key signature is jets and missing Et
- How to measure a jet
- What can cause missing Et
  - Neutrinos
  - Undetected muons
  - Cracks and defects in calorimetry
  - Lack of total coverage in 4π (beampipe)
  - Energy mismeasurement by calorimeter

Jets – Cone Algorithm

CONE center - (η^C, φ^C)

CONE i $\subset C$ *iff* $\sqrt{(\eta^i - \eta^C)^2 + (\varphi^i - \varphi^C)^2} \leq R$

Energy $E_T^C = \sum_{i \subset C} E_T^i$

Many ways to define cluster in calorimetry.

Newer algorithm → particle flow. Use full information from detector

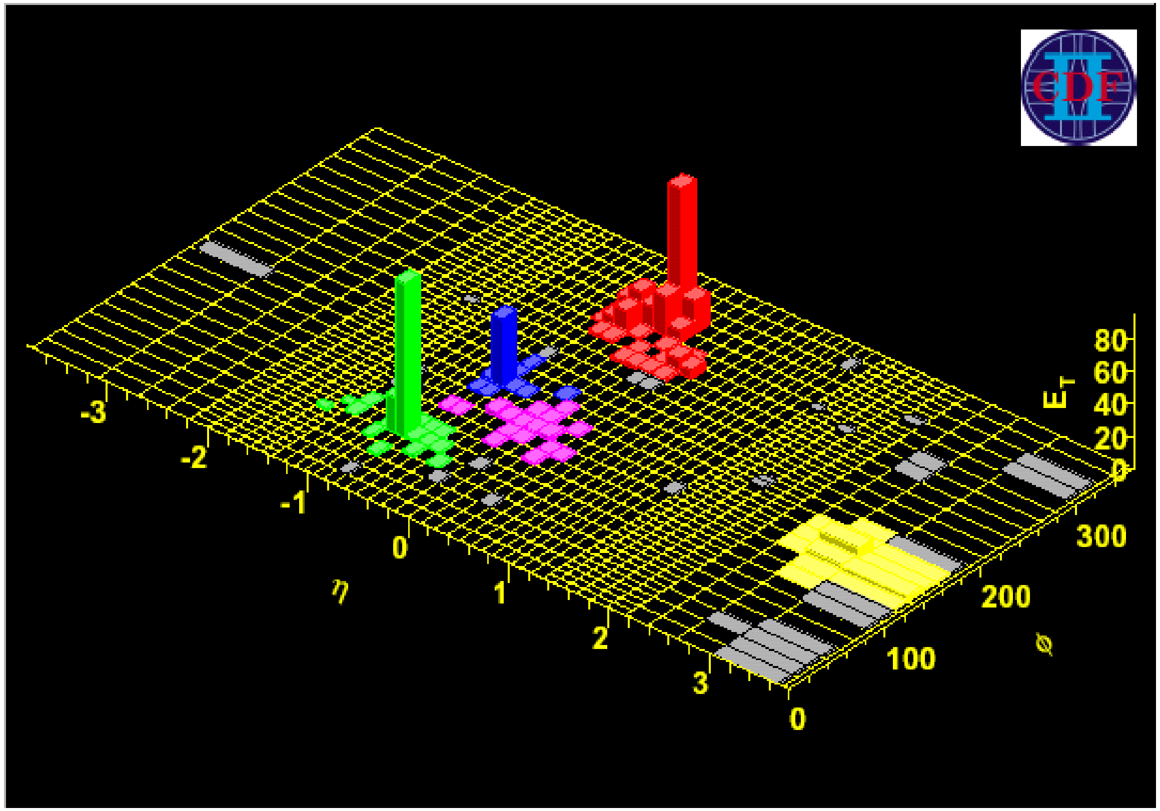

Particle Flow Jets (the future)

- In a typical jet:
  - 60 % of jet energy is from charged hadrons
  - 30 % from photons (mainly from π^0)
  - 10 % from neutral hadrons (n and $K_L{}^0$)
- The traditional approach to jet reconstruction:

  Measure all of jet energy in calorimeters

  → ~ half of energy measured in HCAL

  Poor HCAL resolution limits jet energy resolution: $\Delta E/E \sim 60\% / \sqrt{E}$

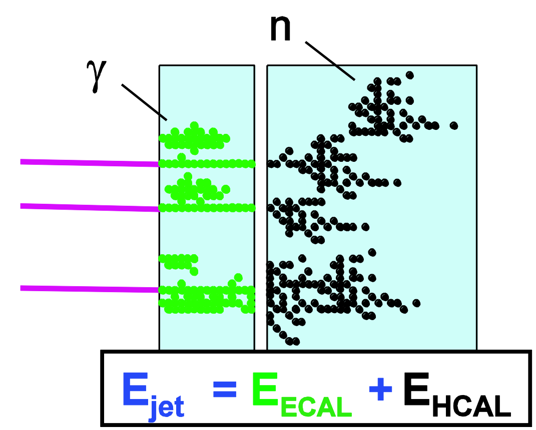

- Particle Flow approach:
  - Charged particles well measured in tracker
  - Photons in ECAL
  - Neutral hadrons (only) in HCAL

  → Only 10 % of jet energy taken from HCAL

  $\Delta E/E \sim 30\% / \sqrt{E}$ may be achieved

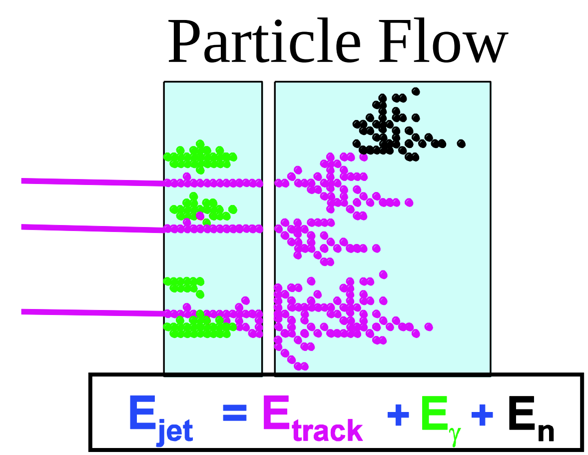

Particle-flow calorimetry

- The main remaining contribution to the jet energy resolution comes from the confusion of contributions, from overlapping showers etc
- Most important is to have high *granularity* of calorimeters to help the (complicated) pattern recognition
- This is the approach being studied for detectors at the future e^+e^- linear collider (ILC or CLIC)
- A motivation for CMS HCAL upgrade

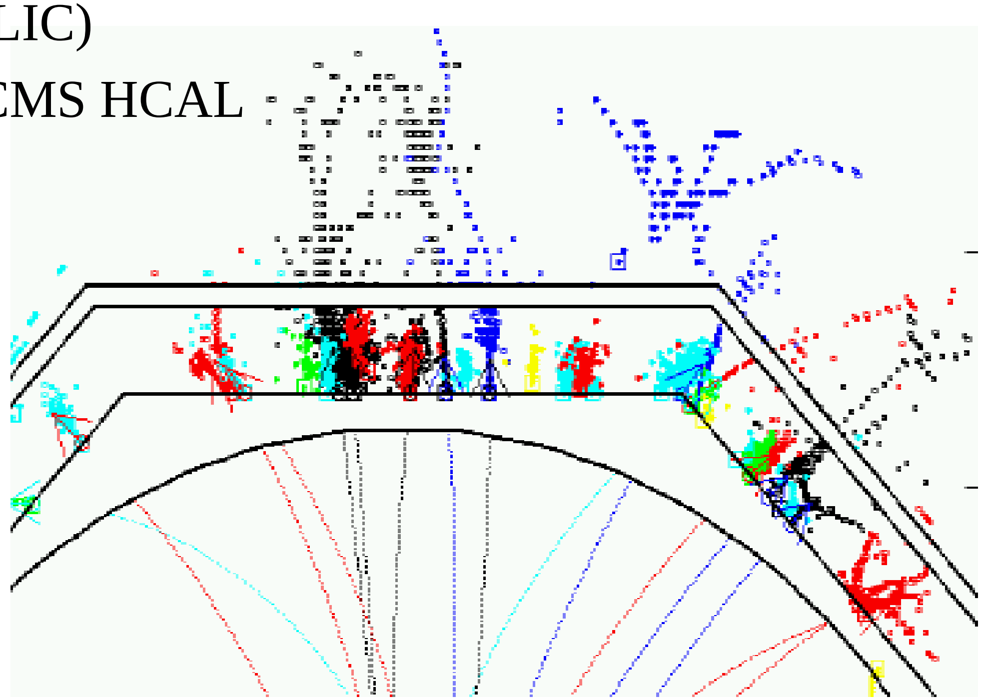

Simulated event in an ILC detector

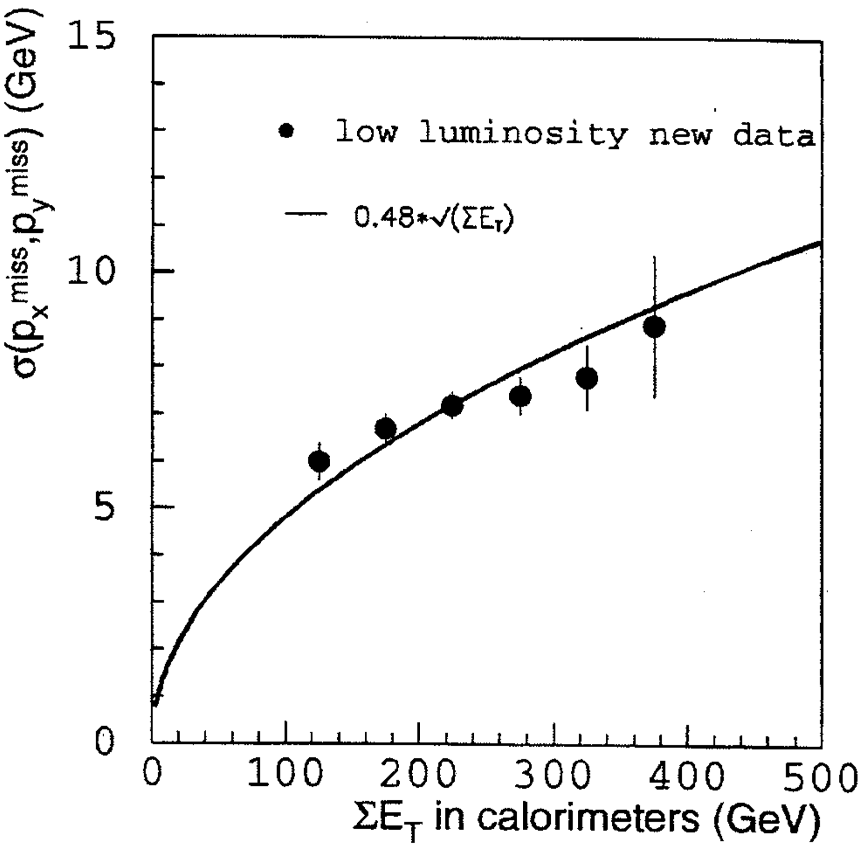

Missing Et is a global variable

dE/E ~ a/√∑(Et)
summed over all Et in the event

Missing Et significance

$$S = \not{E}_T / \sqrt{\sum E_T}$$

Energy Containment for pions vs int length

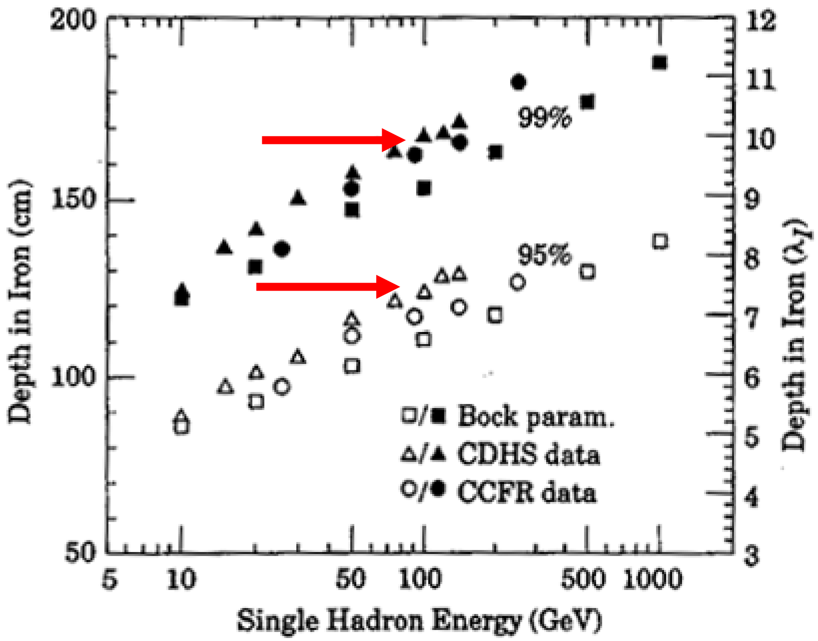

For 95 % containment, the Fluctuation in the leakage is

- 5 %.

With 7 λ total depth, single pions are

- 95 % contained for energies < 100 GeV

As the LHC is a 7 TeV + 7 TeV machine,
That is a bit thin.

Missing Et due to leakage, pion non-interaction (0.001 for 7 lambda), cracks

Particle identification through ionization losses

$$p = m\beta\gamma$$

$$\frac{dE}{dx} \propto \frac{1}{\beta^2}\ln\left(\beta^2\gamma^2\right)$$

Simultaneous measurement of *p* and *dE/dx* defines *m*.

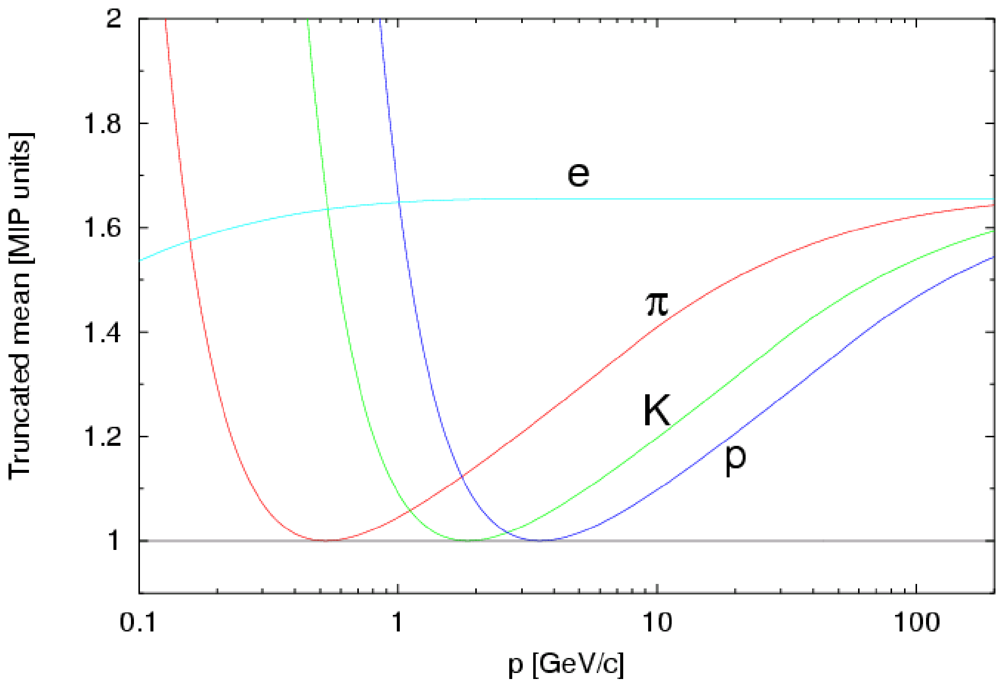

π/K separation at a 2σ level requires a *dE/dx* resolution in the range of 2 to 3% - depending on the momentum range

But:
Large fluctuations and Landau tails !

Average energy loss in 80/20 Ar/CH_4 (NTP)

Distribution of Energy Loss

Amount of energy lost from a charged particle going through material can differ greatly from the average or most probable

Figure 3.9: The Landau distribution of the total energy loss across a gas volume. Note the long *Landau tail* on the distribution.

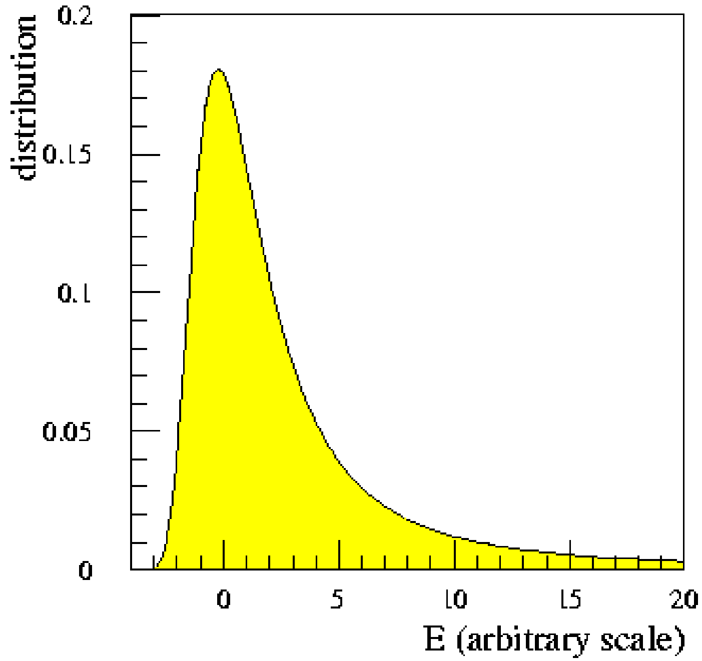

The long tail of the energy loss distribution makes particle ID using dE/dx difficult.

To use ionization loss (dE/dx) to do particle ID typically measure many samples and calculate the average energy loss using only a fraction of the samples.

dE/dx in OPAL Jet Chamber

The chamber is 4 m long with an inner diameter of 0.5 m and an outer diameter of 3.7 m. The sensitive volume is divided into 24 identical sectors, each containing a plane with 159 sense wires.

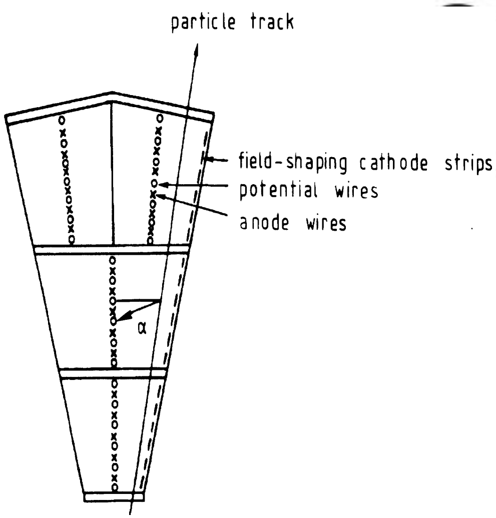

Jet Chamber

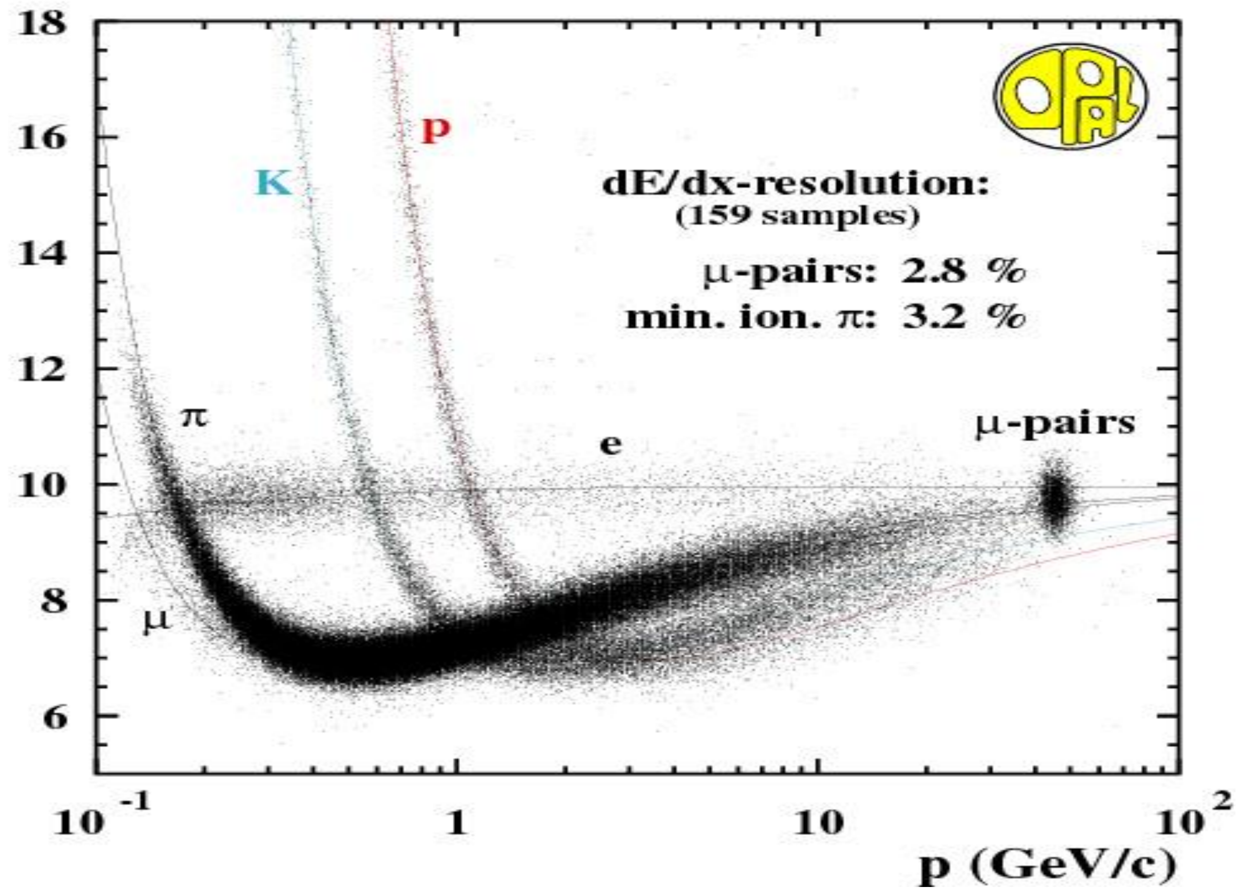

OPAL, NIM A314 (1992) 74

Transition Radiation

- TR is emitted when a charged particle traverses the boundary between two media with different dielectric constants ε_1 and ε_2. Related to cerenkov light $n = \sqrt{\epsilon_r \mu_r}$
- TR is the result of the reformation of the particle's field when traveling from a medium with ε_1 to a medium with ε_2
- TR is not related to the charge acceleration ($v=const$)
- $\Delta E \sim \gamma$. For a 10 GeV electron, $\gamma \sim 2 \times 10^4$, $\Delta E \sim$ keV
- Radiation probability low (1%) so need many layers of radiator.
- Radiation emitted in the very forward direction, in cone of angle $1/\gamma$ around the particle direction → photons will be seen in same detector as the ionization from the track

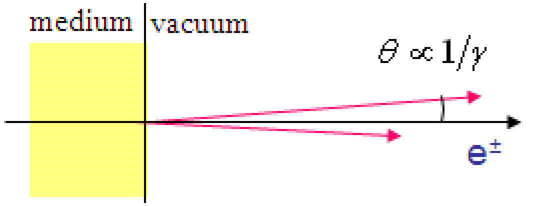

Transition Radiation Detector

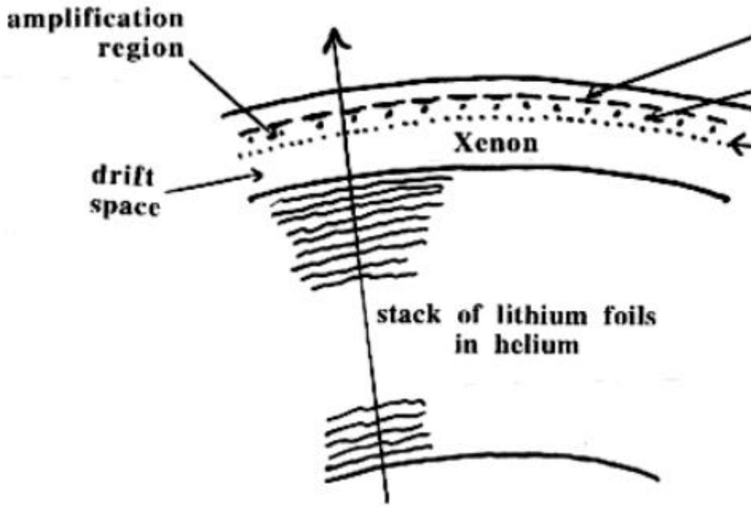

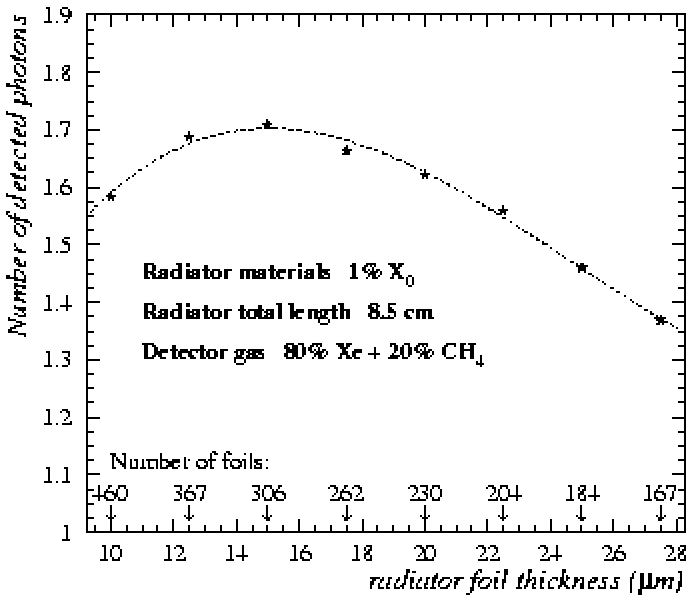

Fig. 2.4. Number of detected TR photons as a function of the radiator foil thickness, for given radiator length and allowed amount of material. The curve shown results from a smoothing algorithm.

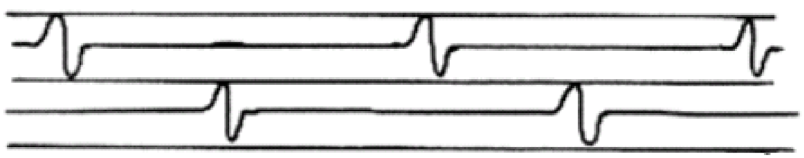

The radiator is made of a low atomic number material, to minimise absorption of the X-ray photons. Lithium foils in a helium atmosphere is ideal, for example 400 foils of thickness 40 microns, spaced 160 microns apart by corrugations on alternate foils.

ATLAS TRT (Transition Radiation Tracker) -30000 channels

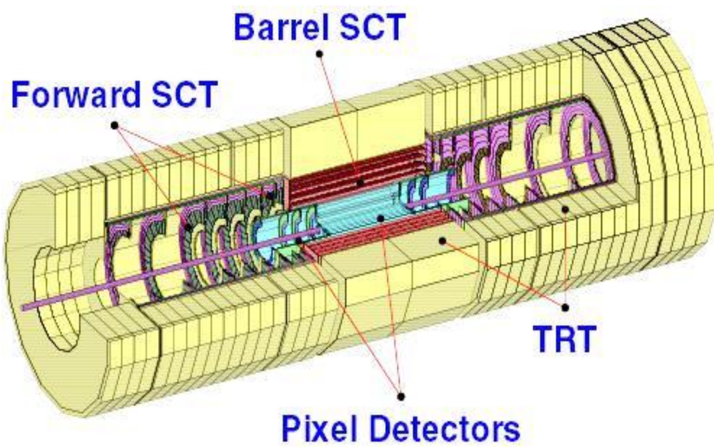

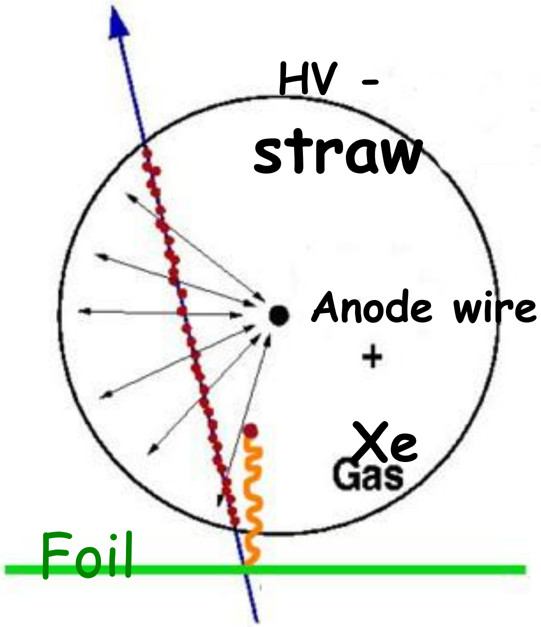

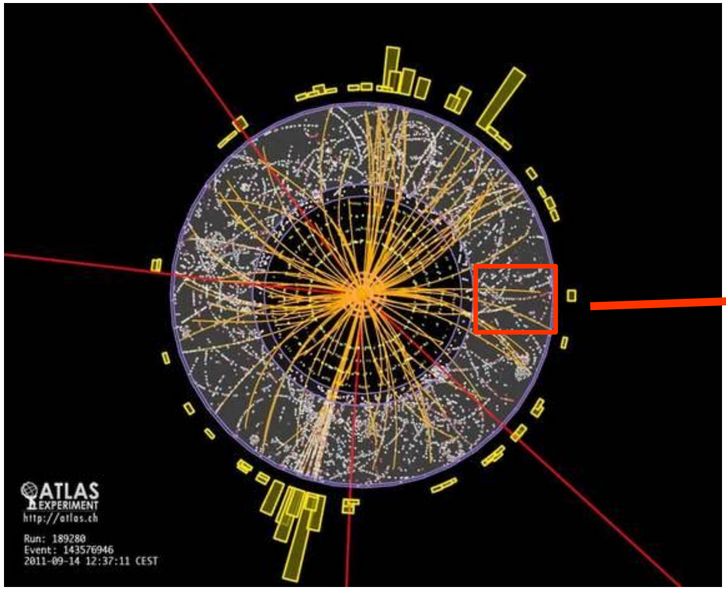

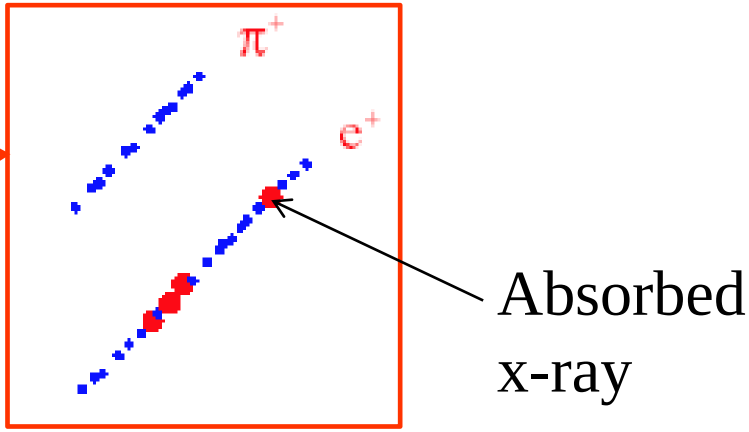

AMS-02 on ISS: Measure Cosmic ray species

AMS made from familiar components

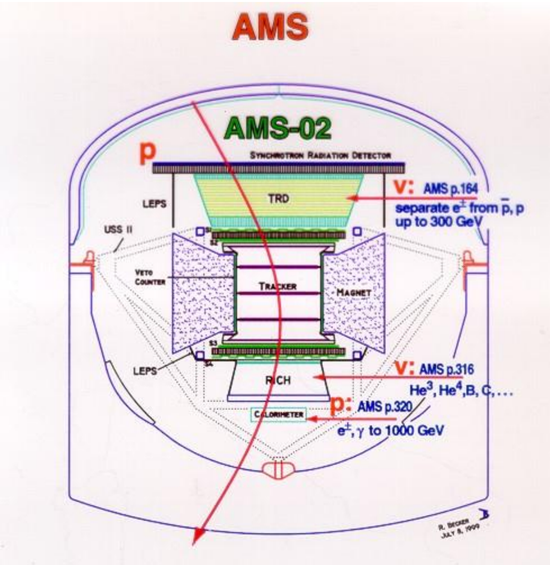

AMS Goals

- Search for Antimatter (H, He, C) in space
- High statistics precision measurements of D, ^{3}He, ^{4}He, B, C, ^{9}Be, ^{10}Be spectrum

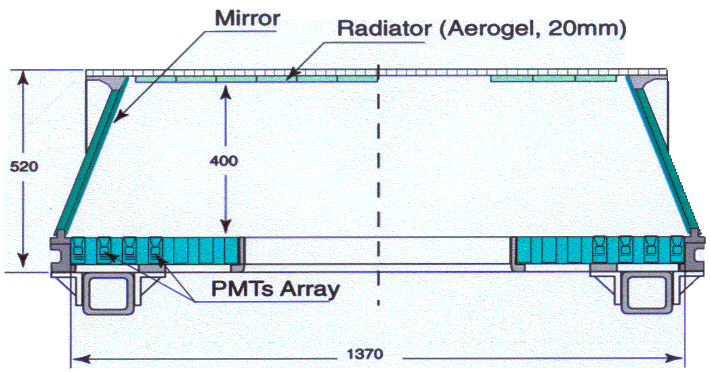

Ring imaging cerenkov

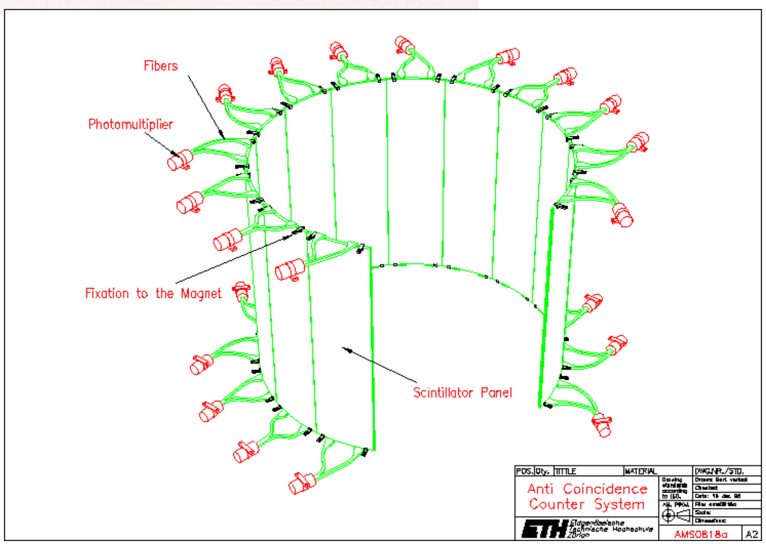

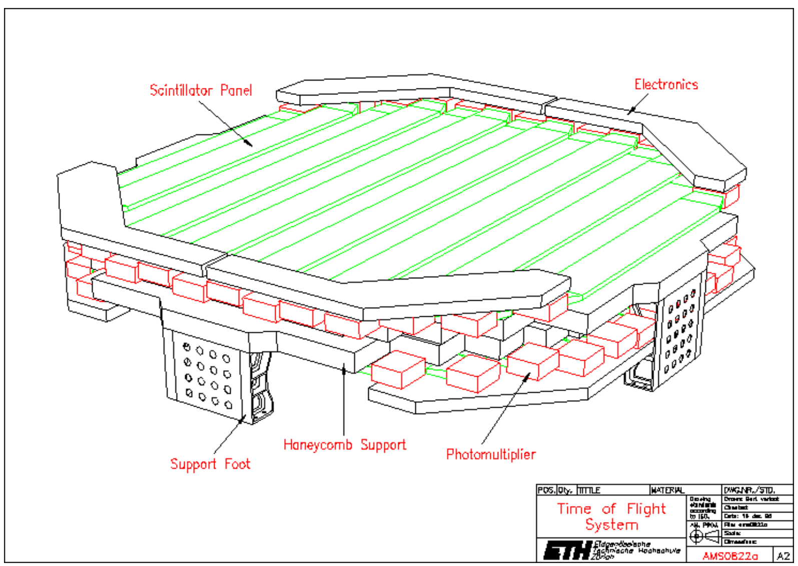

Last Topic: Magnetic Monopoles

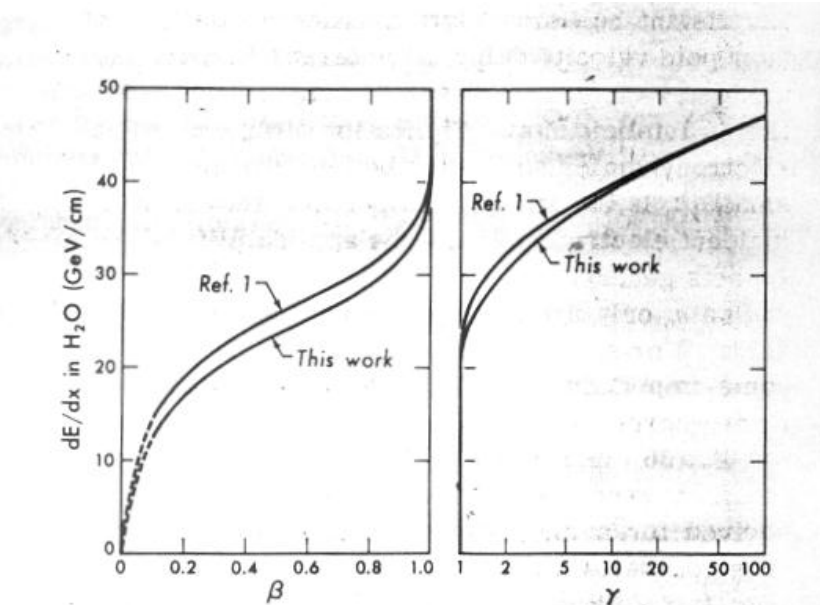

$$\mathbf{F} = g\left(\mathbf{B} - \frac{1}{c^2}\mathbf{V} \times \mathbf{E}\right)$$

Lorentz force for magnetic monopole. Gains energy by falling through magnetic field.

Charge of Monopole n*137 times larger than electron → very heavily ionizing

Magnetic Monopole Exercise: calculate Dirac Quantization Relation

Dirac Quantization Relation

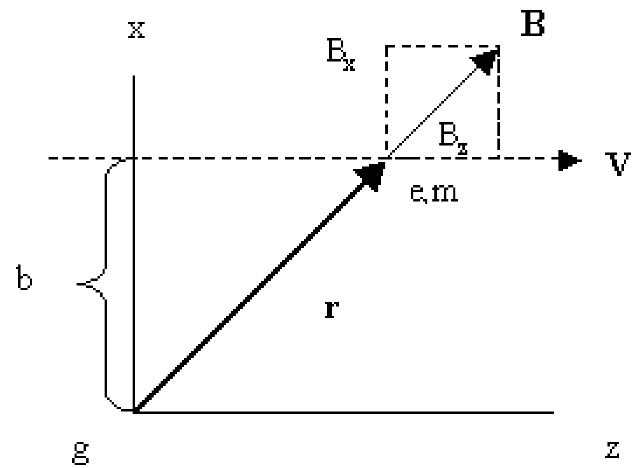

$$g\,e = \frac{\hbar c}{2} n,\; n = 1, \ldots$$

$$\mathbf{B} = g\,\frac{\mathbf{r}}{r^3}$$

$$F_y = \frac{ev}{c} Bx = \frac{eg}{c} V \frac{b}{\left(b^2 + V^2 t^2\right)^{3/2}}$$

rotation around x axis

$$\Delta Py = \frac{egVb}{c} \int_{-\infty}^{+\infty} \frac{dt}{\left(b^2 + V^2 t^2\right)^{3/2}} = \frac{2eg}{cb}$$

$\Delta L = b\,\Delta Py = \dfrac{2\,eg}{c} = n\hbar \rightarrow eg = \dfrac{\hbar c}{2} n$ assuming quantized angular momentum.

Monopole Experiments

- Cosmic Rays
  - Price reported event from 18 m^2 plastic detector in 1975. Later excluded by Alvarez. Then they published an upper limit.

- Moon Rocks
  - One of the first scientific experiments with moon rocks was to search for a concentration of magnetic monopoles by Alvarez.

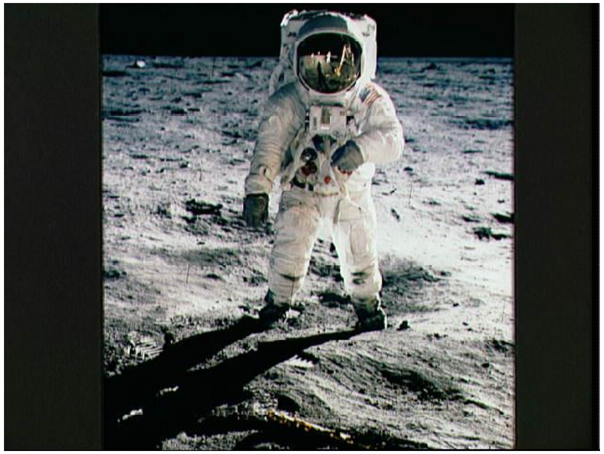

How to design an experiment—magnetic monopoles at collider

- At general purpose experiments like ATLAS, CMS you can "design" your own specialized experiment.
- You know the experiment, operation of the subdetectors
- You know how your signal (monopole) is produced (MC) and interacts (Geant)
- Design the trigger you need. (Maybe existing trigger path?)
- Design the analysis using details of particle interaction in your experiment.
- Monopole bends "wrong way" in magnetic field
- Accelerated by magnetic field
- Loses energy very rapidly in matter

Trigger	Threshold (GeV or GeV/c)	Rate (Hz)	Cumulative Rate (Hz)
Inclusive electron	29	33	33
Di-electrons	17	1	34
Inclusive photons	80	4	38
Di-photons	40, 25	5	43
Inclusive muon	19	25	68
Di-muons	7	4	72
Inclusive τ jets	86	3	75
Di-τ jets	59	1	76
1 jet * E_T^{miss}	180 * 123	5	81
1 jet OR 3 jets OR 4 jets	657, 247, 113	9	89
Electron * Jet	19 * 45	2	90
Inclusive b jets	237	5	95
Calibration etc. (10%)		10	105
TOTAL			**105**

Detectors: Things don’t always go as planned

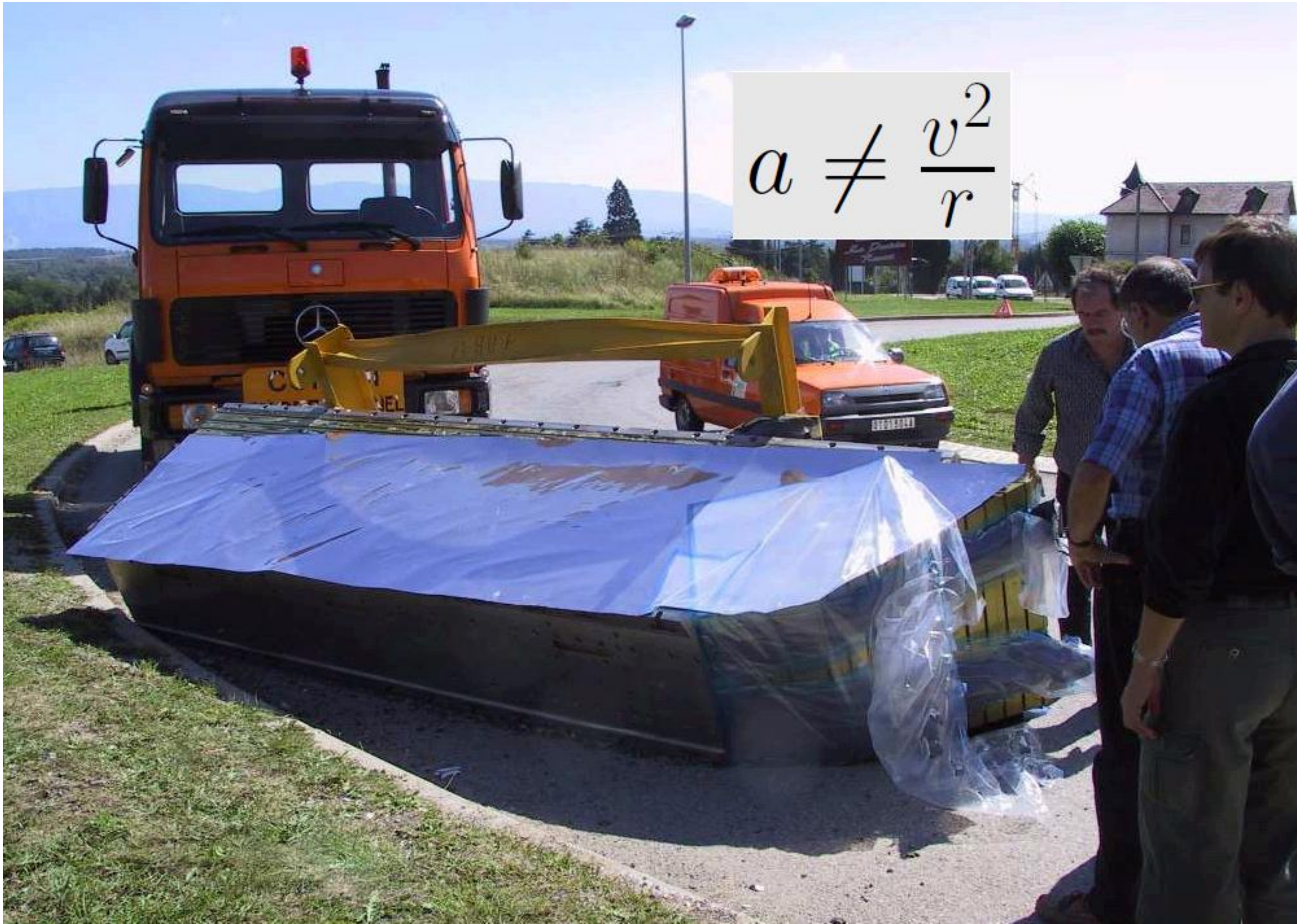

$$a \neq \frac{v^2}{r}$$

CMS HCAL – Fiber Readout of Scintillator

- One 0.94 mm fiber per tile (4 from HO)
  - Optical grouping into readout depths

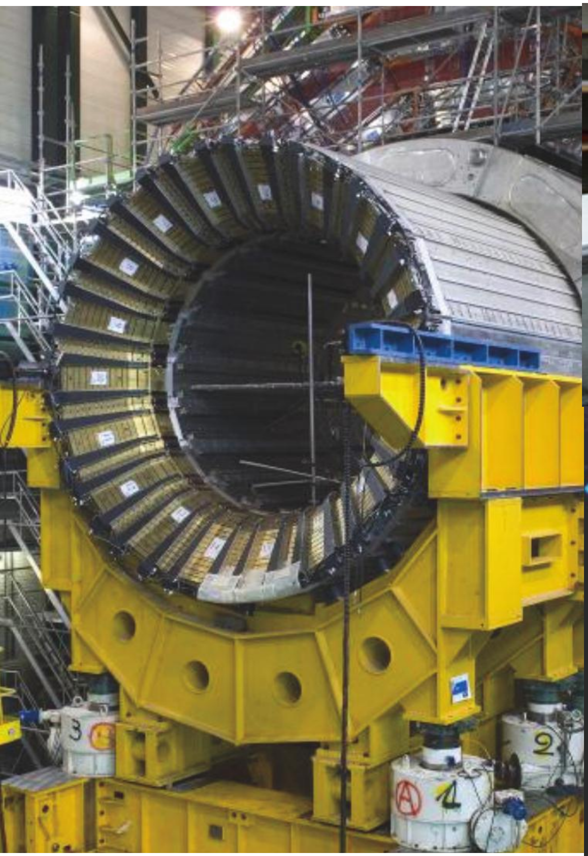

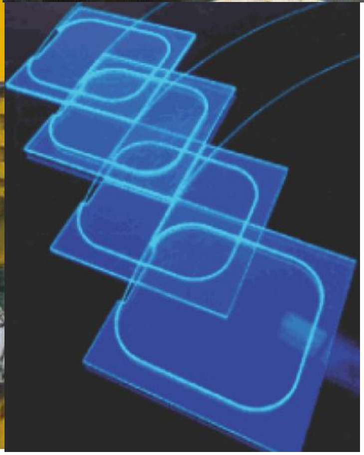

~71,000 Barrel/Endcap 0.94 mm fibers

~670 cm^2 total photodetection area

Barrel Readout Module

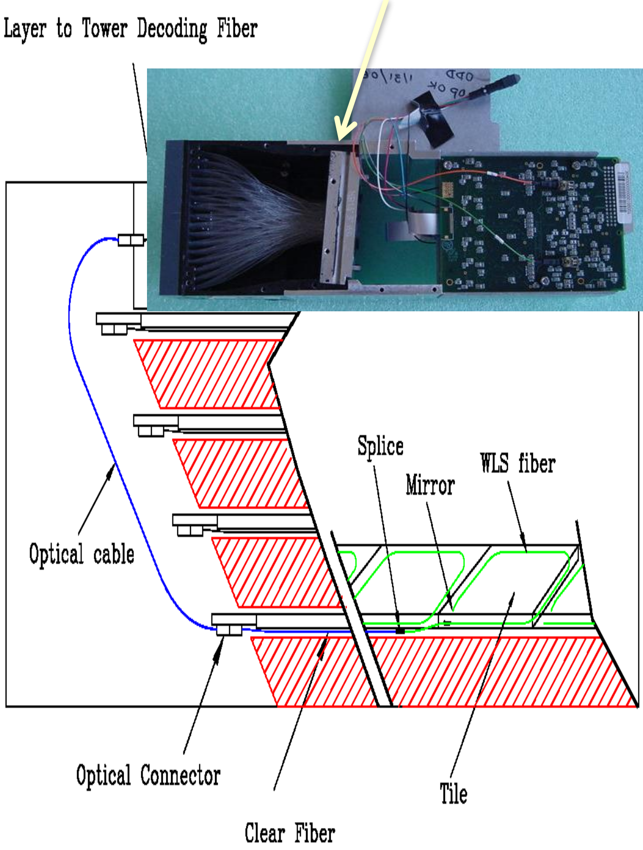

Hybrid Photo-diode (HPD)

- QE ~ 15%
- Gain 1500 ~ 2000 depending on voltage
  - Running at high voltage, 7~8kV
- optical-to-HPD mapping (ODU)

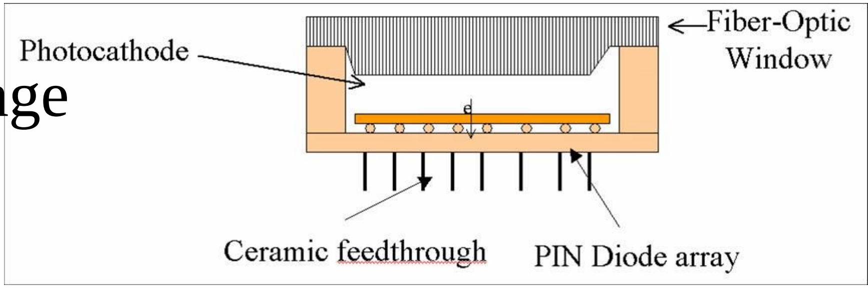

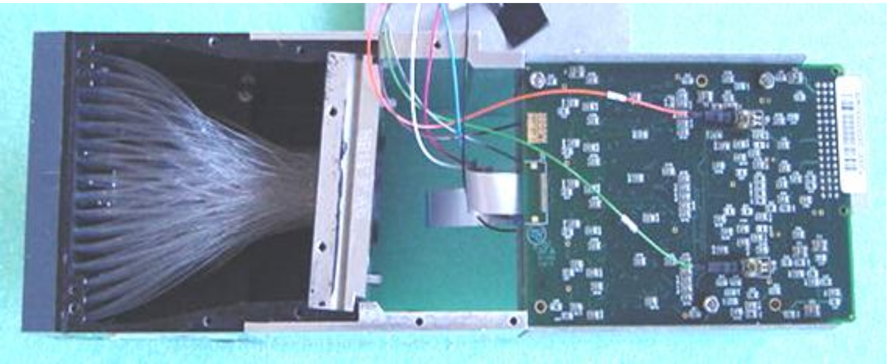

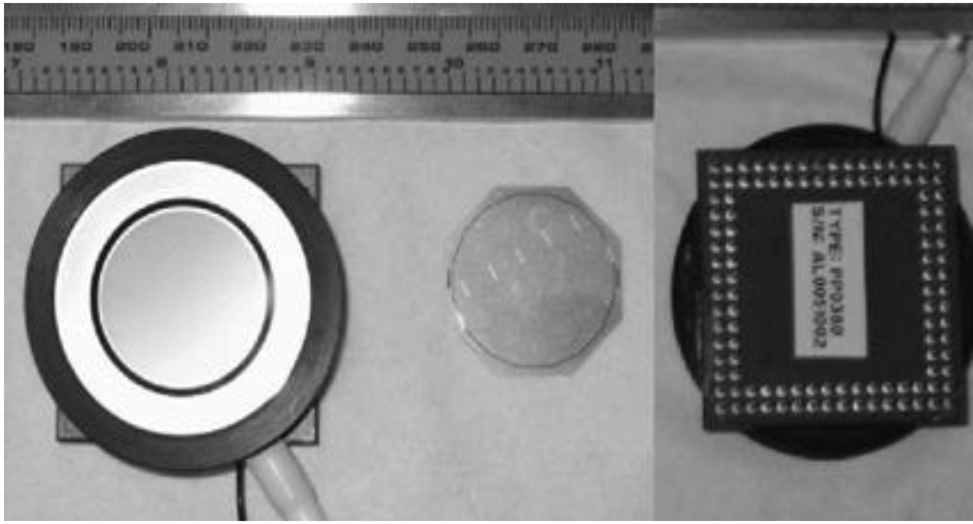

Problems: HPD

•HPD was a long development path for CMS HCAL
•No existing photodetector worked in 4T with enough gain. (20pe/GeV)
•HPDs tested extensively for planned operating environment,
E parallel to B, B = 4T (and at B=0T)
•No problems found
•But – In real CMS B field was not as modeled: E not completely parallel. Also not tested at intermediate field (worked at 0 and 4T)

•We discovered that there were problems

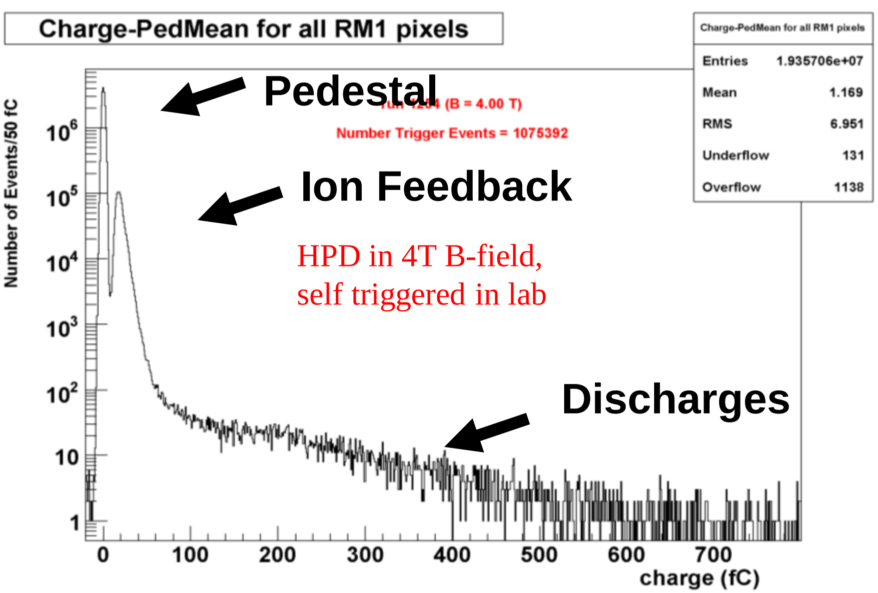

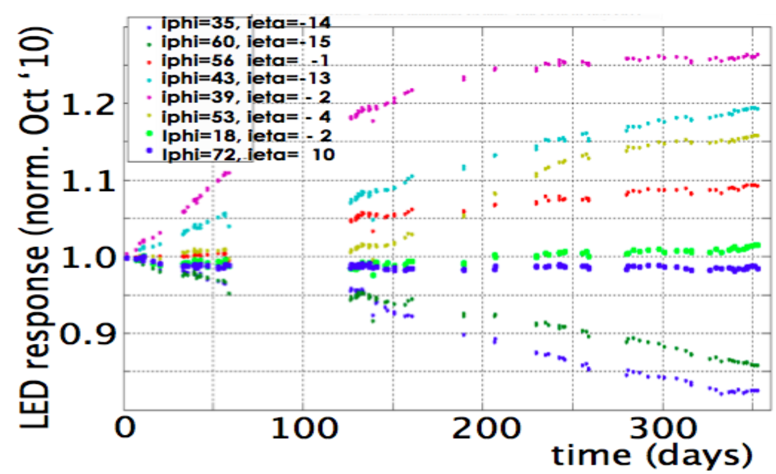

SIPM "Drop-in" replacement for HPD

- Using Hamamatsu 3mm x 3mm, 50 μm pitch, SiPM, we can mimic the layout of the HPD.
- These are coupled to the existing optical decoders and read out using the same ADC.

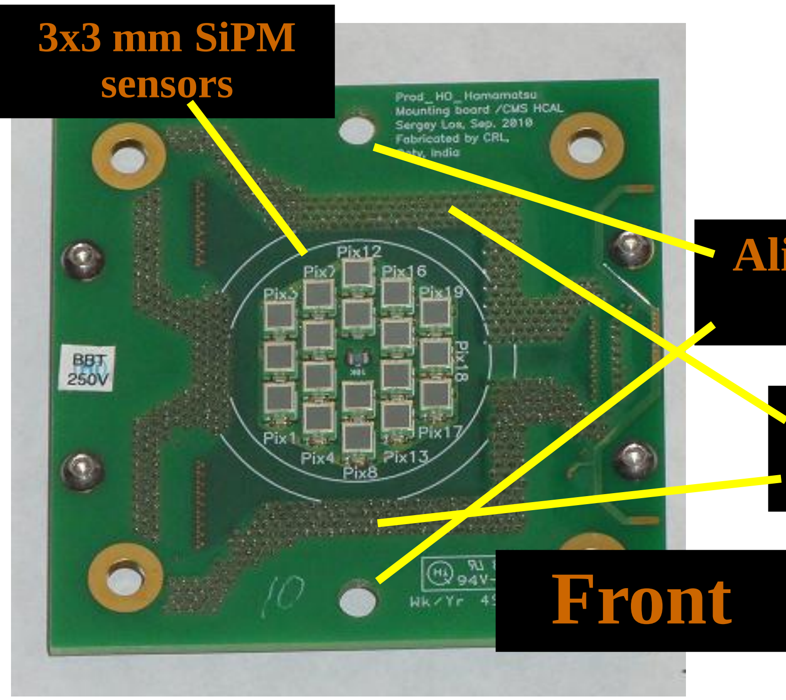

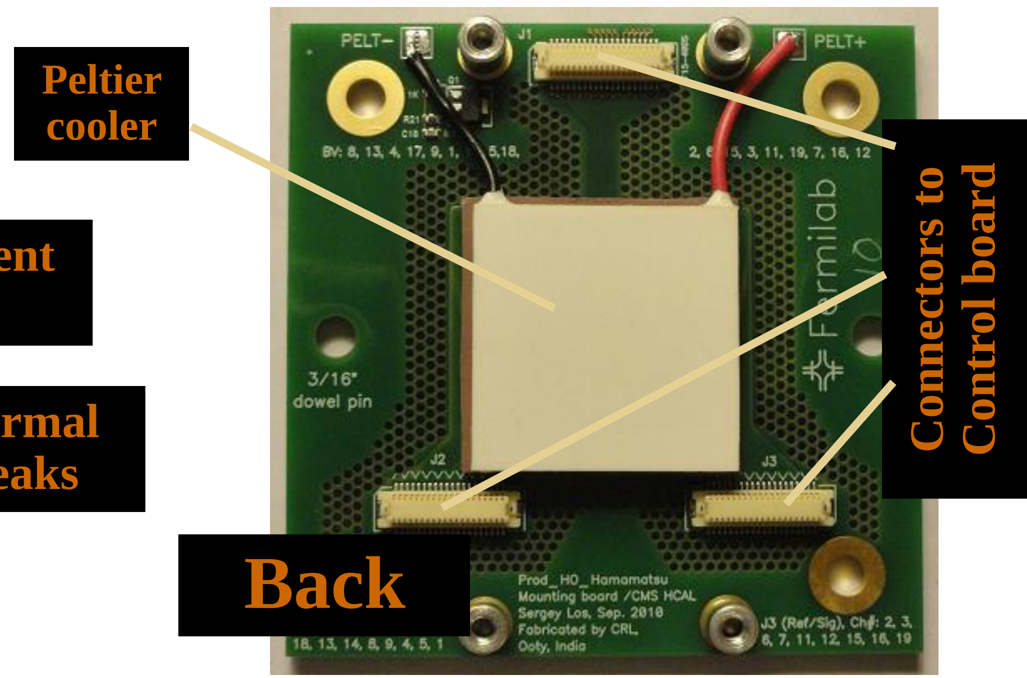

CMS Forward calorimeter HF

HF is located about 11 m from the interaction point, covers $3 < |\eta| < 5$ with depth 10 λ_{int}

Consists of iron absorber embedded with quartz fibers parallel to the beam direction in a 5x5 mm matrix

Charged particles from showers produce Cherenkov light

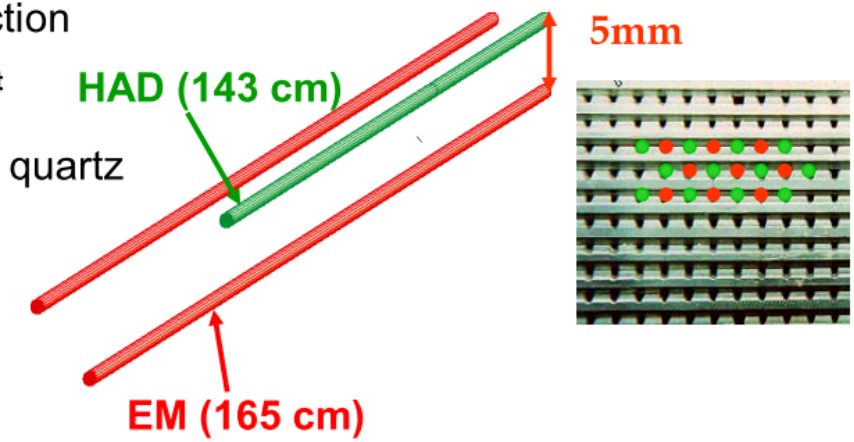

HF signal generation and collection is very fast ~10 ns

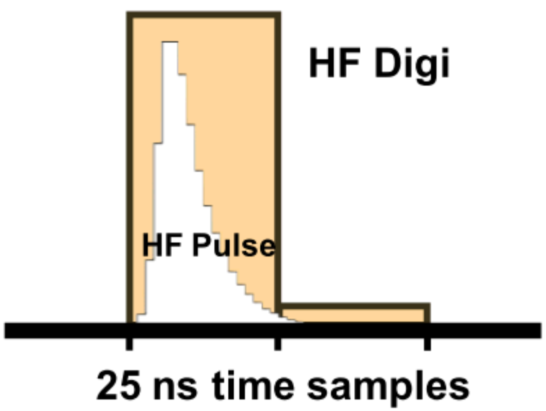

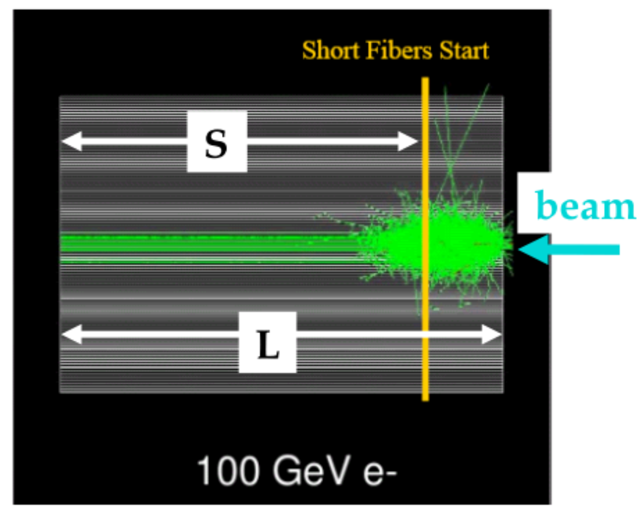

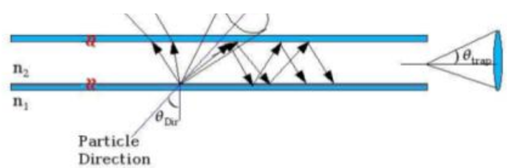

CMS HF Calorimeter

Quartz-fiber Čerenkov calorimeter

First device of its kind.

200k quartz fibers.

Test beam results Aug. 2003

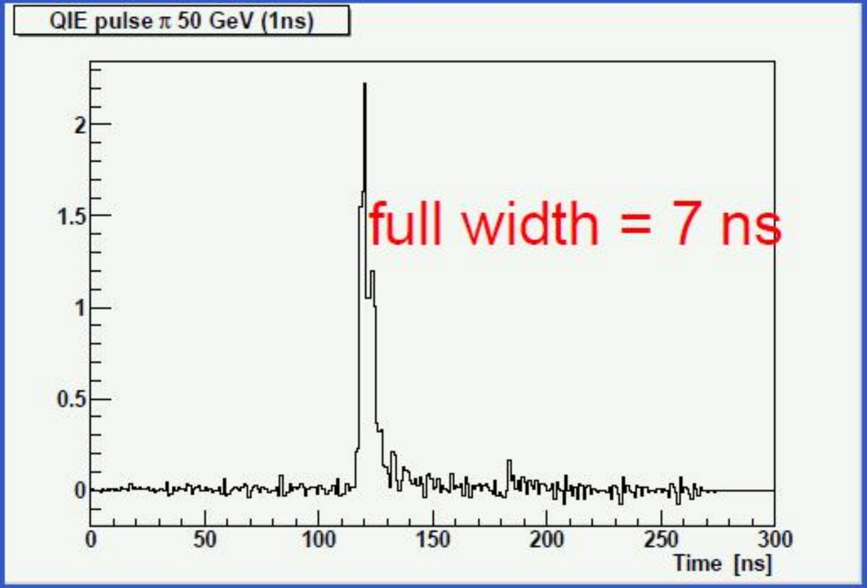

Readout: 2000 pmts

HF side view

Each calorimeter tower has two PMTs: one reading bundle of LONG fibers, the other SHORT fibers (143cm), for some EM/HAD separation

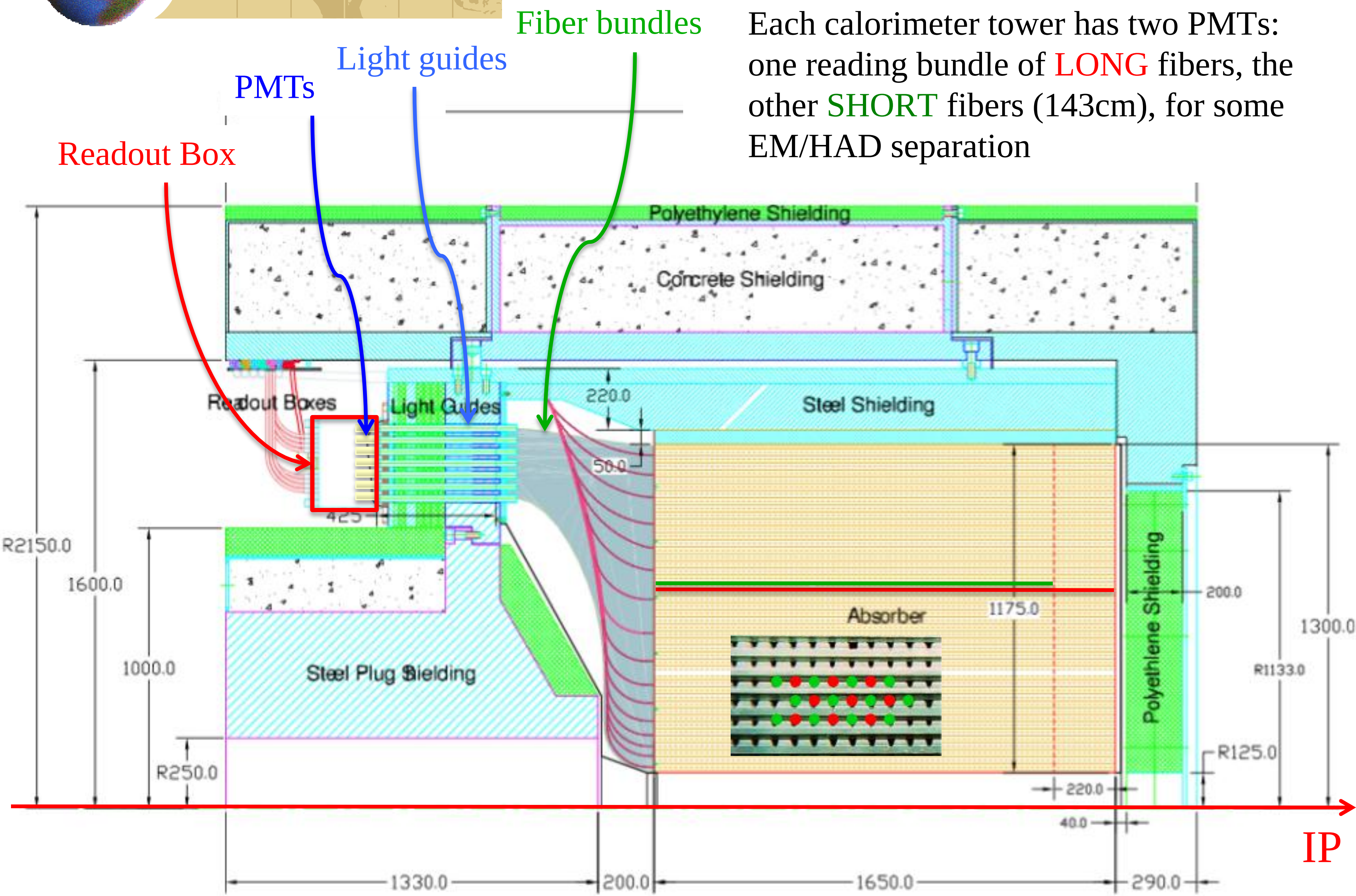

HF PMT : Abnormal Events

150GeV Muon / Wedge 2-6

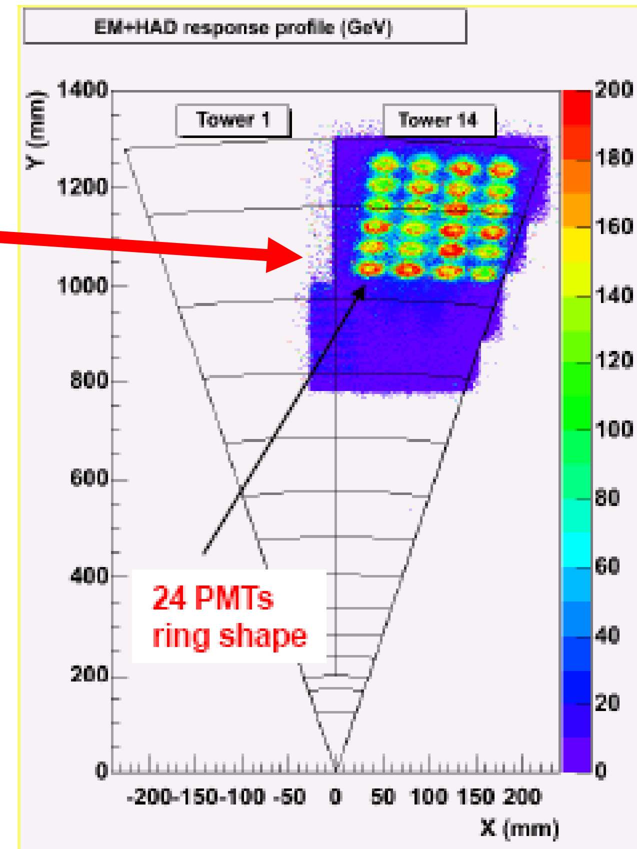

TB2004 elog 3601 Aug. 2, 2004

- These events are most likely to be from Cerenkov radiation from particles directly hitting the PMT window.
  - peak of muon signal ~ 200 GeV
- The glass window is plano-convex.
  - 2mm thick in center
  - 6.1mm thick at the edge

MIP Cerenkov light in HF

It was discovered that minimum-ionizing tracks hitting the pmt front window created cerenkov light, large false signals. Solution→ replace pmts with thin window pmt

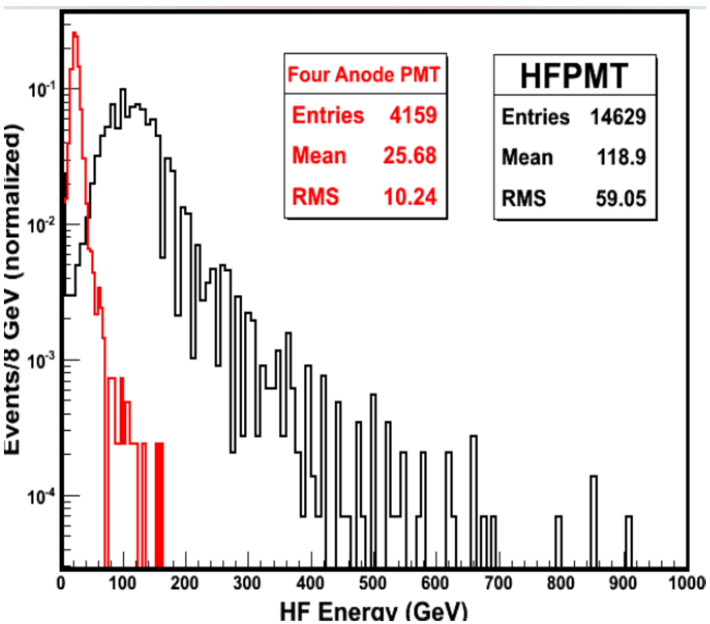

Window: ~2 mm thick at the center, ~6 mm thick at the edges.

R7600U-200-M4

Four Anode Square PMT

Window: < 1 mm thick

Now that you know detectors, I need…

Scintillating fiber trigger counter

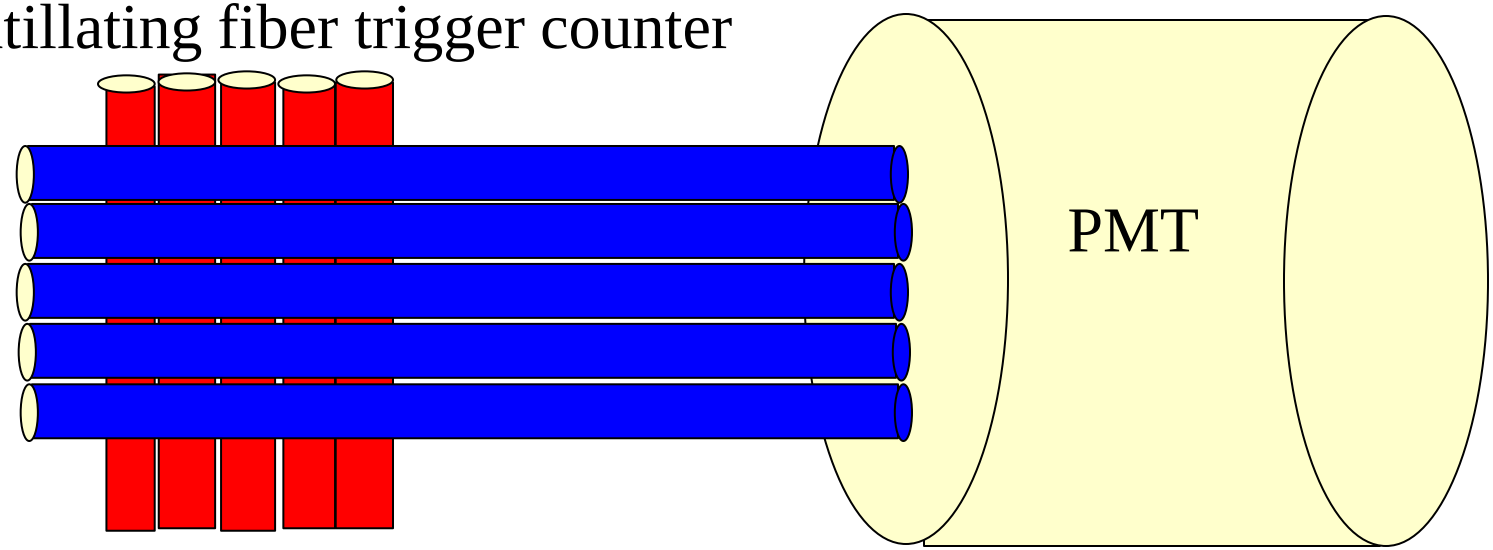

3mm fiber diameters
6mm wide, ~20 cm long
2 of them for SIPM test beam at CERN
in October.

References

- **Web**
  - http://www-physics.lbl.gov/~spieler/physics_198_notes/PDF/

    A nice set of lectures about particle detectors, emphasis on detectors
  - http://www.physics.ohio-state.edu/~kass/p880_06.html Richard Kass

    A nice set of lectures about particle detectors, emphasis on physics
  - http://rkb.home.cern.ch/rkb/titleD.html

    The Particle Detector BriefBook. An encyclopedia of particle detector terms, formulae.
- Books
  - Techniques for Nuclear and Particle Physics Experiments, W.R.Leo, Springer-Verlag
  - Introduction to Experimental Particle Physics, Richard Fernow, Cambridge Press

Backup

LHCb overview

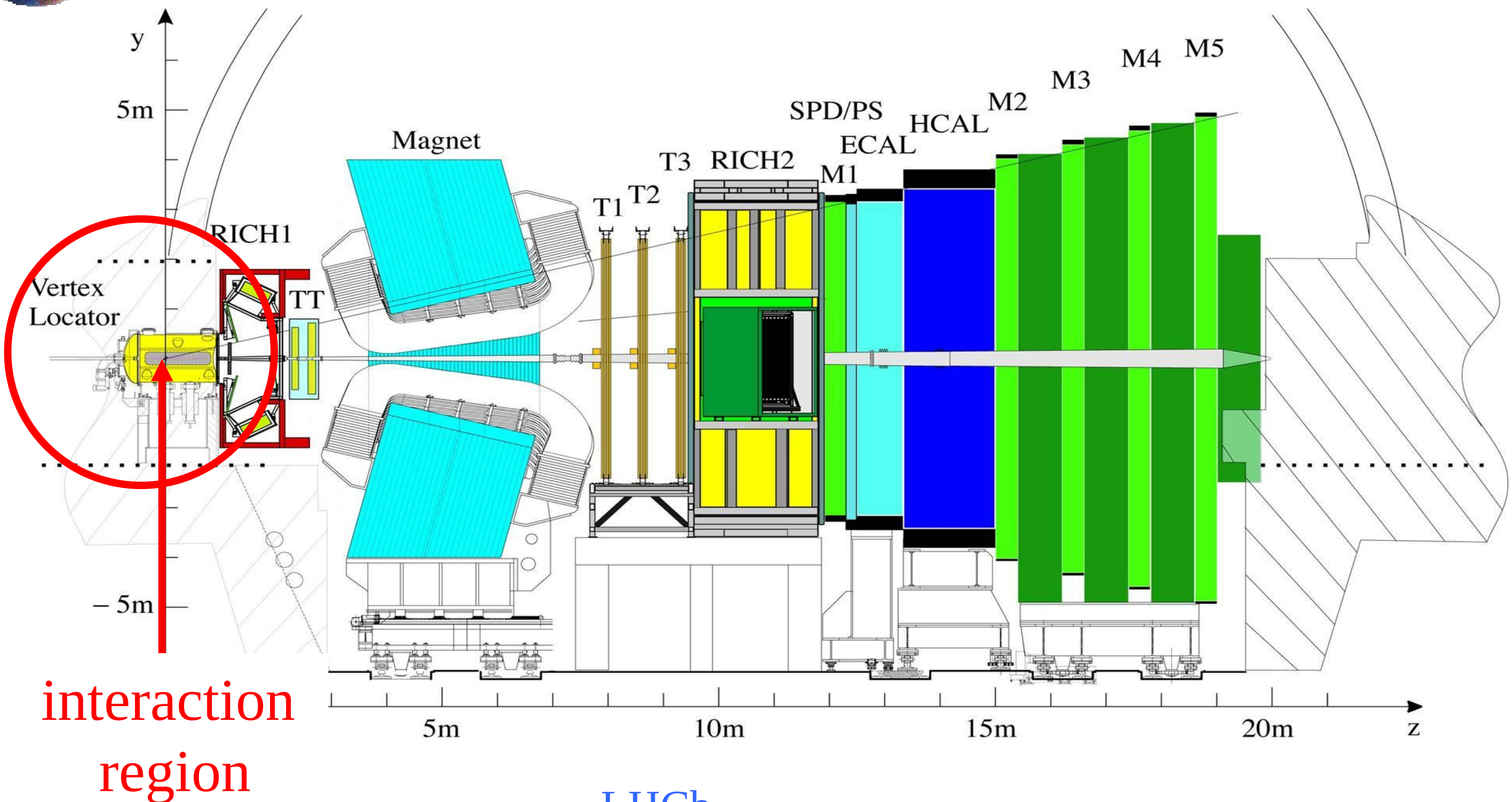

Large Hadron Collider

- pp collisions: $\sqrt{s}$ = 14 TeV
- bunch crossing every 25 ns

LHCb

- Studies physics of b-flavoured hadrons (CP violation)
- B-hadrons produced at small angles
  - -> Single arm forward spectrometer
- 10 – 300 (250) mrad in bending plane (non bend.)
- Luminosity 2 – 3.5 X 10^{32} cm^{-2} s^{-1}

In-time pileup events

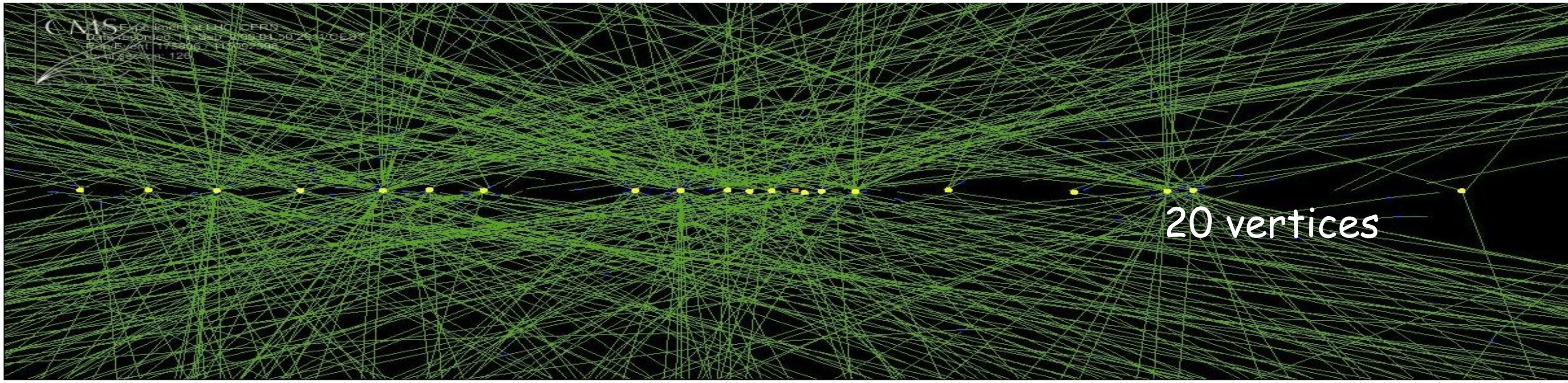

<n>≈33 for highest luminosity in 2012

-> challenges to trigger and computing!

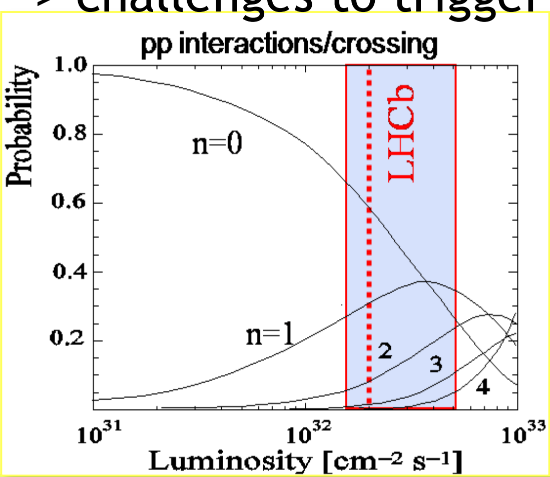

$$\mathcal{P}_n = \frac{\langle n \rangle^n}{n!} e^{-n}$$

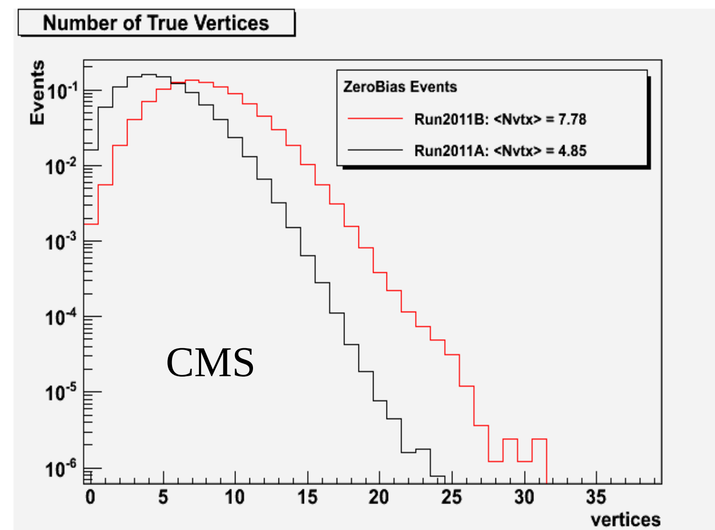

Vertex resolution better than ~200 μm (CMS), ~100 μm (LHCb), vertices a few cm apart, beam spot size 16 μm at collision point. Average number of interactions at nominal LHC luminosity and 25 ns bunch spacing: 23.

LHCb luminosity leveling

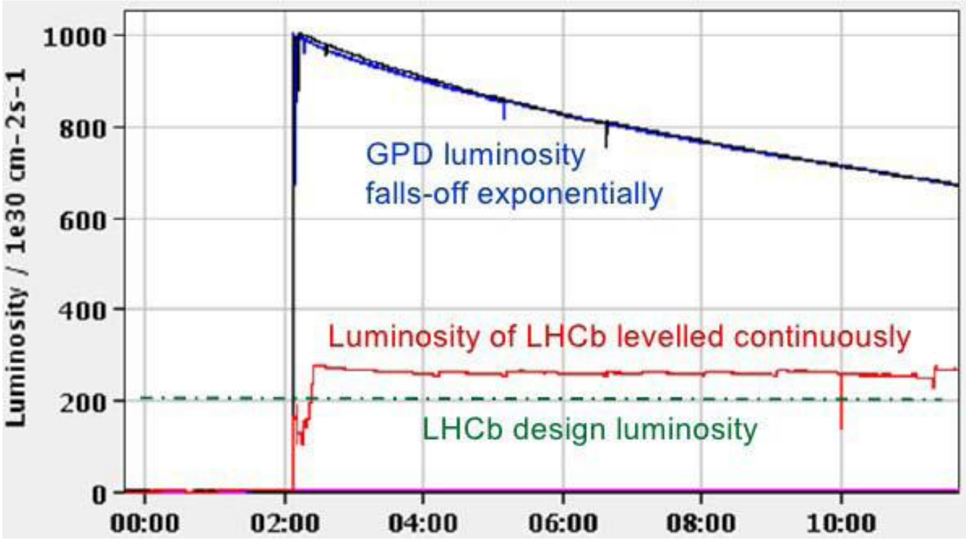

- <u>Luminosity leveling</u>
- LHCb already running above design lumi
  - Average L~3×10^{32} cm^{-2}s^{-1} (nominal 2×10^{32})
- Need to cope with higher occupancies
  - More pile-up: average ~1.5 (nominal 0.5)
- Continuous, automatic adjustment of offset of colliding beams.
- Allows optimal conditions throughout a fill.

Silicon microstrip modules, vertex

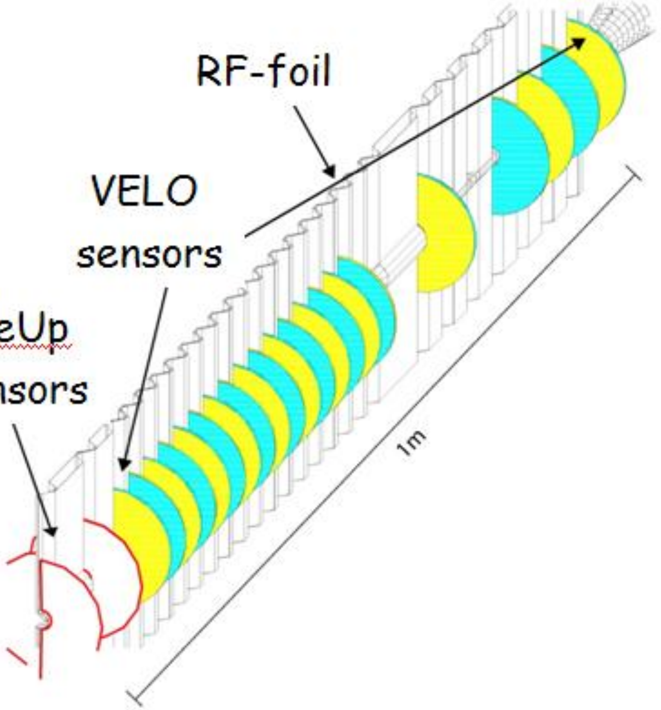

Pileup veto trigger

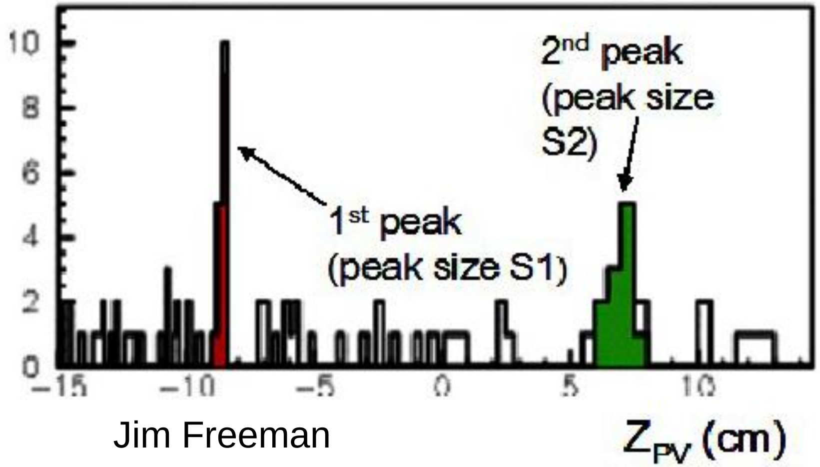

- 21 stations with R-Φ geometry
  - Fast R-Z tracking in trigger farm
  - Overlap of right and left det. halves
  - Total of 176k strips
- 2 stations with R-sensor for L1 PileUp trigger

Jim Freeman

Auger Experiment - Argentina

- Detector field: 3000 km^2
- 24 Fluorescence cameras on 4 observations points
- 1600 Surface detectors (1.5 km spacing)

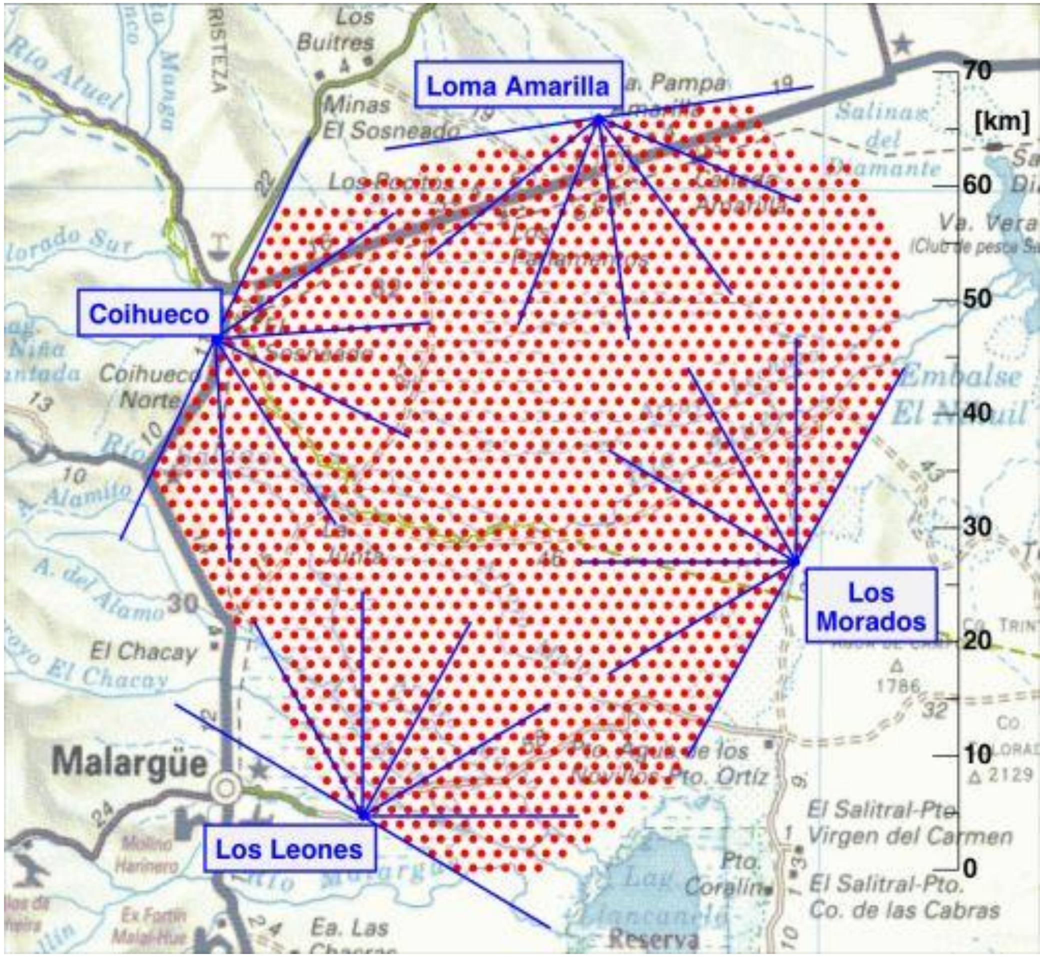

Fluorescence detector

- Charged particles in an air shower also interact with atmospheric nitrogen (excitation)
- Emitted ultraviolet light via a process called fluorescence
- Direction and energy of the cosmic particle can be determined

Fluorescence detector

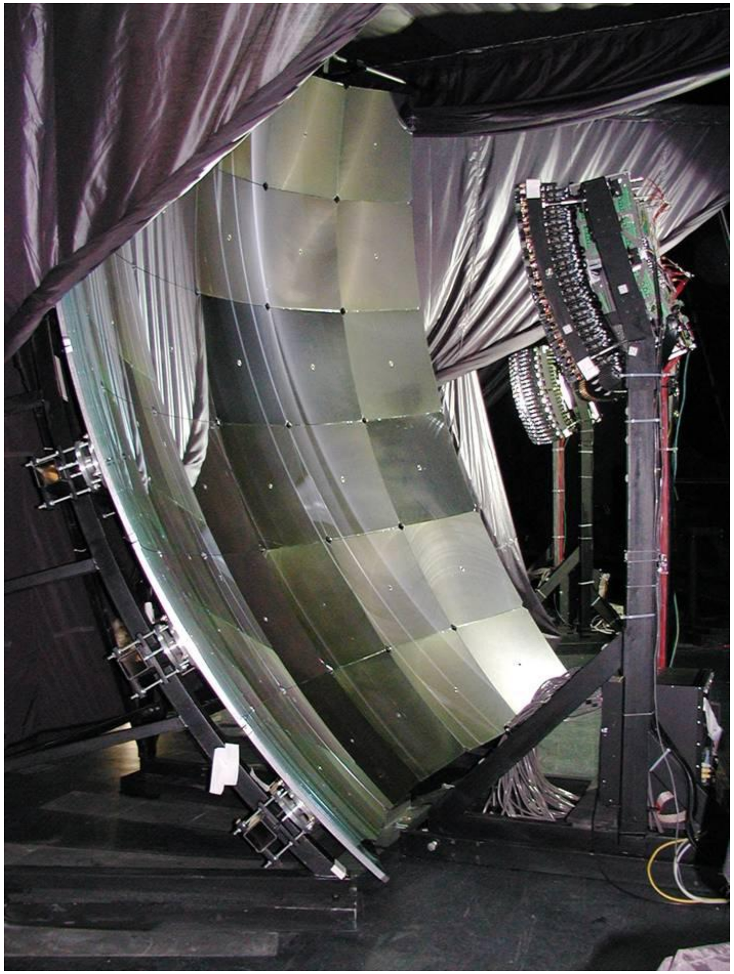

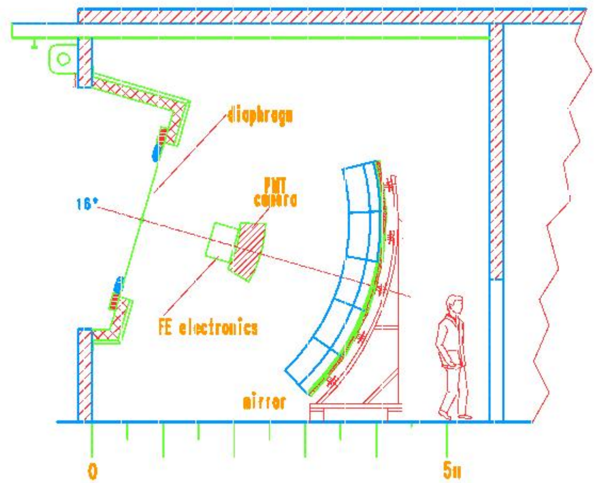

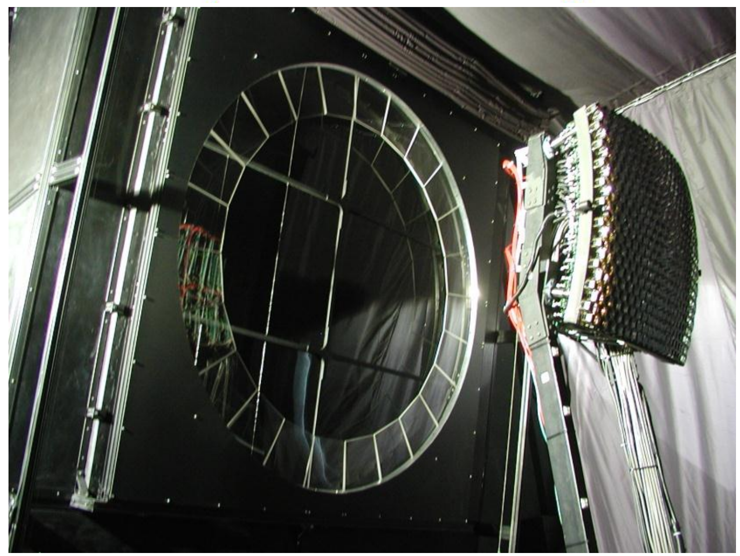

Surface detector

Surface detector

- Base of detector = $10m^2$
- 12 tons of very pure water as detection material
- 3 Photomultipliers detect cerenkov signals
- With GPS antenna high time correlation to different detectors
- Energy given in VEM (Vertical Equivalent Muon)

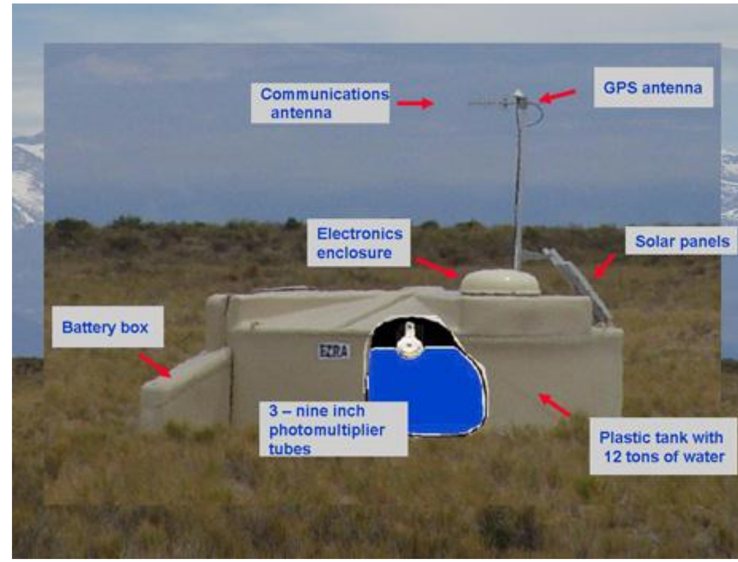

Combination of FD and SD

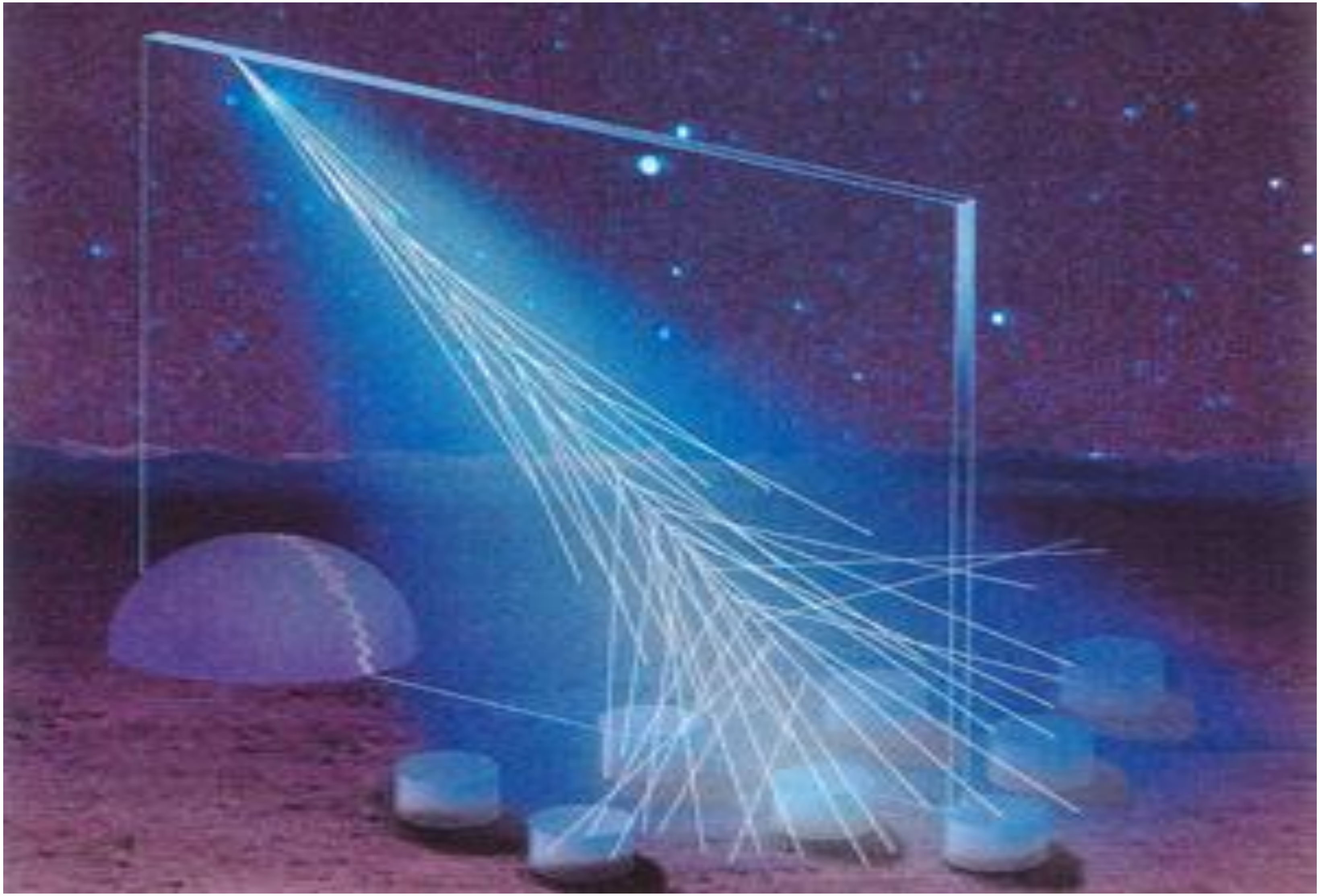

Results

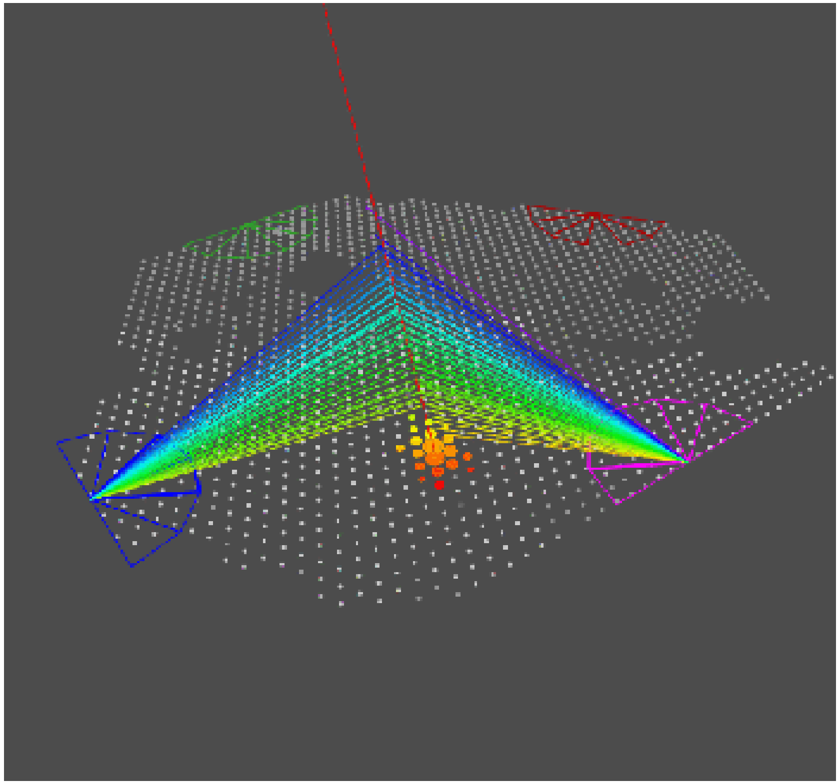

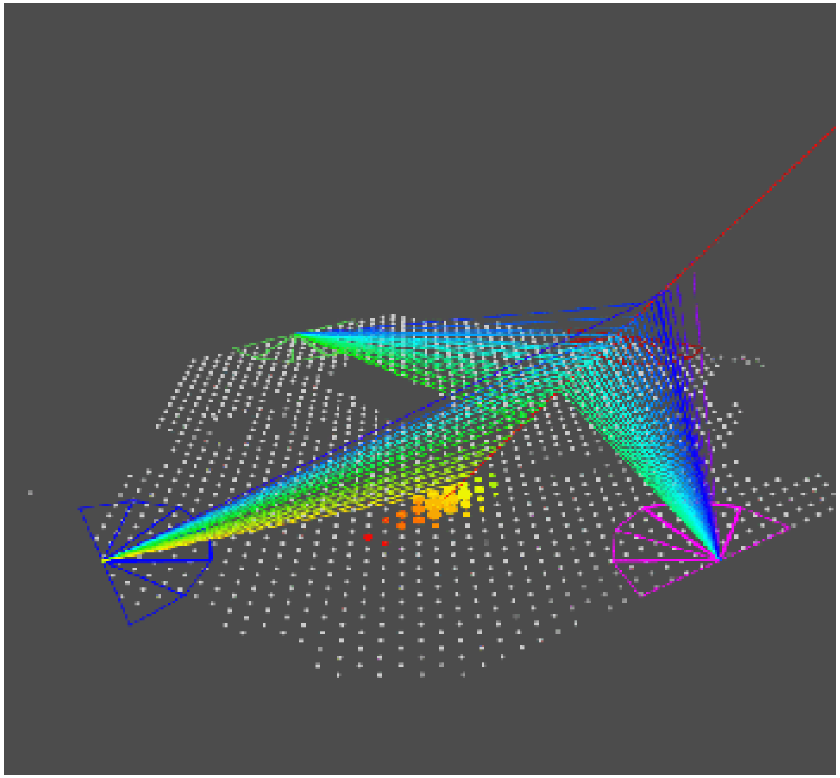

Auger Results